TERRESTRIAL RADIOACTIVITY IN HUNGARIAN ADOBE BUILDING MATERIAL AND DWELLINGS WITH A FOCUS ON THORON (^{220}RN)

by

Zsuzsanna Szabó

Master in Environmental Science
Lithosphere Fluid Research Lab at the Department of Petrology and Geochemistry,
Eötvös Loránd University, Budapest

Ph.D. thesis

submitted to the
Environmental Physics Ph.D. program (Ádám Kiss, Prof., Imre Jánosi, Prof.)
Doctoral School of Environmental Sciences (Ádám Kiss, Prof., András Galácz, Prof.)
Eötvös Loránd University, Budapest

Advisors:

Csaba Szabó, Ph.D.

Associate professor
Lithosphere Fluid Research Lab at the Department of Petrology and Geochemistry,
Eötvös Loránd University, Budapest

Ákos Horváth, Ph.D.

Associate professor
Department of Atomic Physics,
Eötvös Loránd University, Budapest

Budapest
2013

ACKNOWLEDGMENTS

This work was financially supported by the **Doctoral School of Environmental Sciences, Eötvös Loránd University** (led by **Ádám Kiss** and **András Galácz**), Ph.D. scholarship of Hungary and by **Radosys Ltd.** (led by **Erik Hülber**) providing 200 passive track etched detectors. The work was carried out at the **Lithosphere Fluid Research Lab, Eötvös University**, partially at the **Department of Atomic Physics, Eötvös University** and the thesis was finished at the **Centre for Energy Research, Hungarian Academy of Sciences**.

I am highly thankful for **Csaba Szabó**, my advisor and mentor and for **Ákos Horváth**, my advisor to be with me on this path. I must say many thanks to **István Csige** and **Győző Jordán**, whose knowledge helped a lot to improve the quality of my work. **Szabina Török** highly contributed with pushing me to finish this work. I am thankful for **Tibor Kovács** and **Péter Zagyvai** for their constructive comments in the prereview of the thesis. I got a lot of help from many friends-colleagues, first of all late **Ottó Csorba**, who first introduced me to the topic of radioactivity and who cheered me up with his kindness many times and **Gábor Kocsy**, **Zoltán Kis**, **Botond Papp**, **Péter Szabó**, **Zsolt Homoki**, **Beatrix Udvardi**, **Dániel Breitner**, **Mária Balogh di Gleria**, **Helge Hellevang**, **Zoltán Szalai**, **Katalin Zsuzsanna Szabó**, **Gyula Pávó** and all of you from **Institute of Radiochemistry and Radioecology, University of Pannonia** and your collaborators. Thank you! **I emphasize the importance of the help of all local people who gave anything to this work. Without their patience, understanding or sometimes active help I would have failed. I am happy that I could have met them.** Many thanks to **Angéla Barossné Szőnyi** for helping in some measurements, administration and for her kindness and also to **Andrea Förherczné**, **Henrik Kulla** and **Éva Bíró** for other administration issues during the doctoral process. Thank you **LRG guys**, it was fun to meet you in the cold (but sometimes too warm) basement! Also thank all of you from the **Environmental Physics Department**. And at last but not least, there are no enough thanks to say to the following people whose permanent presence gave me my life and strength in this period: **Zsuzsanna Kincses**, my mother, **László Szabó**, my father, **Óskar Halldórsson Holm**, who was so far but still always here, **Margit Cuczor**, my grandmother, **Ákos Szabó**, my cousin, all of **my other family members**, **Hedvig Éva Nagy** and **Péter Völgyesi**, my friends and colleagues, **Adrienn Szaniszló**, **Krisztina Kármán** and **Zsanett Pató**, my friends. I am also thankful for **Andrea Burovinyecz**, **Judit Szabó** and "**Kringsjå Friends**" to contribute to a harmonic living environment while finishing this work.

KÖSZÖNETNYÍLVÁNÍTÁS

A disszertációban összefoglalt munkát az **ELTE Környezettudományi Doktori Iskola** (**Kiss Ádám** és **Galácz András**) állami ösztöndíja és a **Radosys Kft.** (**Hülber Erik**) 200 felajánlott radon-toron detektora tette lehetővé. A kutatást az **ELTE Litoszféra Fluidum Kutató Labor**ban, valamint részben az **Atomfizikai Tanszék**en végeztem, a disszertációt pedig az **MTA Energiatudományi Kutatóközpont**jában fejeztem be.

Először is nagy köszönetem fejezem ki **Szabó Csabá**nak, témavezetőmnek és mentoromnak, majd **Horváth Ákos**nak, témavezetőmnek, hogy velem voltak az idáig vezető úton. Sok köszönettel tartozom **Csige István**nak és **Jordán Győző**nek, akik szakmai tudása nagyban hozzájárult munkám elmélyítéséhez. Köszönöm **Török Szabiná**nak, hogy ösztönzött a disszertáció befejezésére, valamint **Kovács Tibor** és **Zagyvai Péter** konstruktív megjegyzéseit a dolgozat előbírálata során. Rengeteg segítséget kaptam a következő személyektől: először is néhai **Csorba Ottó**tól, akinek sosem felejtem el, hogy mind szakmailag, mind emberileg mennyit tanultam tőle, majd **Kocsy Gábor**tól, **Kis Zoltán**tól, **Papp Botond**tól, **Szabó Péter**től, **Homoki Zsolt**tól, **Udvardi Beatrix**tól, **Breitner Dániel**től, **Baloghné di Gleria Mária**tól, **Helge Hellevang**tól **Szalai Zoltán**tól, **Szabó Katalin Zsuzsanná**tól, **Pávó Gyulá**tól és tőletek mind a **Pannon Egyetem Radiokémiai és Radioökológiai Intézet**éből. Nagyon hálás vagyok mindannyitoknak! **Kiemelem a vizsgált területek helyi lakosainak segítségének fontosságát. Türelmük, megértésük és néhányuk aktív segítsége nélkül megbuktam volna. Köszönöm, hogy ezt a nagyszerű tapasztalatot megszerezhettem!** Sok köszönet illeti **Barossné Szőnyi Angélá**t mérésekért, ügyintézésekért és kedvességéért, valamint **Förherczné Andreá**t, **Kulla Henrik**et és **Bíró Évá**t, mert mindig hatékonyan segítettek a doktori folyamat különféle lépcsőinek ügyintézésében. Köszönöm **LRG-sek** a hideg-meleg alagsorban. Örülök, hogy megismertelek Titeket! Illetve köszönöm Nektek, a **Környezetfizika Labor**ban, hogy befogadtatok. És végül, de nem utolsósorban nincs elég mondható köszönet azoknak, akik állandó jelenléte és akár aktív segítsége adta az erőt ehhez a munkához: **Kincses Zsuzsanna**, édesanyám, **Szabó László**, édesapám, **Óskar Halldórsson Holm**, aki messze de mégis közel volt végig, **Cuczor Margit**, nagymamám, **Szabó Ákos**, unokatestvérem, összes további **családtagjaim**, **Nagy Hedvig Éva** és **Völgyesi Péter**, barátaim és kollégáim, valamint **Szaniszló Adrienn**, **Kármán Krisztina** és **Pató Zsanett**, barátaim. Továbbá köszönöm **Burovinyecz Andreá**nak, **Szabó Judit**nak és nektek, „**Kringsjå Friends**”, hogy a legvégénél ott voltatok.

„ …Fülelt a csend – egyet ütött.
Fölkereshetnéd ifjúságod;
nyirkos cementfalak között
képzelhetsz egy kis szabadságot –
gondoltam. S hát amint fölállok,
a csillagok, a Göncölök
úgy fénylenek fönt, mint a rácsok
a hallgatag cella fölött…”

József Attila
Eszmélet (1934)

TABLE OF CONTENTS

1. INTRODUCTION AND OBJECTIVES

Natural ionizing radiation originates from various sources. These can affect the human body via different pathways, causing both external and internal exposure. For example at high altitude cosmic radiation, and its induced radionuclides cause elevated effective doses but at sea level the largest contribution is from terrestrial radionuclides such as radon and thoron.

Radon (^{222}Rn, Rn) and thoron (^{220}Rn, Tn) isotopes, from the ^{238}U and ^{232}Th decay chains respectively, are responsible for approximately the half of the total annual effective dose from natural sources to an average human (e.g. Eisenbud and Gesell 1997, UNSCEAR 2000). Elevated concentrations of radon and thoron are generally considered to increase the risk of lung cancer based on epidemiological data (Darby et al. 2005) and, given the acceptance of the linear non-threshold (LNT) model (ICRP 2005), even low doses have significant cumulative effect when considering the human population. In the past, exposure to thoron was often ignored due to its very short half-life which was believed to prevent its indoor accumulation. It is already known that thoron and its progenies can significantly contribute to the radiation dose in certain environments (UNSCEAR 2006). Thus, it is important to identify these environments. Before the start of this research project, not many indoor thoron data were available in Hungary, i.e. only those published by Hámori (2006) and Kávási et al. (2007). Therefore, the subject of this study was instead found based on international experiences.

Several studies (Németh et al. 2005, Sciocchetti et al. 1992, Shang et al. 2005, Yamada et al. 2005, Yonehara et al. 2005) show elevated radon and thoron activity concentrations in dwellings built of soil and mud. These dwellings are very similar to Hungarian adobe dwellings. In Europe, Germany has also targeted the very similar half-timbered houses (wood structure filled in with clayey material) for a current research project (HZM, http://www.helmholtz-muenchen.de). The porous and permeable structure of these similar building materials, the lack of any burning procedure in their preparation (Sas et al. 2012, Sas 2012) and probably the fact that they consist of mostly small sized grains is proven to lead to increased radon and thoron exhalation and indoor accumulation. In the case of radon in Hungarian adobe dwellings, this was already pointed out by Minda et al. (2009). For this reason, Hungarian adobe dwellings are chosen to be good candidates to find the possible environments with significant thoron presence.

Adobe, made from clay, sand (soil), water, and various organic materials, is a typical building material of cultural heritage which used to be frequently used in rural areas of

Hungary. The adobe dwellings still provide a cheap housing option for a high-number of people. Adobe dwellings are generally considered to have a low energy cost, a small environmental impact and a healthy, well ventilated, natural indoor environment. For this reason the tradition of building adobe houses is being revived. Therefore, the consideration of all possible health hazards, such as external radiation doses and both indoor radon and thoron activity concentrations becomes more important.

For another aspect, Tokonami (2010) pointed out the importance of indoor thoron measurements along radon for the correct inhalation dose estimation. Kávási et al. (2007) also stated that the possible interfering effect of thoron, in the already available radon indoor results, has to be also considered in Hungary. However, not only indoor activity concentration and inhalation dose estimation methodologies should be improved as was experienced during this study.

The main objective of this research was to evaluate the assumed elevated terrestrial radiation risk in Hungarian adobe dwellings via studying adobe building material samples and also via indoor measurements. The focus is on external radiation, radon, and as a new point, thoron indoor accumulation. The regional and local geological differences might significantly affect the terrestrial radioactivity levels in locally made adobe building materials and dwellings. Therefore, the spatial distribution of these terrestrial radioactivity levels and also possible affecting parameters, like grain size distributions and connected specific surface areas, needs to be studied as well as the seasonal variation of indoor radon and thoron activity concentrations. The effect of moisture content studied by numerous authors (e.g. Hosoda et al. 2007, Ingersall 1983, Megumi and Mamuro 1974, Stranden et al. 1984, Strong and Levins 1982) found to be interesting to consider indirectly in seasonal results. The results are aimed to help later studies to find high risk localities and periods. During this study, also some problems occurred in the reliability of the available radon and thoron emanation determination methods of building material samples. To provide solution for these became a specific aim of this study.

2. TERRESTRIAL RADIOACTIVITY

2.1. Effective doses from and sources of natural ionizing radiation

The worldwide average annual exposure to natural radiation sources remains 2.4 mSv y^{-1} (UNSCEAR 2000). Its sources and their contribution to the average annual effective dose of humans are presented on *Fig.1*. Basically, three types of natural ionizing radiation sources dominate. Among these, *cosmic radiation* contributes 15 % (cosmic including neutrons, *Fig.1.*), *cosmic radiation induced radionuclides* contribute 0.6 % (cosmogenic nuclides, *Fig.1.*) and *terrestrial radionuclides* altogether (^{40}K, ^{87}Rb, radon and ^{214}Pb, other from ^{238}U series, thoron and ^{208}Pb and other from ^{232}Th series on *Fig.1.*) contribute 84.4 % to the average human effective dose (Eisenbud and Gesell 1997).

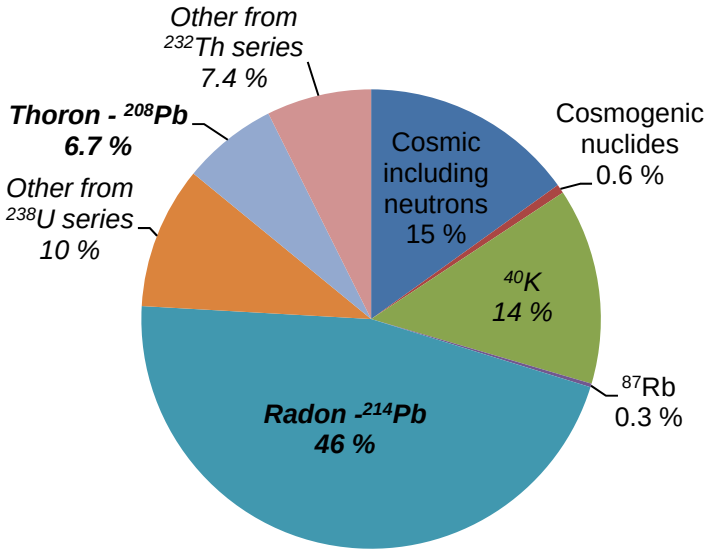

Fig.1.: Average contribution of natural sources to the human effective dose (data used from Eisenbud and Gesell 1997). Radon -^{214}Pb and Thoron - ^{208}Pb indicate radon, thoron and their short half-lived decay products.

Among these natural ionizing radiation sources, cosmic radiation contributes only to the external exposure of humans, whereas cosmic radiation induced radionuclides (for example ^{14}C) and terrestrial radionuclides (detailed below) contribute to both external and internal exposures. External exposure of these radionuclides is mostly due to their emitted γ-rays and internal exposure is due to their deposition in the human body and their emitted α- and also β- and γ-radiation.

Contributions from radon and thoron, and their respective progenies to the effective dose need to be considered separately. Radon and its decay products contribute 46 %, whereas thoron and its decay products only 6.7 % (*Fig.1.*) to the worldwide average value. These amount to about 1.1 mSv y^{-1} and 0.16 mSv y^{-1}, respectively, which is mostly due to internal, in this case inhalation exposure. Assuming that (1) these average effective doses of both radon and thoron are generated mostly due to inhalation and that (2) the inhalation dose from any other sources is ignored, it can be calculated that 87 % of the inhalation dose is due to radon and its progenies and 13 % is due to thoron and its progenies in an average environment (Eisenbud and Gesell 1997). Based on UNSCEAR (2000), the contribution of thoron to the inhalation dose is only 8 %. However, elevation of this average contribution can be expected in special environments, like adobe dwellings of this study.

2.2. Physics and geochemistry of terrestrial radionuclides

Among terrestrial radionuclides the ^{238}U and ^{232}Th decay series, including radon and thoron (*Fig.2.*) and ^{40}K contribute with the most significant proportions to the average annual effective dose of humans, both externally and internally. For this reason, also the NORM (Naturally Occurring Radioactive Material) and TENORM (Technically Enhanced Naturally Occurring Radioactive Material) acronyms generally refer to the amount of these radionuclides in any material, for example in building materials and all of the building material radiation hazard indices used in the literature are based on their activity concentrations.

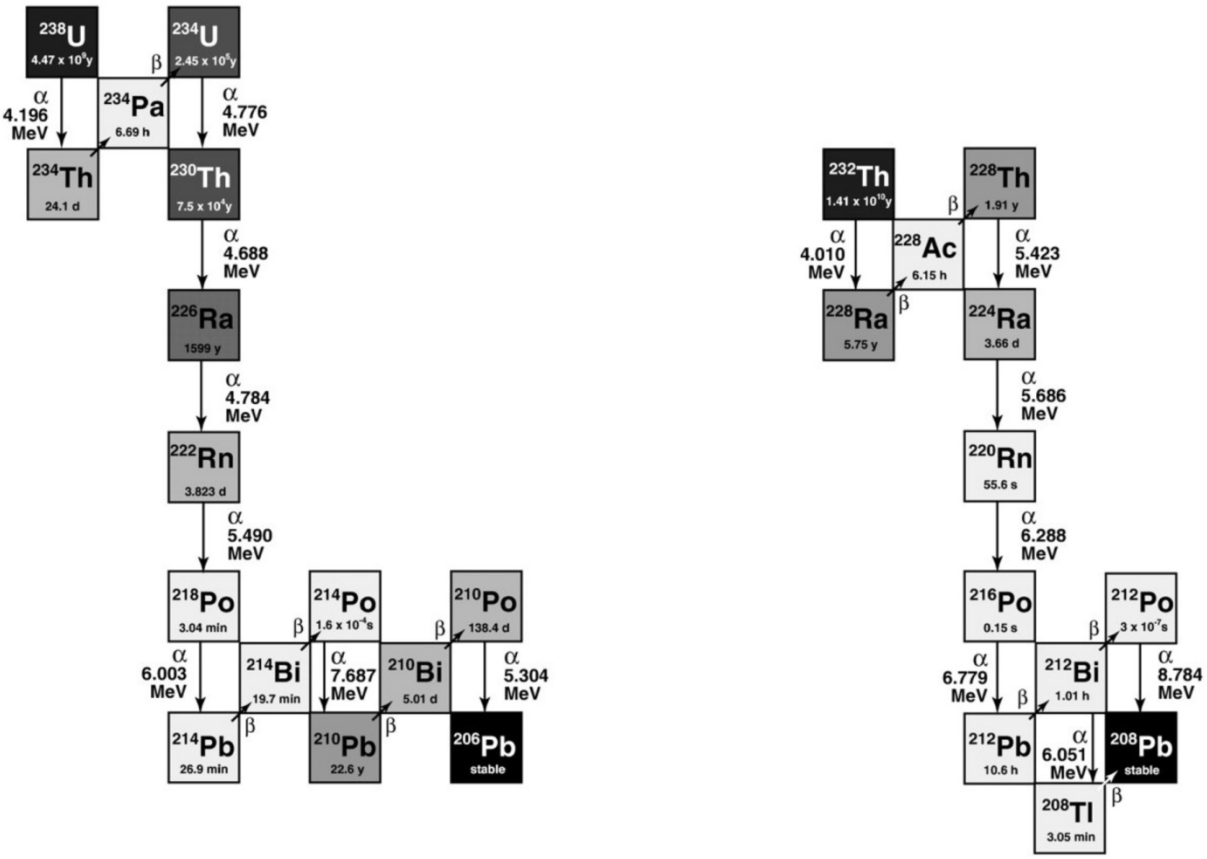

Fig.2.: The ^{238}U and ^{232}Th decay chains showing the half-life (given exact numbers and tone) and the decay type and energy of each isotope.

It is known that in both of the ^{238}U and ^{232}Th decay series, secular equilibrium can be present due to the long half-lives of parent nuclides and the much shorter half-lives of their progenies (*Fig.2.*). This equilibrium is usually considered to set after five times the half-lives of the progenies, and then the activity of the progenies becomes equal to that of the parent with 3 % accuracy. Deviations from secular equilibrium in these decay chains occur frequently due to the fact that radon and thoron can leave the solid materials due to their gaseous forms. In the ^{238}U decay series the different geochemical behavior of ^{226}Ra together with its significantly long half-life can also break the equal activities of nuclides. Other deviations are not probable.

Below the most important physical, nuclear (NuDat 2.6, http://www.nndc.bnl.gov/nudat2/) and geochemical (Takeno 2005) properties of the long half-lived parent nuclides, ^{238}U and ^{232}Th, and the secular equilibrium breaking nuclides, ^{226}Ra, radon and thoron are summarized together with the properties of ^{40}K.

2.2.1. ^{238}U parent nuclide

The ^{238}U has a half-life of 4.47 billion years and decays through α-radiation as $^{238}U \rightarrow {}^{234}Th + \alpha$. Its average activity concentration in Hungarian soils is 29 Bq kg^{-1} and concentration is 2.3 ppm (UNSCEAR 2000), it is the most abundant isotope of the element uranium with 99.3 % (NuDat 2.6).

Uranium element occurs in three oxidation states: U^{6+} in oxidative environment, U^{4+} in reductive environment and U^{5+} (Takeno 2005). Its solubility in water is the highest in the form of U^{6+}, therefore uranium is dissolved in water when the environment is oxidative as uranyl ion (UO_2^{2+}) or it forms complexes, for example, with CO_2^{3-}. As soon as the environment gets reductive, uranium precipitates in minerals like uraninite (UO_2) or coffinite (Takeno 2005). Dissolved uranium may be reabsorbed by an ion exchange mechanism on clay minerals. Uranium is an incompatible element, thus its abundance is higher in the Earth continental crust than in the mantle. Igneous silicate-rich rocks, like granite, rhyolite and pegmatite usually have elevated uranium content.

2.2.2. ^{232}Th parent nuclide

The ^{232}Th has a longer half-life than ^{238}U, 14.0 billion years. Its abundance in the environment is higher than that of ^{238}U, its average activity concentration is 28 Bq kg^{-1} in Hungarian soils (UNSCEAR 2000) which is equal to about 6.9 ppm. Its isotopic abundance is 100 %. It decays via emitting α-particle: $^{232}Th \rightarrow {}^{228}Ra + \alpha$ (NuDat 2.6).

The thorium – as an element – exists only in one oxidation state such as Th^{4+}, which is indissoluble in water. It occurs in oxide-, silicate- and phosphate-minerals, for example, thorianite (ThO_2), thorite [$(Th)SiO_4$] and cheralite [$(Ce,Ca,Th,U)(P,Si)O_4$] in the monazite group (**PV1., 2. and 4.**), respectively (Takeno 2005). Any thorium released into solution is rapidly sorbed by clay minerals and hydrolyzed to $Th(OH)_4$ which is intimately associated with the clay mineral fraction. Thorium, such as uranium, is an incompatible trace element, however it can enter some rock-forming minerals, therefore it is not as strongly concentrated in the pegmatite phases as uranium.

2.2.3. ^{40}K parent nuclide

The ^{40}K has a half-life of 1.25 billion years. Its 89 % decays through β^--radiation as $^{40}K \rightarrow {}^{40}Ca + e^- + \bar{\nu_e}$ and its 11 % through electron capture as $^{40}K + e^- \rightarrow {}^{40}Ar + \nu_e + \gamma$. Its average activity concentration in Hungarian soils is 370 Bq kg^{-1} and concentration is

11 970 ppm (UNSCEAR 2000). Its isotopic abundance is 0.0117 % (NuDat 2.6), however other natural potassium isotopes are not radioactive.

The element potassium occurs in the oxidation state of K^+ (Takeno 2005), it is a major element in the Earth crust. In soils the K^+ ions are fixed in 2:1 type clay minerals' interlayers such as in illite group.

2.2.4. ^{226}Ra

This radium isotope has a half-life of 1600 years and, such as ^{238}U and ^{232}Th, decays via emitting an α-particle: $^{226}Ra \rightarrow {}^{222}Rn + \alpha$ (NuDat 2.6). Its average activity concentration in Hungarian soils is 33 Bq kg^{-1} (UNSCEAR 2000).

The element radium exists in one oxidation state, Ra^{2+}, in the environment. It forms strong complexes in natural waters and can be present in $RaSO_4$ form at pH between about 2 and 12 and in $RaCO_3$ form at pH above about 12 (Takeno 2005). Radium ion is absorbed on clay minerals, and on oxides, carbonates, as well (IAEA 1986). As shown above (*Fig.2.*), the ^{226}Ra is the only isotope in both ^{238}U and ^{232}Th decay chains before radon and thoron, which potentially can lead to deviations in the secular equilibrium. It is due to the different geochemical properties of uranium and radium and its significantly long half-life which last property is not true for the ^{224}Ra isotope in the ^{232}Th decay chain.

2.2.5. Radon and thoron

The 222 mass number isotope of radon (^{222}Rn, Rn) in the ^{238}U decay chain has a half-life of 3.82 days but its 220 mass number isotope, called thoron (^{220}Rn, Tn) in the ^{232}Th decay chain has a much shorter half-life of 55.6 seconds (NuDat 2.6). Parent nuclide of both isotopes is a radium isotope, the ^{226}Ra for radon and the ^{224}Ra for thoron decaying via emitting α-particles. When radon and thoron are formed in the rock, soil or building material from radium, they are recoiled into the opposite direction as the α-particle goes. The recoil length of radon is typically 30-50 nm in solid materials, 95 nm in water and 64 000 nm in air (Tanner 1964, 1980, Porstendörfer 1994). These values for thoron are considered to be the same, although they should be slightly higher due to the higher α-energy in its formation (5.69 MeV vs. 4.78 MeV, *Fig.2.*). Radon element is a heavy inert gas which can recoil out from, migrate in and leave solid materials, get to their pore volume filled with air or water, and then reach the free air before it decays. It is soluble in water (e.g. groundwater, soil water, pore water etc.) in which its diffusion coefficient is reduced. Radon and thoron themselves also

decay through α-radiation: $^{222}Rn \rightarrow {}^{218}Po + \alpha$ and $^{220}Rn \rightarrow {}^{216}Po + \alpha$. Their decay products are polonium, lead, bismuth and thallium isotopes (*Fig.2.*) and they emit α-particles, electrons (β-decay) and consequently γ-radiation with the given energies on *Fig.2.*

2.3. Radon and thoron in the human environment

Among terrestrial radionuclides, radon and thoron cause the highest average effective doses (*Fig.1.*). In this chapter the processes leading to their interactions with the human body are summarized.

2.3.1. Radon and thoron emanation and exhalation of rock, soil and building material

Characterizing potentials of solid materials for emitting radon and thoron, two processes and measures are applied in the literature (e.g. Porstendörfer 1994). *Emanation* is the process of the radon and thoron nuclei recoiling into or diffusing (Porstendörfer 1994) to the pore volume of the rock, soil or building material. Whereas, *exhalation* is the process of the emanated radon and thoron leaving the pores and reaching the atmosphere or a closed air volume.

The radon and thoron emanation of any solid material depends on its parent nuclide (^{226}Ra and ^{224}Ra) activity concentration and the emanation fraction (also called as emanation power or factor). The emanation itself is usually given as the activity of radon or thoron leaving a unit mass of a sample (*E'*, Bq kg^{-1} s^{-1}) but also can be calculated for a unit sample volume named later as thoron generation rate (*G*, Bq m^{-3} s^{-1}). These two values can be transferred simply to each other by knowing the density (kg m^{-3}) of the material. However, in this work the emanation of adobe building material samples is given as the number of radon or thoron atoms leaving a unit mass of a sample (*E*, kg^{-1} s^{-1})[1]. This unit provides the possibility to better compare the results for the two isotopes[2]. The *emanation fraction* describes the proportion (%) of radon or thoron atoms in the pore volume and the total number of radon or thoron in the sample. The typical radon emanation fraction for rocks and soils ranges from 5 to 70 % (Nazaroff et al. 1988, **PV9.**). Some experimental studies show that this value ranges from 0.2

[1] $E[kg^{-1}s^{-1}] = \frac{E'[Bqkg^{-1}s^{-1}]}{\lambda\,[s^{-1}]}$, where λ is the decay constant of radon or thoron.

[2] When the activity is given (Bq kg^{-1} s^{-1}), any emanation measurement results show orders of magnitude higher values for thoron isotope than for radon due to their highly different half-lives, consequently decay constants.

to 30 % for building materials and in case of thoron, from 0.2 to 6 %. Building materials treated under relatively high temperatures are characterized by the lowest emanation fractions (Porstendörfer 1994 and references therein, Sas et al. 2012, Sas 2012).

The radon and thoron exhalation depends on the emanation, consequently the radium content and the emanation fraction, and the exhalation fraction. The exhalation is meaningful to give as the radon and thoron activity leaving the solid material through a unit surface (Bq m^{-2} s^{-1}), however, sometimes it is expressed like emanation, for a unit mass or volume of a sample. This causes inconsequences in the literature which should be solved. Mostly in this last case, the geometry of the sample strongly influences the exhaled and measured radon and thoron activity concentrations, which are used then to calculate the exhalation of the material. The *exhalation fraction* describes the proportion (%) of radon or thoron atoms leaving the material and the total number of emanated radon or thoron atoms in the pore volume. When samples are analyzed (not soil or surfaces of thick walls), and at least one of their widths is smaller than the diffusion length of radon or thoron in them, the exhalation fraction gets close to 100 %. Due to the difference between the half-lives of the two isotopes, this sample width, which the nuclides can diffuse through, is much higher for radon than for thoron.

There are more properties of a rock, soil or building material which influence its radon and thoron emanation and exhalation fractions. Two of them, the grain size distribution and the moisture content are highly relevant to this research and described below. In this work the grain size distribution is determined and it is considered directly, whereas the moisture content is considered indirectly.

2.3.1.1. The grain size distribution as emanation-exhalation affecting property

The grain size distribution significantly influences the value of the specific surface area on which the radon and thoron can be emanated trough from the grains. In soils the smallest sized minerals are usually the clay minerals originated from weathering processes of rocks. Small grains have a comparably higher specific surface area than large grains (e.g. Weiszburg and Tóth 2011). This is resulted in an expected positive correlation between the proportion of the small grain size fraction and the emanation fraction (partially in **PV1.**, **2., 5.** and **7.**) which is studied in this work. Beside this, a relationship with the value of specific surface area estimated from the grain size distribution can also be expected. These considerations above assume that uranium, thorium and radium are homogeneously distributed in the grains.

However, note that Greeman and Rose (1996) showed that about half the soil gas radon in their study results from radium in organic matter and related surface coatings on grains, with a relatively high emanation coefficient.

At the same time, the grain size distribution influences the permeability of materials and, therefore, its radon and thoron exhalation. Thoron exhalation is expected to be more significantly influenced than radon due to its much shorter half-life. However, both of the exhalation fractions are reduced with a decrease in permeability. This decreased value can be due to a heterogeneous grain size distribution (small grains fill the pore volume of large grains) or when swelling clay minerals are present.

As shown above, the uranium, thorium and radium are all can be also enriched in clay minerals in the small grain size fraction due to their geochemical properties. As a consequence, the parent nuclide contents of different materials can show correlation with the proportion of small grains in their grain size distributions. This might be influencing the emanation and exhalation via the total number of radon and thoron.

2.3.1.2. The moisture content as emanation-exhalation affecting environmental factor

The influence of moisture content on emanation and exhalation fractions and consequently emanation and exhalation was studied and described by many authors (e.g. Tanner 1980, Porstendörfer 1994 and references therein: e.g. Ingersall 1983, Megumi and Mamuro 1974, Stranden et al. 1984). This influence first originates from that the recoil length of radon and thoron is three orders of magnitude longer in air than in water (64 000 nm vs. 95 nm, Tanner 1980). Therefore, some water present around the source grains (hygroscopic water) is advantageous ("optimal") to keep the gases in the pores via avoiding them to recoil into a neighboring grain and not get emanated. Secondly, if the whole pore is filled with water, the emanated radon and thoron cannot leave the pores easily. In this case they dissolve in the water filling the pores and since their diffusion length is shorter in water than in air, the exhalation gets reduced.

Experimental studies pointed on a great decrease of the emanation for moisture contents below 5 % (e.g. Sas 2012, Strong and Levins 1982) or a sporadic increase in exhalations up to moisture content of 8 % and a decreasing tendency over this value (Hosoda et al. 2007). In the latter study the porosity was given to be 30 %. Therefore, the some %-es of moisture content refer to the presence of some thickness of hygroscopic water, whereas the rest of the pore

volume is filled with air. This must have been the case in the study of Hassan et al. (2011) for the “wet” samples, which all showed increased radon emanation fractions compared to “normal” and “dry” conditions.

2.3.2. Indoor accumulation of radon, thoron and their solid decay products

Radon is usually considered to accumulate indoor originated from the *rock* or *soil* below the buildings. This is the reason why radon risk mapping can be performed based on the properties of geological environments, like ^{238}U-^{226}Ra content (**PV3.** and references therein: Kemski et al. 2001, Kohli et al. 1997, Wattananikorn et al. 2008) or more precisely and frequently based on soil gas radon activity concentration (**SJ3.**), and permeability measurements (e.g. Szabó et al. 2013). In other cases, indoor radon activity concentration measurements are performed when the results can highly be influences by the structure of the studied buildings (e.g. Minda et al. 2009). Note that in this present study all adobe dwellings are one-storied buildings without basements, hence further evaluation of their structure can be avoided. Radon can also accumulate indoor originating from *building materials* which can be typical of different areas. In this case, its short half-lived isotope, thoron also should be taken into account. Thoron does not have enough time to migrate far before it decays. Therefore, while the radon gas is approximately homogeneously distributed in the indoor air, thoron activity concentration is high close to its source, some types of walls and drops drastically towards the center of the room. However, thoron decay products are evenly distributed (e.g. Urosevic et al. 2008).

The most important aspects of radon and thoron solid decay products are summarized based on Porstendörfer (1994). After their formation, these freshly generated radionuclides react very fast and become small particles, called clusters or "unattached" radionuclides. Then they attach to the existing aerosol particles in the atmosphere. In buildings, the deposition of the radionuclides on walls and furniture is an important parameter. Describing the amount of progenies in buildings three values are defined here. One of these is the *potential alpha energy concentration* (PAEC), which is the sum of alpha energies emitted during the decay of radon up to ^{210}Pb progeny or thoron up to ^{208}Pb progeny (*Fig.2.*). The *equilibrium-equivalent concentration* of a non-equilibrium mixture of short-lived progenies in air is the activity concentration of radon or thoron in radioactive equilibrium with their short-lived progenies, which has the same potential alpha energy concentration as the actual non-equilibrium

mixture. The *equilibrium factor* is the ratio of equilibrium-equivalent concentration to the actual activity concentration of radon or thoron. This factor characterizes the disequilibrium between the progeny mixture and their parent nuclide. Determinations of the equilibrium factor for radon indoors generally confirm a typical value of 0.4 (UNSCEAR 2000, 2006), i.e. most of the values are within 30 % deviation (Hopke et al. 1995, Ramachandran and Subba Ramu 1994). In case of thoron this value is expected to be one order of magnitude lower, and a 0.04 average equilibrium factor is determined by Harley et al. (2010) based on measurements in numerous dwellings. However, this average value is determined with a much high standard deviation than radon.

2.3.3. Characteristics of radon and thoron health effects and modifying circumstances

Since both radon and thoron and most of their progenies emit high-LET (linear energy transfer) α-radiation, the resulting ionization after their inhalation mostly happens in tissues of the lung. Some already almost twenty years old publications (e.g. Porstendörfer 1994, Steinhäusler 1996) already note that due to its comparably long, i.e. 10.6 hours half-life, the ^{212}Pb thoron descendant (*Fig.2.*) can even reach the blood flow and affect other parts of the body beside the lung. The differences between the effects of the radon and thoron isotopes are also shown in their dose conversion factors, which are 9 nSv $(\text{Bq h m}^{-3})^{-1}$ for radon and 40 nSv $(\text{Bq h m}^{-3})^{-1}$ for thoron (UNSCEAR 2000, 2006). This high value for thoron is intended to also include the dose to organs other than lung. In this study the above presented values are applied, however, it should be noted that these values might need general reevaluation (Zagyvai, personal communication, 2013) for the following reasons: (1) the dose from thoron decay products affecting the organs other than lung is missing from the lung itself and in the opinion of the author (2) the not negligible proportion of thoron gas itself in the inhalation dose (e.g. Steinhäusler 1996) needs to be recognized and evaluated for different thoron gas and thoron decay product mixtures (for a continuum from near wall to middle of room environments). The actually received effective doses also depend on the indoor present aerosol concentration and aerosol size distribution (e.g. Porstendörfer 1994, Steinhäusler 1996).

As seen above, all of the average effective doses received from natural sources (2.4 mSv y^{-1}) are much below the 100 mSv order of magnitude level, which above it is seen to have significant stochastic radiation risk increase (e.g. ICRP 2008). However, due to the

natural variation in the presence of radionuclides, in some environments significantly higher inhalation doses can be derived from radon and thoron than the average in the 1 mSv y^{-1} order of magnitude. Although, even if these elevated effective doses are received the radiation risk increases only with the acceptance of the still recommended LNT (linear non-threshold) model in the low dose range (ICRP 1990, 2005, 2007, 2008), which assigns the borders of this research.

At the same time for radon and, consequently, also for thoron the 100 mSv effective dose "threshold" for low doses is not obvious. Recent studies (Madas and Balásházy 2011) describe a much higher local tissue dose resulted from the determined effective dose of radon inhalation because of its inhomogeneous distribution in the lungs. This explains why it has an elevated health impact resulted in the observed elevation of lung cancer risk in epidemiological data (Darby et al. 2005, WHO 2009). Considering that the number and size distribution of aerosol particles are characterizing the behavior of radon and thoron decay products, smoking habits seem to increase the radiation risk originated from their inhalation (Bochicchio 2008).

2.4. Applied thresholds and reference levels

To limit the building materials' excess external γ doses due their NORM and TENORM contents, different building material hazard indices are used in the literature. These and their applied threshold values are detailed in Chapter 4.1.3.1. However, the reference dose is similar and it falls into the 1 mSv y^{-1} (EC 1999, Trevisi et al. 2012) order of magnitude.

Whereas IAEA (2003) also reports radiation protection against radon at workplaces, in this study solely the recommendation of the World Health Organization (WHO 2009) is considered for residential indoor radon activity concentrations. WHO proposes an annual indoor radon activity concentration reference level of 100 Bq m^{-3} and declares that the chosen national reference level of any country should not exceed 300 Bq m^{-3} (ICRP 2007). This corresponds to about 10 mSv y^{-1} order of magnitude effective dose (ICRP 2009). In Hungary the 300 Bq m^{-3} level seems to be more reasonable to compare the measured indoor radon activity concentration values also fitting into the ALARA (as low as reasonable achievable) principle and lower the expectations to a reasonable level. Such a recommendation, i.e. reference value does not exist for thoron gas itself. The author decided to compare the results to the same activity concentration of 300 Bq m^{-3}, however, its much lower connected dose is emphasized mostly due to the one order of magnitude lower equilibrium factor of thoron.

3. HUNGARIAN ADOBE DWELLINGS

3.1. The adobe building material

Most of the information collected in this sub-chapter is originated from local people who the author met during the numerous field campaigns.

The adobe used to be the cheapest building material at certain parts of the country mostly because it was always made locally. People building their own houses made the adobes, sometimes referred as adobe bricks, also themselves or with the help of local professionals, who were well appreciated in this era. Where the suitable raw materials were easily available, several adobe dwellings were built and still a significant portion exists. Most of these dwellings are from between 1930 and 1960, so about 50-80 years old. The tradition of building adobe houses is also being revived since they are considered to provide a healthy, "breathing" natural indoor environment.

Adobes are always made of inorganic and organic raw materials which are mixed with water to provide a muddy body, and then this mud is pressed into wooden frames to dry out in sunshine. No burning procedure is applied in this process. The inorganic raw material is basically a suitable, usually clayey, loamy soil either collected at the edge of the settlement or right next to the building itself. It is already very difficult or even impossible to find the original place of adobe preparation. The clay mineral content of the used soil has an important role to contain the natural radionuclides, the parent nuclides of radon and thoron and also to provide a significant specific surface area for the emanation process. The organic raw materials used are most frequently shelling, straw or chopped straw and they are added to build up the structure of adobe and make it more solid and elastic. After the evaporation of water from the adobe structure, the organic materials make the blocks to keep their shapes. If swelling clay minerals (e.g. smectites) are present, the inorganic component volume decreases leaving pores behind after losing the water content during the drying procedure. The remaining increased pore volume and permeability helps the exhalation process. For these reasons, beside the lack of burning treatment (Sas et al. 2012, Sas 2012), adobe building material is quite probable to exhale significant amounts of radon and thoron even if their NORM content is close to that of regular soils (29 Bq kg^{-1} for ^{238}U, 28 Bq kg^{-1} for ^{232}Th, 370 Bq kg^{-1} for ^{40}K, 33 Bq kg^{-1} for ^{226}Ra, UNSCEAR 2000).

Adobe dwellings are usually one-storied buildings without cellars. Their bases are even strengthen by stones or concrete only if located close to possible flooded areas, otherwise

rammed soil is found below the floor. The raw materials, the lack of burning process and the separation between the wall and the soil are all contributing to the sensitivity of adobe dwellings for precipitation.

3.2. The studied areas

3.2.1. Relevant information in the selection process

For the study of terrestrial radioactivity in adobe dwellings several distinct areas were decided to choose. In the selection process the following relevant factors were needed to take into account. Among these the most important one was the existence and the relatively high frequency of adobe buildings at the area. Another property taken into account was the geology of the well-known typical areas with many adobe dwellings. Different geological settings were considered to be advantageous in the general representativeness of the study to be able to make a statement about maximum health impact of living in Hungarian adobe dwellings. In the selection process, the level of the already published RAD Labor indoor radon data (Hámori and Tóth 2004, Minda et al. 2009, Tóth 1999) played also an important role. Due to a correlation between the amount of ^{226}Ra and ^{232}Th and also between radon and thoron measures indicated in many studies, the elevated radon level selection criterion seemed to be ensuring to find the most significant localities of elevated thoron presence. Note that the planned field work highly involved the contribution of local people, hence the selection process made a preference to sites where the author or her supervisors, colleagues had relatives or friends.

3.2.2. The locations of sampling and in-situ measurements

Based on the aspects detailed above, three distinct areas were selected for collecting *adobe samples*. These areas of study are (1) the central-north part of *Békés County* (SE-Hungary), which is the largest size area among the three and located at the geographical unit of the Grate Hungarian Plain, this is the most typical and hence representative area of average Hungarian adobe dwellings, (2) the *E-Mecsek Mts.* (S-Hungary) which is well-known for its granite bedrock and the connected elevated indoor radon activity concentrations at some settlements (RAD Labor), and (3) the *Sajó and Hernád Rivers Valleys* (*S-H Rivers Valleys*, NE-Hungary) where also high indoor radon levels were detected (RAD Labor) (*Fig.3.*). Six-seven settlements at each area, 19 settlements in total were selected to find help from local people in the collection of building material samples. These settlements are

Gyomaendrőd, Gyula, Kondoros, Sarkad, Sarkadkeresztúr, Újiráz (officially not belonging to Békés County), Vésztő at Békés County; Bátaapáti, Erdősmecske, Fazekasboda, Feked, Mórágy, Véménd at E-Mecsek Mts.; and Alsódobsza, Hernádnémeti, Sajóhidvég, Sajókeresztúr, Sóstófalva, Újcsanálos at Sajó and Hernád Rivers Valleys (*Fig.3.*). The number of areas of study for *in-situ measurement* campaigns was more limited by different reasons (e.g. budget, time and the local help). Therefore, this part of the research was performed only at one of the three areas, which was chosen to be *Békés County*. The campaigns focused on the same settlements (*Fig.3.*, Békés County) as the building material sampling, however in very few cases on the same dwellings due to the low number of volunteers.

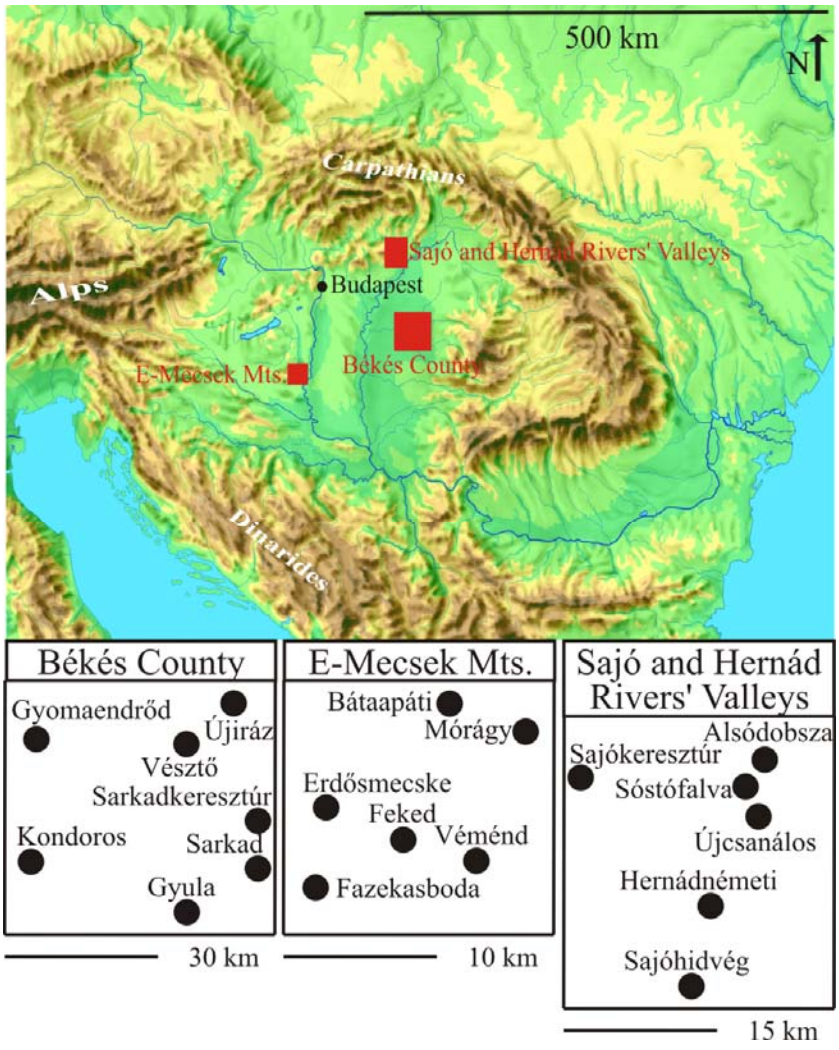

Fig.3.: The location of the three studied areas, Békés County, E-Mecsek Mts. and Sajó and Hernád Rivers Valleys in the Pannonian Basin and the approximate locations of the 19 selected settlements.

Influencing the indoor radon and thoron activity concentrations and their variations, the climatic conditions of the studied areas are summarized below (OMSZ, http://www.met.hu/eghajlat/magyarorszag_eghajlata/). The whole area of Hungary is characterized by a European continental climate with warm summers (20 ºC), cold winters (0 ºC) and mild springs and autumns (10 ºC). However, small differences among the studied areas are observed. The annual average temperature is 10-11 ºC at the Great Hungarian Plain (Békés County), which is slightly lower at the E-Mecsek Mts. and the Sajó and Hernád Rivers Valleys (9-10 ºC). The precipitation falls mostly during the summer months (especially June) and the least in the winter season (especially February). The annual average precipitation is 500-550 mm at the studied areas of Békés County and Sajó and Hernád Rivers Valleys; and about 100 ml more at E-Mecsek Mts.

3.2.3. Geology of the studied areas

Since the inorganic raw material of adobe is always originated from the edges of the settlements or right next to the buildings, the type of local geology can be expected to play an important role in the terrestrial radioactivity levels in adobe building material and dwellings. Therefore, in this sub-chapter, the most probable geological sources of adobe building materials are summarized at each studied areas and settlement, based on the 1:100 000 geological map of Gyalog (2005) and the online geological map on the home site of MFGI (http://loczy.mfgi.hu/fdt100/).

3.2.3.1. Békés County

The major raw material of local adobe at this area is the prevailing fluvial sediments of Körös and Berettyó rivers, tributaries of Tisza River. All sediments located at the studied settlements are Quaternary formations originated most probably from the Carpathians (*Fig.4.*, where the missing right-bottom part today does not belong to the area of Hungary.).

Due to the comparably simple geology of Békés County and the good enough information from local people, each selected settlement can be characterized by one specific geological formation. Therefore, based on the type of the most probable geological source of adobe (Gyalog 2005), the settlements are divided into three groups:

- *clay*: Gyomaendrőd, Vésztő, Kondoros,
- *loess*: Gyula, Sarkad, Sarkadkeresztúr, and
- *turf*: Újiráz.

Based on the geological age, the following two groups can be distinguished:

- *Pleistocene*: Gyula, Kondoros, Sarkad, Sarkadkeresztúr, and
- *Holocene*: Gyomaendrőd, Újiráz, Vésztő.

All of these groups are used later in the evaluation process of in-situ measurement results. However, note that the adobe making process might have inorganic raw material preference, hence more homogeneous than the geology predicts.

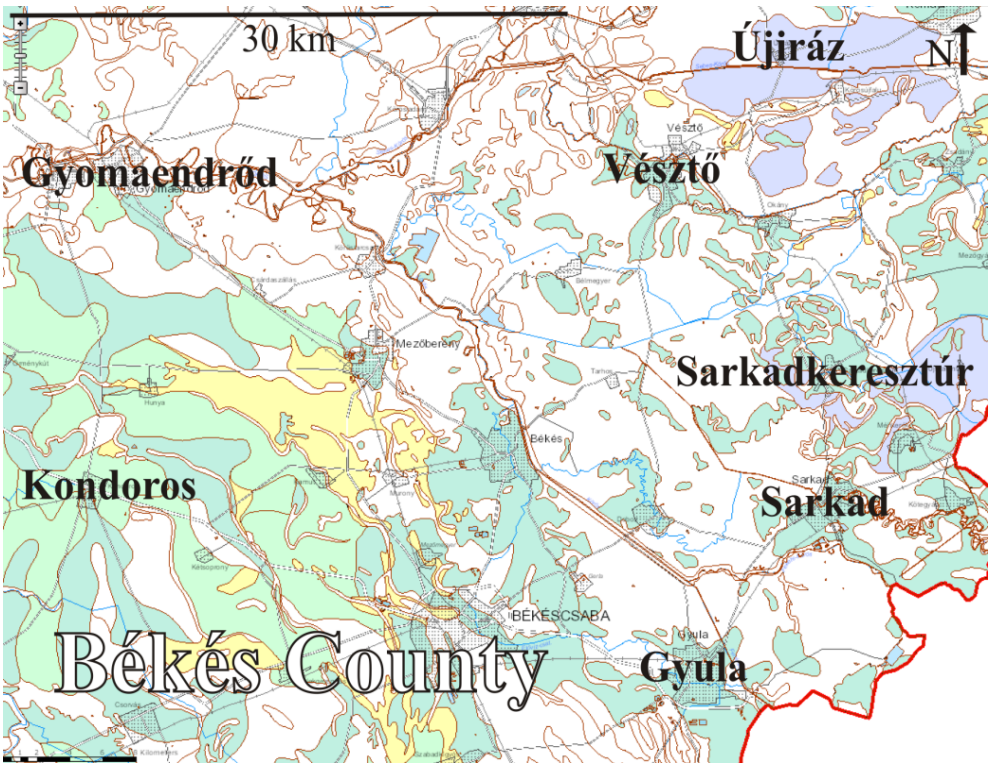

Fig.4.: The location of the studied settlements at Békés County, SE-Hungary on the geological map of the area (MFGI, http://loczy.mfgi.hu/fdt100/). The relevant colors on the map are the white, light green, dark green, and purple representing Holocene clay, Pleistocene clay, Pleistocene loess, and Holocene turf formations, respectively.

3.2.3.2. E-Mecsek Mts.

This studied area is known about its *Paleozoic granite* bedrock (*Fig.5.*), which type of rock tends to have elevated terrestrial radionuclide content. However, here the major raw material of local adobe is probably the characteristic *Pleistocene loess*, which is followed in abundance by *Pleistocene-Holocene aleurite* and then *Holocene alluvial sediment* formations.

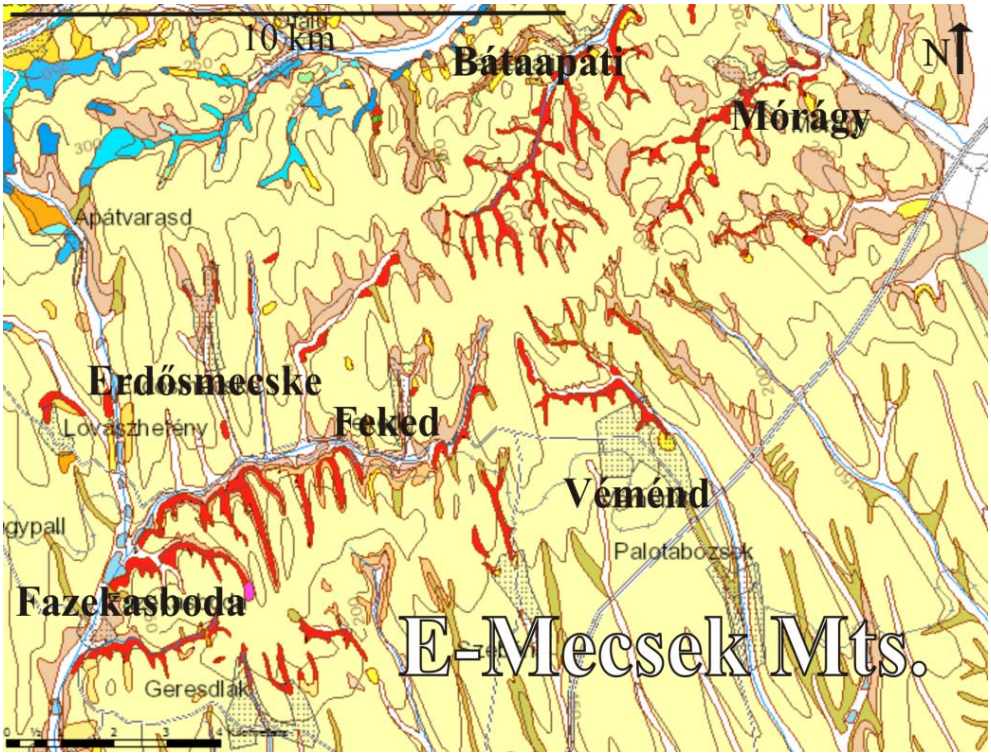

Fig.5.: The location of the studied settlements at E-Mecsek Mts., S-Hungary on the geological map of the area (MFGI, http://loczy.mfgi.hu/fdt100/). The relevant colors on the map are the red, mauve, sand (yellow), and white representing Paleozoic granite, Pleistocene-Holocene aleurite, Pleistocene loess, and Holocene alluvial sediment formations, respectively.

3.2.3.3. Sajó and Hernád Rivers Valleys

The area of Sajó and Hernád Rivers Valleys is the most characterized by the fluvial sediments of Sajó and Hernád rivers, tributaries of Tisza river. Therefore, the major raw material of local adobe is *Holocene* and *Pleistocene-Holocene fluvial sediments* like clay mixed with aleurite or sand mixed with aleurite, or it can either be *Pleistocene loess* and *Pleistocene deluvial sediment*, which are also characteristic of the environment of studied settlements (*Fig.6.*).

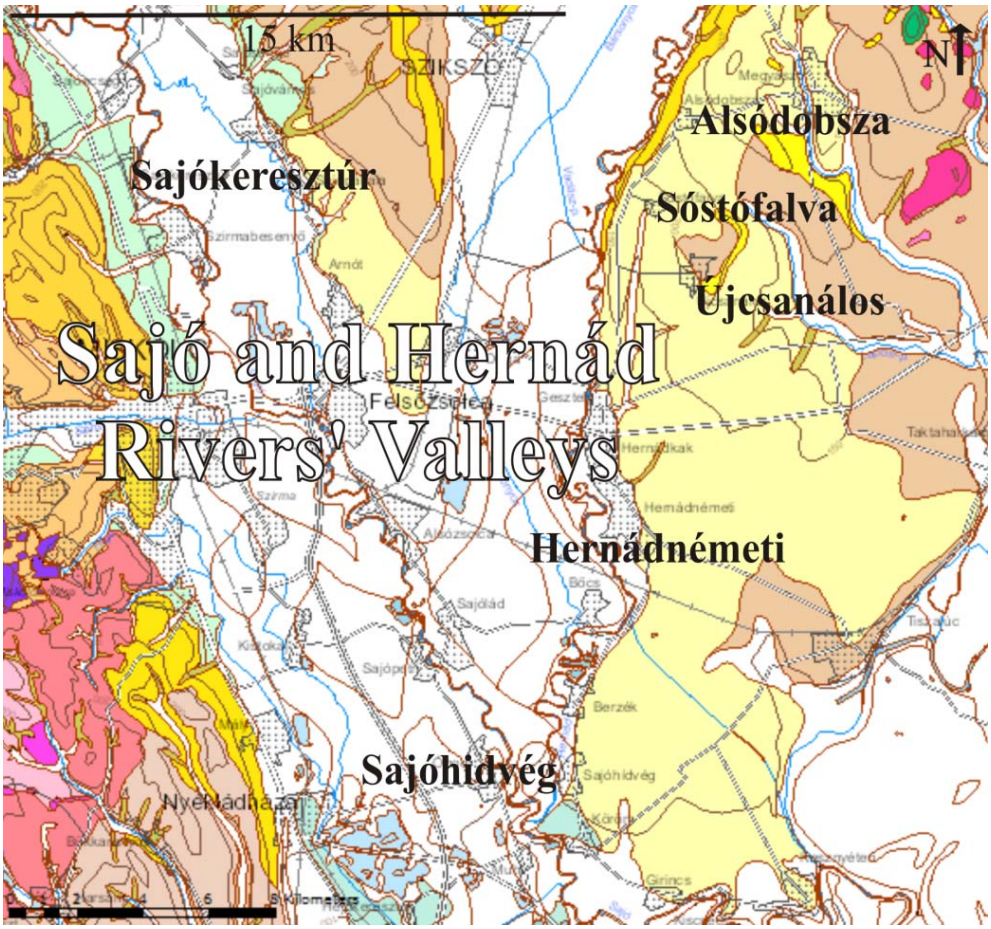

Fig.6.: The location of the studied settlements at Sajó and Hernád Rivers Valleys, NE-Hungary on the geological map of the area (MFGI, http://loczy.mfgi.hu/fdt100/). The relevant colors on the map are the white, sand, mauve and turquoise representing Holocene fluvial sediments like clay mixed with aleurite or sand mixed with aleurite, Pleistocene loess, Pleistocene deluvial sediment and Pleistocene-Holocene fluvial sediment formations, respectively.

4. MEASUREMENT AND STATISTICAL METHODS

4.1. Methods of laboratory measurements on samples

4.1.1. Sampling strategy

Adobe building material blocks and pieces were collected at all the 19 selected settlements of all three studied areas of Békés County, E-Mecsek Mts. and Sajó and Hernád Rivers Valleys (*Fig.3.*). Altogether *46 adobe samples* were collected and studied; among these *18 from Békés County* (three-three from Gyomaendrőd, Gyula, Sarkad, Újiráz and Vésztő; two from Kondoros; one from Sarkadkeresztúr), *18 from E-Mecsek Mts.* (three-three from all settlements of Bátaapáti, Erdősmecske, Fazekasboda, Feked, Mórágy and Véménd) and *10 from Sajó and Hernád Rivers Valleys* (three-three from Alsódobsza and Sajóhidvég; one-one from Hernádnémeti, Sajókeresztúr, Sóstófalva and Újcsanálos).

The sampling campaigns were carried out in five turns in 2009 and 2010 years. Only very few samples were taken after these campaigns. At each settlement always three adobe samples were aimed to collect, however, this was not always possible. The help of local mayors, people from mayor offices or widely known local people and also volunteering house owners were needed to find adobe building material samples to take. The most effective way of gaining samples was to try to find adobe dwellings under renovation or where a part of the building itself or any of its side buildings had collapsed and ask for a block from the owners if they were available[3]. The samples had usually the sizes of the blocks being in the buildings (widths in the 10 cm, mass in the 1 kg order of magnitude). All collected adobes were kept on lab air before any laboratory analysis to reduce their moisture content to the same natural level best representing the real conditions in dwellings.

Representativeness

The number (one - three) and quality of collected samples from each settlement are considered to represent the adobe building material of that given settlement. The samples at a studied area (10 - 18 pieces) are assumed to represent the adobe building material of that given studied area. Some samples were collected from collapsed dwellings or side buildings; these are considered originating from the same soil and made on the same way as other

[3]It represents well, how difficult any building material sampling is that on a sampling trip, the author was almost arrested by the police thanking to a belligerent house owner. At the end, the policemen provided one of the adobe blocks.

adobes of the settlement. Keeping the natural moisture content of the samples (no oven drying) ensures that they behave as in their original environment in the dwelling.

4.1.2. Radon and thoron emanation determination by closed chamber technique

The applied closed chamber technique provides appropriate radon and thoron emanation data of the analyzed samples after some methodological considerations as seen below. However, at the end of the analysis procedure, the gained values are connected and considered to refer to the radon and thoron exhalation potential of the building material.

4.1.2.1. The general description of the experimental setup

The determination of emanation values was carried out at Lithosphere Fluid Research Lab, Eötvös University. The suitable experimental setup (*Fig.7.*) consists of a cylindrical aluminum sample holder with a height of H = 9.5 cm and a cross-sectional area of A = 38.5 cm^2, plastic tubing, a gas-drying unit filled with desiccant ($CaSO_4$ with 3 % $CoCl_2$, as indicator), an aerosol filter and a RAD7 radon-thoron detector with a calibrated induced air flow rate of q = 11 cm^3 s^{-1} (*Fig.7.*) (Durridge Co. 2013). All connections were insulated by parafilm (product of the Pechiney Plastic Packaging Company). $V_{standard}$ (*Fig.7.*) represents a volume equal to that of a "standard RAD7 inlet filter, a 3-foot long, 3/16 inch inner diameter vinyl hose, and a small (6 inch) drying tube" (Durridge Co. 2013) and V_{det} (*Fig.7.*) is the 750 cm^3 detector volume of RAD7 (Durridge Co. 2013, **SJ4.**). The values of h, d and V_{net} (*Fig.7.*) also play important roles in the followings, h is the sample thickness in case of cylindrical samples, d is the sample width in case of cubical samples and V_{net} is the rest of the volume of the sample container above the sample, which is determined as $V_{net} = A(H - h)$ or $V_{net} = AH - d^3$.

The measurement device RAD7 (*Fig.7.*) determines radon and thoron activity concentrations by measuring the α-counts of their progenies (^{218}Po, ^{216}Po, ^{214}Po, ^{212}Po and ^{212}Bi), which are formed in the detector cell. However, the vendor of RAD7 needs to provide a correction with the instrument to determine the correct ^{218}Po counts and consequently the correct radon activity concentration as this radon progeny overlaps with the thoron progeny ^{212}Bi in the α-spectra (100% 6.115 MeV and 36% 6.207 MeV, respectively, NuDat 2.6). However, this built in correction in some cases was proven not to be sufficient enough and a further correction was needed (**PV1. and 2.**). In this present study of adobe building material

samples, this further correction provided by the author (**PV1. and 2.**) turned out to be not necessary to apply, hence not described in details.

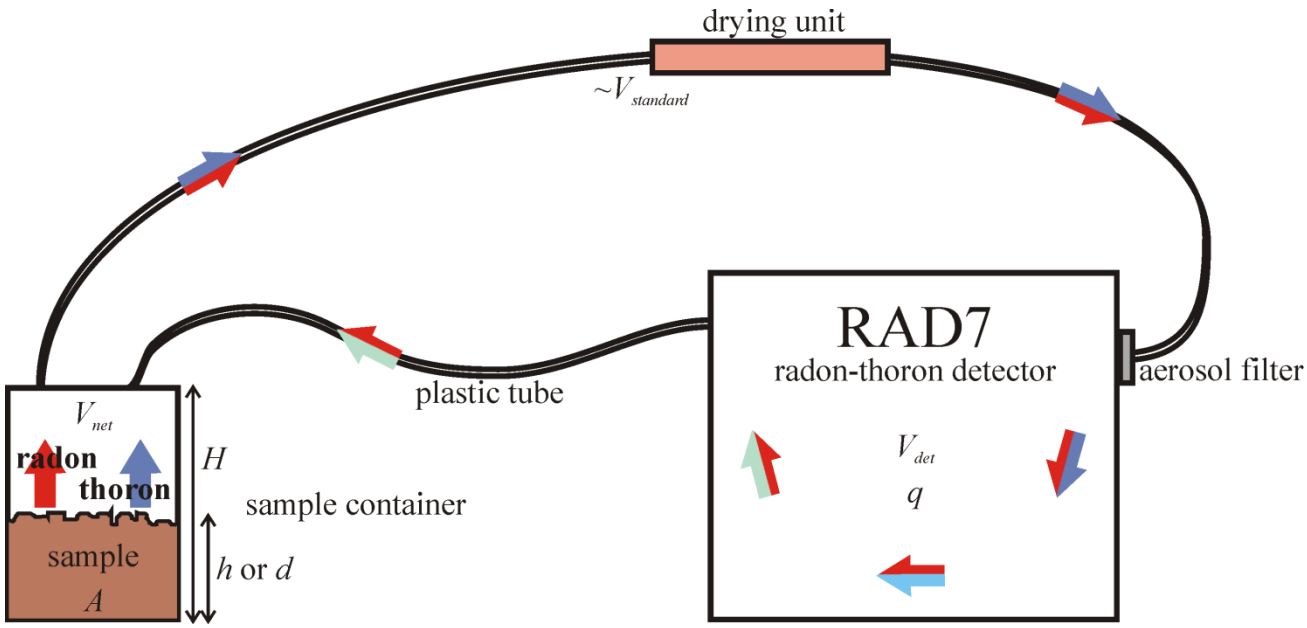

Fig.7.: Schematic representation of the experimental setup. The red/blue arrows mark the path of radon and thoron. Find further explanation in the text above and ***SJ4.***

4.1.2.2. Behavior of radon and thoron in the experimental setup – explaining specific aims of the study

After closing an air volume above the sample, the activity of radon and thoron leaving the sample is accumulating as *Eq.1.* (Stranden, 1988) describes.

$$T(t) = \frac{R(1-e^{-\lambda t})}{\lambda} \quad (Eq.1.)$$

where *T(t)* is the increasing total radon or thoron activity in the air volume available above the sample (Bq), *R* represents the rate of radon or thoron activity leaving the sample within a unit time (Bq s^{-1}), λ is the decay constant of radon or thoron (s^{-1}) and *t* is the accumulation time, i.e. the time elapsed since the closure of the sample (s). The described activities increase following the exponential growth and attain near constant values when $t >>$ the half-life of radon or thoron (e.g., $t \geq$ five times the half-lives) (e.g., Krishnaswami and Cochran, 2008). Then the exponential part of *Eq.1.* gets negligible. Therefore, it is stated that it takes about three weeks (19 days) until the equilibrium activity (and consequently the equilibrium activity

concentration) sets for radon in ideal circumstances and takes about five minutes until it sets for thoron with 3 % accuracy.

For the determination of radon and thoron emanation is the best to measure the equilibrium activity concentrations. However, some modifying processes make their determination complicated.

4.1.2.2.1. Modifying processes for radon

In case of radon, the emanated and exhaled amounts are closely equal in the given experimental setup[4] due to its long enough, 3.82 days half-life. Hence, the accumulated equilibrium activity concentration above the sample directly refers to its radon emanation without the need to consider the sample geometry. However, for the same reason, a significant portion of radon may leak from the measurement setup via the not perfectly sealed connections and the sample container itself. This leakage reduces the total radon activity just as its decay and hence modifies *Eq.1.* to *Eq.2.* for radon isotope.

$$T(t) = \frac{R(1-e^{-(\lambda+\alpha)t})}{\lambda+\alpha} \qquad (Eq.2.)$$

where α is the measure of radon leakage giving the proportion of radon atoms leaving the experimental setup within a unit time (s^{-1}, or later given in h^{-1} or % h^{-1} units due to easier handling). Leakage causes deviations in the normal run of radon accumulation on a way that it seems to reduce its half-life ($\lambda+\alpha$, *Eq.2.*). This is resulted in a reduced accumulation time required ($t \geq$ five times the "reduced" half-live) until the set of a reduced equilibrium activity (or equilibrium activity concentration).

The author notes that a further modifying process exists for radon, the so-called back diffusion (Tuccimei et al. 2006). However, its role is negligible if the pore volume of the sample is below 10% of the total volume of the experimental setup (V_{net} + $V_{standard}$ + V_{det}) (Petropoulos et al. 2001). Therefore, it is concluded that the back diffusion effect is not needed to consider with the given experimental setup (*Fig.7.*) and the studied sample volumes.

An appropriate radon emanation measurement method which takes into account the radon leakage (Chapter 4.1.2.3.1.) is already available. However, it is quite time consuming. One of

[4]Maximum 5% decrease occurs in the measurable radon activity concentration (exhaled radon) compared to that of in the pore volume of the sample (emanated radon). This negligible value is calculated based on the thoron model calculations detailed in **SJ4.** and Chapter 5.2.1. modified for radon isotope.

the specific aims of this work is to *test an already existing, less time consuming method* (Chapter 4.1.2.3.2.) for further consideration to use, see Chapter 5.1.

4.1.2.2.2. Modifying processes for thoron

Unlike radon, thoron cannot escape from the measurement system due to its short half-life (55.6 s). However, there are other difficulties not possible to avoid from:

(1) In case of this isotope, a significant proportion decays before leaving the pore volume of the sample. This means that the emanated and exhaled amounts are not equal from samples with sizes larger than a limit determined by the diffusion length of thoron. Therefore, the equilibrium thoron activity concentration in the air above the sample is not a linear function of the sample thickness (*h*, *Fig.7.*) or sample width (*d*, *Fig.7.*), hence not directly refers to the thoron emanation of the sample.

(2) Another significant amount of thoron decays along its path in the experimental setup (represented by the lightning tone of blue in the arrows on *Fig.7.*). This decay is already considered in the RAD7 factory calibration for $V_{standard} + V_{det}$ (*Fig.7.*, Durridge Co. 2013). Its consequence is that the RAD7 displays the thoron activity concentration assumed to have at its inlet, which is about the double of the concentration in the detector chamber (Durridge Co. 2013) calculated based on the calibrated induced air flow rate of $q = 11$ cm^3 s^{-1}. Despite of this calibration, the resulted equilibrium thoron activity concentration attenuation in the volume of V_{net} in the sample container (*Fig.7.*) still has to be taken into account when calculating thoron emanation.

There was not an appropriate thoron emanation measurement/determination method available in the literature for the given experimental setup (*Fig.7.*), which considers both (1) and (2) processes. A *new data analysis method* was required with the regular measurement strategy (Chapter 4.1.2.3.2.). *Making this available* got to be the other specific aim of this work, see Chapter 5.2.

4.1.2.3. Basic types of measurement strategies

Below two measurement strategies and analysis methods for radon emanation determination are described. Both of them aim to measure the equilibrium activity concentration above the samples, which is then used for the calculation of radon emanation results. In Chapter 5.1. their results are compared. The measurement strategy applicable for thoron emanation determination is also signed out which can be used with the new data analysis method detailed in Chapter 5.2.

For all of the routine measurements, the adobe building material samples were cut to about 200 g cubic bodies with widths of about 5 cm.

4.1.2.3.1. Growth curve method for radon emanation determination

The growth curve (or also named as ingrowth curve) method is frequently found in the literature (e.g. Jonassen 1983, Petropoulos et al. 2001, Sakoda et al. 2008, Stranden 1988, Tuccimei et al. 2006) and it is based on measuring the accumulation of radon activity concentration in the experimental setup from the background until the maximum value. For this, the measurement circle (*Fig.7.*) is closed right after the sample is placed into the sample holder and the RAD7 is started. In this study, 30 minutes measurement cycles (integration times) were applied for about 10 days of measurement durations[5].

For the analysis of raw data, *Eq.3*. is described and used.

$$C(t) = \left(C_{max} - C_{bg}\right)(1 - e^{-(\lambda+\alpha)t}) + C_{bg} \qquad (Eq.3.)$$

where *C(t)* is the increasing radon activity concentration above the sample in the air volume of the experimental setup (Bq m^{-3}), C_{max} is the maximum of radon activity concentration reached during the measurement (Bq m^{-3}), C_{bg} is the radon activity concentration of the background, i.e. the starting point of the growth curve (Bq m^{-3}), which is usually close to 0 (zero). Note that the unit of λ and t must be consequent.

Fitting *Eq.3.* for the raw measurement data was performed by Microcal Origin software and it gives the values of the two missing but needed parameters, C_{max} and α (its unit is the same as chosen for λ). These parameters are used in the radon emanation calculations described by *Eq.4*. All of the other needed parameters are known or can be determined easily.

$$E = \frac{1}{M}\frac{\lambda+\alpha}{\lambda}C_{max}(V_{net} + V_{standard} + V_{det}) \qquad (Eq.4.)$$

where E is the radon (or later also thoron) emanation (kg^{-1} s^{-1}) and M is the sample mass placed into the sample container (kg)[6].

[5]As described above any radon leakage from the experimental setup reduces the accumulation time until the set of a reduced equilibrium activity concentration. Therefore, 19 days (five times the radon half-life) for the measurement duration would be unnecessarily long.

[6]$E = \frac{R}{M\lambda}$

Advantages and disadvantages

This method does not require preliminary closing of the sample into the sample container and appropriately regards the possibility of radon leakage from the experimental setup. Therefore, any randomly occurring, uncontrolled but systematic error is avoided in the calculated emanation results. However, the measurement duration by RAD7 is in the 10 days of order of magnitude.

4.1.2.3.2. Equilibrium method for radon emanation estimation

The equilibrium method was taken into use because it saves time to make the RAD7 device available for a higher number of experiments and studies.

In this method, as the first step, the samples studied are closed into separate sample holders for at least 19 days. When the accumulation time is over the sample holders, one by one, are connected to the RAD7 detector (*Fig.7.*) theoretically for the determination of the radon equilibrium activity concentration. However, the lack of any radon leakage should be assumed because it cannot be controlled by calculations. In this study 15 minutes measurement cycles for four hours measurement durations (significantly less than 10 days) were applied.

The analysis of raw data is using the following information. The sum of the equilibrium activity in V_{net} and the background activity in $V_{standard}$ and V_{det} is equal to the activity of the mixed volume of the experimental setup (V_{net}, $V_{standard}$ and V_{det} together) which is measured. Adjusting this equality, the radon emanation can be calculated according to the *Eq.5.*

$$E = \frac{1}{M}(C_{meas}V_{net} + (C_{meas} - C_{bg})(V_{standard} + V_{det})) \quad (Eq.5.)$$

where C_{meas} is the average of measured radon (or later also thoron) activity concentrations by RAD7 (Bq m^{-3}).

Advantages and disadvantages

The most important advantage of this method is that the measurement time by RAD7 is enough to be in the maximum some hours of order of magnitude. This fact highly reduces the total measurement time for large number of samples, even if it requires the 19 days preliminary closing of the samples into sample containers. However, using the equilibrium method does not give the possibility to take into account any radon loss due to leakage during the actual measurement. Therefore, it is possible that randomly occurring, uncontrolled but

systematic error is present in its determined radon emanation values. For testing this method, see Chapter 5.1.

In case of thoron isotope, gaining correct equilibrium activity concentration data above a sample is simpler since it is set after about five minutes of closure and even no significant thoron leakage occurs within this time. Equilibrium thoron activity concentration data can be gained from both types of measurement strategies applied for radon. However, a new and more complicated data analysis method is required to apply, see Chapter 5.2.

4.1.3. ^{226}Ra, ^{232}Th and ^{40}K activity concentration determination by γ-ray spectrometry

Activity concentrations of ^{226}Ra, ^{232}Th and ^{40}K in the adobe building material samples were determined for the aims of the calculation of different building material hazard indices, estimate effective doses and for gaining radon and thoron emanation fractions.

The measurements were carried out by γ-ray spectrometry using GC1520-7500SL HPGe detector[7] at the Department of Atomic Physics, Eötvös University. All of the cubic samples from emanation measurements were powdered[8] filled back to the containers and their γ-rays were measured for a minimum of 16 hours. The detection efficiency for γ-photons of characteristic energies was determined by the measurement system provided Monte Carlo simulation, in which a theoretical elemental composition of montmorillonite (clay mineral) was assumed. It ranges from about 0.5 % to 8 % depending on photon-energy, geometry and density of the sample. Absolute transition probabilities were taken from the NuDat 2.6.

The ^{226}Ra analysis was performed based on its 186.1 keV peak, taking into account that it overlaps with the 185.7 keV peak of ^{235}U. Both the natural isotopic abundance between ^{238}U (99.3 %) and ^{235}U (0.7 %) and secular equilibrium between ^{238}U and ^{226}Ra were assumed leading to a 58.3 − 41.7 % ratio (Ebaid et al. 2005) in the count number of the appearing peak of ^{226}Ra and ^{235}U, respectively. The latter, more possibly disturbed assumption of secular equilibrium between ^{238}U and ^{226}Ra (Chapter 2.2.4.) can be supported by data published about surface soils. For example Al-Hamarneh and Awadallah (2009) report the wide presence of ^{238}U – ^{226}Ra secular equilibrium in 220 surface soil samples. Additionally, in a parallel study

[7]Detector shielding of 10 cm thickness was applied to reduce the background radiation. The detector was cooled to liquid nitrogen temperatures and coupled to a PC-based 4K multichannel analyzer. The energy resolution of the detector is 2.0 keV at 1332.5 keV (^{60}Co peak) and its relative efficiency is 15%.

[8]To have a standard cylindrical geometry varying only in height.

of the author, its generally acceptable existence was determined in coal slag building material samples.

These assumptions had to be applied in the calculations, first of all, because the use of peaks of radon decay products for ^{226}Ra activity concentration determination was considered disadvantageous in the given experimental setup. The reason is that radon exhaling from the sample fills the free volume of the sample container and progenies attach to the inner wall also where no sample is present in the upper parts of the volume. Hence, detection efficiency of their gamma-photons is undeterminable. This effect can be avoided only if the sample fills the whole volume of the container which was difficult to perform for technical reasons. Moreover, despite sealing, some radon leakage can also occur in containers without special design (**SJ5.**), which is further reducing the count number of radon decay product peaks. Second of all, any possible 186.1 keV peak correction (Yücel et al. 2009), for example with the use of 63.3 or 92.6 keV peaks of ^{234}Th (Dowdall et al. 2004, Kaste et al. 2006, Saidou et al. 2008) or with the 1001 keV peak of ^{234m}Pa (Yücel et al. 1998, Papachristodoulou et al. 2003) could not be applied neither for different technical reasons.

The ^{232}Th analysis was done by an interference free ^{228}Ac peak at 911 keV and the ^{40}K activity concentration was determined by using its peak at 1461 keV.

Possible errors and uncertainties

In γ-ray spectrometry measurement results the statistical uncertainty is mostly originated from the γ-peak area determination and the efficiency simulation uncertainties. Systematic error might be able to occur due to deviations in secular equilibrium state of ^{238}U and ^{226}Ra.

4.1.3.1. Hazard indices calculations

To qualify safety of building materials and limit external dose received by residents, many different building material hazard indices are applied in the literature based on activity concentrations of ^{226}Ra, ^{232}Th and ^{40}K. They are all widely used in recent publications (e.g. Al-Sulaiti et al. 2011, Damla et al. 2011, Moura et al. 2011, **SJ2.**). In case of adobe building materials these indices are not expected to exceed the threshold values, however calculated for the aim of gaining a proof, scaling their external radiology hazard and also to provide the comparative evaluation of indices (Chapter 7.1.1.1.).

The most frequently used radium equivalent index is given in the following expression (*Eq.6.*) (Beretka and Mathew 1985, Hamilton 1971):

$$Ra_{eq} = C_{226Ra} + \frac{10}{7} C_{232Th} + \frac{10}{130} C_{40K} \quad (Eq.6.)$$

where Ra_{eq} is the radium equivalent index (Bq kg^{-1}), C_{226Ra} is the activity concentration of ^{226}Ra, C_{232Th} is that of ^{232}Th and C_{40K} is that of ^{40}K (Bq kg^{-1}). The value of Ra_{eq} in building materials is required to be less than the limit value of 370 Bq kg^{-1} (OECD 1979) for safe use, i.e. to keep the external dose below 1.5 mSv y^{-1}.

The RP112 (EC 1999) recommends to use the unitless activity concentration index for building material qualification. This index is derived to indicate whether the annual dose, due to the excess external γ-radiation in a building, may exceed 1 mSv y^{-1}. The applied dose criterion was chosen based on Trevisi et al. (2012) who showed that the adoption of another possible criterion, 0.3 mSv y^{-1} is probably too ambitious a health goal, since too many materials exceed the value. A background cosmic and terrestrial dose rate of 50 nGy h^{-1} has been used in deriving the index (EC 1999) which is defined in the following way (*Eq.7.*).

$$I = \frac{C_{226Ra}}{300\ Bq\ kg^{-1}} + \frac{C_{232Th}}{200\ Bq\ kg^{-1}} + \frac{C_{40K}}{3000\ Bq\ kg^{-1}} \leq 1 \qquad (Eq.7.)$$

where I is the activity concentration index and its threshold is 1 (unit). Notice that the value of the activity concentration index is not directly an estimate for the effective dose. The only case, where the index has the same numerical value as the assessed annual effective dose in mSv, is the limit value of 1 (unit, EC 1999). For dose estimation see below in Chapter 4.1.3.2.

External and internal hazard indices also exist with threshold values 1 (unit), below which the building materials can be qualified being safe. The *Eq.8.* shows the calculation of the external hazard index.

$$H_{ex} = \frac{C_{226Ra}}{370\ Bq\ kg^{-1}} + \frac{C_{232Th}}{259\ Bq\ kg^{-1}} + \frac{C_{40K}}{4810\ Bq\ kg^{-1}} \leq 1 \quad (Eq.8.)$$

where H_{ex} is the external hazard index. The objective of this index is to limit the radiation dose to 1 mSv y^{-1} (ICRP 1990). This calculation does not take into account the wall thickness and the existence of doors and windows (Hewamanna et al. 2001). The internal hazard index is described by *Eq.9.*

$$H_{in} = \frac{C_{226Ra}}{185\ Bq\ kg^{-1}} + \frac{C_{232Th}}{259\ Bq\ kg^{-1}} + \frac{C_{40K}}{4810\ Bq\ kg^{-1}} \leq 1 \quad (Eq.9.)$$

where H_{in} is the internal hazard index. This calculation tries to better consider that ^{226}Ra decays to radon, which can accumulate indoors and increase the radiation hazard. The denominator of ^{226}Ra activity concentration has been decreased from 370 to 185 Bq kg^{-1} (*Eq.8.* and *Eq.9.*) (Krieger 1981). This estimation neglects other factors, such as airflow patterns, frequency of air changes, and type and porosity of the building materials (Beretka and Mathew 1985). The methodology regarding these last two indices is further discussed with the help of the results of this study (Chapter 7.1.1.1.).

4.1.3.2. External effective dose estimation from ^{226}Ra, ^{232}Th and ^{40}K activity concentration data in building materials

According to the RP112 (EC 1999), the total absorbed external dose rate in a room with dimensions of 4 × 5 × 2.8 m^3, wall thickness of 20 cm and wall density of 2350 kg m^{-3} (concrete) can be calculated by using the *Eq.10.* The background cosmic and terrestrial dose rate of 50 nGy h^{-1} is taken into account like in the case of the activity concentration index (*I*).

$$D_a = aC_{226Ra} + bC_{232Th} + cC_{40K} \qquad (Eq.10.)$$

where D_a is the absorbed dose rate (nGy h^{-1}) and *a*, *b* and *c* are the dose rates per unit activity concentrations of ^{226}Ra, ^{232}Th and ^{40}K [nGy h^{-1}(Bq kg^{-1})$^{-1}$], respectively. The values of *a*, *b* and *c* were taken to be 0.92, 1.1 and 0.08.

The external, annual effective dose can be estimated using the following formula (*Eq.11.*).

$$D_e = 10^{-6} OFD_a \quad (Eq.11.)$$

where D_e is the calculated annual effective dose rate (mSv y^{-1}), *O* is the annual indoor occupancy time (0.8×24 h×365.25 d=7012.8 h y^{-1}) and *F* is the dose conversion factor, 0.7 Sv Gy^{-1} (EC 1999).

To calculate the excess of building materials to the external dose received outdoors one can subtract the assumed 50 nGy h^{-1} background radiation (EC 1999) from result provided by *Eq.10.* and *Eq.11.*

4.1.4. Grain size distribution determination by wet sieving and laser grain size analysis

The grain size distribution and the resulting specific surface area of any material is considered to be related to its radon and thoron emanation and exhalation fractions as described in Chapter 2.3.1.1. However, it was not clear whether it has an influence on terrestrial radionuclide contents, influences radon and thoron emanations differently and whether it varies among the studied areas. Therefore, grain size distributions and specific surface areas of the adobe building material samples were determined by wet sieving and laser grain size analysis carried out at the Lithosphere Fluid Research Lab, Eötvös University and the Research Centre for Astronomy and Earth Sciences, Hungarian Academy of Sciences.

4.1.4.1. Wet sieving

After soaking 200-500 g of each of the samples in distilled water for at least two days, the author carried out the wet sieving by Fritsch sieves with diameters of 2, 1, 0.5, 0.25, 0.125 mm and 63 μm or only with diameters of 2 mm and 63 μm[9] coupled with Fritsch Analysette3 sieve shaker. The sieves with the separated grain size fractions were dried on lab air for making possible to remove the individual grains to sheets by a brush. The mass of each grain size fraction (0.063-0.125, 0.125-0.25 0.25-0.5, 0.5-1, 1-2 and > 2 mm) then was measured by an electronic balance from the Sartorius Basic series with a readability of ≥ 0.01 g. By this method mass% data is provided for each grain size fraction.

4.1.4.2. Laser grain size analysis

The finest grain size fraction of wet sieving (< 63 μm) dispersed in distilled water was collected into plastic vessels. After sampling these homogenized liquids to glass holders and adding some detergent, the grain size distributions were measured by two different models of Fritsch Analysette 22 laser grain size analyzer (different grain size resolutions).[10] These instruments measure the angular variation in intensity of light scattered as a laser beam passes through a dispersed particulate sample. Large particles scatter light at small angles relative to

[9]During the lab work, it became obvious that there are almost no grains staying on some sieves. Therefore, the number of applied sieves has been reduced.

[10]The instrument at Lithosphere Fluid Research Lab stopped functioning after 19 adobe samples. Therefore, the other 27 adobe samples were analyzed at the Research Centre for Astronomy and Earth Sciences, Hungarian Academy of Sciences.

the laser beam and small particles scatter light at large angles. By this method volume% data of a range of grain sizes or a middle grain size (< 63 μm) is provided.

4.1.4.3. Data evaluation methods

The inorganic raw material contents of adobes were classified to assess their physical characteristics based on the USDA (United States Department of Agriculture) system, which uses twelve classes of clay, silt, sand and their intermediate types, for example loam. The classification was carried out by loading the proportions of clay, silt and sand fractions to the Soil Texture Utility (Wunsch 2009), which is an excel sheet showing automatically the results in the USDA soil texture triangle. The clay size range was taken to be < 2 μm, the silt to be 2-50 μm and the sand to be 0.05-2 mm. These cover all the results of wet sieving and laser grain size analysis. Due to the different mass% data from wet sieving and the volume% data from laser grain size analysis, special care has to be taken while coupling the result. Further useful information about the samples is provided by the positions and amplitudes of characteristic peaks in the clay and silt fractions (data from laser gain size analysis).

The specific surface area of each studied adobe building material was estimated in $m^2\ g^{-1}$ units by assuming that they contain only perfectly spherical grains with densities of SiO_2 (2.65 g cm^{-3}). The surface area and the volume of a spherical particle can be calculated from its given diameter. Then, using the density, the mass of the same particle is estimated. From these data and the mass% and volume% results, the surface area of each grain size fraction can be estimated which weighted sum provides the specific surface area of the sample (Hellevang, personal communication, 2013).

Possible errors and uncertainties

The high clay and silt content of adobe building materials frequently cause plugging in the process of wet sieving, which might lead to some material loss. However, this loss is not relevant compared to that of the process of removing the grains from sieves. This is resulted in an opposite relationship between the systematic error of mass% data and the total mass of the soaked and analyzed sample. Statistical uncertainty occurs due to the readability of the electronic balance. In case of laser grain size analysis, systematic error might be present in the volume% data because of the not sufficient enough grain separation by the detergent. The instruments do not display statistical uncertainty values. Further details about uncertainties of this method can be found in Di Stefano et al. (2010). Additional uncertainty of the estimated

specific surface area results is due to the possible deviations in particle shapes and densities, as well as due to the not considered surface roughness.

4.2. Methods of in-situ measurements in dwellings

4.2.1. In-situ measurement strategy

For the success of in-situ measurement campaigns, the help of local people to find appropriate houses and owners volunteering to participate was again indispensable. The selection criterion was that the room had to have at least one adobe wall, and preferably be in daily use or at least offer the possibility to sleep, live or work in. At the end, the in-situ measurements, consisting of indoor radon and thoron activity concentration and γ dose rate measurements, were performed in *53 adobe dwellings* of the seven selected settlements at *Békés County* (*Fig.3.*). Since Sarkad and Sarkadkeresztúr are considered together[11], five to eleven buildings were studied at each location: eleven at Gyomaendrőd, Sarkad-Sarkadkeresztúr and Vésztő, ten at Gyula and five at Kondoros and Újiráz. It was not possible to measure at all locations during the whole measurement period of one year. In some cases, the owners refused continuing the measurement campaigns or some detector loss or damage occurred.

The indoor radon and thoron activity concentrations measurements were carried out in three months periods for one year in order to represent the four seasons typical of the climate (OMSZ, http://www.met.hu/eghajlat/magyarorszag_eghajlata/): *winter* from December 2010 to February 2011, *spring* from March 2011 to May 2011, *summer* from June 2011 to August 2011 and *autumn* from September 2011 to November 2011. The γ dose rate measurements were performed in each dwelling when the first radon and thoron activity concentration measurements started.

Representativeness

The total number (five to eleven) of measurements at each settlement is considered to represent the adobe dwellings of that given settlement. The number of all studied dwellings (53) represents the adobe dwellings of the given studied area, Békés County.

[11]Due to the proximity, similar geological setting and the low number of studied buildings at Sarkadkeresztúr.

4.2.2. Indoor radon and thoron activity concentration determination by etched track detectors

Raduet type etched track detector pairs, provided by Radosys Ltd. (Budapest, Hungary) were used for the indoor radon and thoron activity concentration measurements. One of the detectors is for radon detection and the other one is for radon and thoron detection together using more permeable filter. The thoron activity concentration, therefore, can be derived based on the track density difference of the two detectors. The detector pairs were placed at a 10±1.5 cm distance from the adobe walls. This distance was chosen to match earlier studies (Chougaonkar et al. 2004, Deka et al. 2003, Luo et al. 2005) so that comparison of the results can be made. However, some recent studies, e.g. by Stojanovska et al. (2013), placed the detectors at a distance of at least 50 cm. Note that these measurements are always expected to show lower thoron activity concentrations than at 10 cm distance because of the inhomogeneous distribution of thoron in the room (Urosevic et al. 2008). For the same reason, special care was taken to avoid double or multiple sided effects at wall edges and corners, as well as any influence of electronic devices

Special care was taken to avoid double or multiple sided effects at wall edges and corners, as well as any influence of electronic devices (Hámori et al. 2006). Detectors were placed at a height between 60 and 240 cm from the ground, while adjusting to the conditions provided by the residents.

For the analysis of detectors, the chemical etching of inner plastic films was performed in the laboratory of the National Research Institute for Radiobiology and Radiohygiene (OSSKI), Budapest, Hungary with 6.25 M NaOH solution at 90 ^{0}C for 5 hours. The counting of α-tracks was carried out by Radosys automatic microscopes in the lab of OSSKI and partly in the lab of the manufacturer, and always at least three parallel counting were run for each plastic film. Radon and thoron activity concentrations for the three months integration times were calculated from the track density of detector pairs, the background track density and the calibration factors provided by the manufacturer. Annual averages were only determined when measurement data were available in all seasons in the given building.

Possible errors and uncertainties

The standard deviation of the three times counted track densities and the uncertainty of calibration factors, provided by the manufacturer, were taken into account in the statistical uncertainty calculations. The uncertainty for thoron activity concentration is about the double of that of radon due to the calculation based on two measurements. Systematic error in the

detector analysis process might occur due to the possibilities of not appropriate etching or automatic microscope settings.

Knowing the lower limits of detection (LLDs) is a critical point of these measurements, mainly in case of thoron. The measurement of this isotope is quite uncertain and low values cannot be detected appropriately due to the subtraction of two separately measured track densities. LLD calculation in this method is complicated because it has to provide a unique value for each radon and thoron activity concentration pair, since radon LLD depends on the thoron activity concentration and thoron LLD depends, in turn, on the radon activity concentration. For details about LLD calculation procedures, the reader is referred to the publication of Stojanovska et al. (2013) or suggested to contact Radosys Ltd. (Budapest, Hungary) for their manuals (Kocsy 2012). As Stojanovska et al. (2013) admitted to provide only a "simplistic approach to estimate the LLD of thoron for the two-detector configuration" the author only accepted to be correct the LLDs calculated based on the way offered by the manufacturer (Kocsy 2012). The author, however, emphasizes the need of the representation of low values in the statistics. As suggested by the Analytical Methods Committee (AMC 2001) and Reimann et al. (2008) the best way to do this is to use all measurement data if available, instead of many existing, however, not ideal solutions (for example, changing to arbitrarily chosen low numbers, e.g., half of the LLDs). For this reason, all measurement data were used in the statistical evaluation even though a part of them were below their LLDs. However, even if LLDs are not involved in the statistical analysis, they are recognized and considered in that data evaluation.

4.2.2.1. Inhalation dose estimation from indoor radon and thoron activity concentration data

The term of inhalation dose, a type of internal exposure, refers to the effective dose originated from radon, thoron and usually considers mostly the inhalation of their solid decay products, which is mostly affecting the tissues of the lung. It can be directly related to the level of health impact of radon and thoron, however, note the possible much higher local tissue dose (Madas and Balásházy 2011). In this study, the inhalation dose can be estimated from the measured annual average radon and thoron activity concentration data using *Eq.12.*

$$D_i = 10^{-6} C_{av} F_{eq} F_c O \qquad (Eq.12.)$$

where D_i is the estimated annual inhalation dose from radon or thoron (mSv y^{-1}), C_{av} is the annual average radon or thoron activity concentration (Bq m^{-3}), F_{eq} is the radon or thoron equilibrium factor (see further details about applied values below) and F_c is the dose conversion factor with a value of 9 nSv (Bq h m^{-3})$^{-1}$ for radon and 40 nSv (Bq h m^{-3})$^{-1}$ for thoron (Chapter 2.3.3, UNSCEAR 2000). It is noted that O is the annual indoor occupancy time (7012.8 h y^{-1}).

As described in Chapter 2.3.2. the typical value of the radon equilibrium factor is 0.4 (UNSCEAR 2000), which was applied in the dose estimation calculations (*Eq.12.*). In case of thoron isotope, the 0.04 average equilibrium factor (Harley et al. 2010) was available to use. Note the resulted uncertainty. Omori et al. (2013) pointed out that without direct determination of thoron decay product activity concentrations and equilibrium factors, any average discrete value has about a 100-200 % uncertainty. However, in this study, most of the many efforts of the author failed to provide information about the actual equilibrium factors. Only six measurement data were available from the spring period which show a similar average as Harley et al. (2010), hence verifying its application for a crude estimation.

4.2.3. Equivalent γ dose rate determination by a portable device

To monitor the actual γ dose rate and to gain further information about possible building material excess external dose in adobe dwellings, some measurements were carried out by FH 40 G-L10 meter (Thermo Scientific 2007) at the beginning of the radon and thoron activity concentration measurement campaigns (winter). This instrument has a proportional detector built in, which detects the 30 keV - 4.4 MeV energy γ-photons originated from cosmic background radiation and most importantly from the terrestrial radionuclide concentration of the soil and the building materials. The latter source is considered to cause any detected spatial variation on the studied area of Békés County. The device is designed to meet the energy response behavior of the SI-units ambient dose equivalent and ambient dose equivalent rate according to the Report 39 of the International Commission on Radiation Units and Measurements (ICRU, 1985). An intelligent rate meter algorithm detects and indicates small changes in dose rate, suppressing random noise. The values can be read directly from the instrument LCD in the units of nSv h^{-1}. Three dose rate values with about one minute time shifts were reported with the device pushed to adobe wall surfaces, lying on ground surfaces and also being hold at one meter height in the middle of the chosen rooms.

Possible errors and uncertainties

The statistical uncertainty of detected γ dose rate results was controlled by the three successive measurements. However, the integration time of the device is not found its manual, hence the possibility of any overlap cannot be neglected, however reduced by one minute waiting time before each read.

4.3. Applied statistical methods

For all data processing purposes, the Microsoft Excel, Statgraphics Centurion and Microcal Origin softwares were used. As the basis of the statistical analysis of all measurement results robust statistics were applied and Tukey's resistant five-letter summary statistics (Tukey 1977) containing the minimum, lower quartile, median, upper quartile and the maximum were calculated, presented in tables and visualized by box-whisker plots. Probability (frequency) histogram, average and its 1σ standard deviation are also presented in some cases. Standardized skewness and standardized kurtosis values are considered for the evaluation of statistical distributions. Relative variabilities are presented by the robust Median Absolute Deviation/median (MAD/median) measure.

For the detailed analysis of the measurement results the following three methods/hypothesis tests, for three different aims were chosen and carried out. All the test were considered at the *95 % confidence level (α)*, which means that the test accepts (cannot reject) the null hypothesis when the *P*-value ≥ 0.05 and that the test rejects the null hypothesis when the *P*-value < 0.05. None of the resulted *P*-values are given among the results because of the predefined decision threshold.

4.3.1. Mann-Whitney (Wilcoxon) test for equality of medians

To be able to show significant *differences between central tendencies of sample groups* (like data from different studied areas, geological environments or periods), the Mann-Whitney (Wilcoxon) non-parametric test, hereafter *MW test*, based on the comparison of pairs of medians was applied (Mann and Whitney 1947). The null hypothesis is that two populations are the same (*P*-value ≥ 0.05). This statistical test points out if a sample group significantly tends to have lower or higher values than any other group (*P*-value < 0.05). It does not assume that the data is normally distributed, which is not expected from some of the data (see below), and it turned out to have satisfying sensitivity for the collected number of samples and data.

4.3.2. Shapiro-Wilk test for statistical distributions of indoor radon and thoron activity concentrations

Significant deviation from lognormal distribution of indoor radon data was described by Bossew (2010) and Tóth et al. (2006) only when non homogeneous regions with uniform geology, building style and living habits were sampled. Based on this finding, it is useful to test the *lognormal distribution assumption* of these data, i.e. normal distribution assumption of the natural logarithm of the data, to find possible deviations referring to sampling heterogeneity. The data was also tested for normality as it is a condition of most parametric tests and it is mentioned as the alternative distribution (Tóth et al. 2006). By the help of determined distributions the proportion of dwellings above reference levels can also be predicted. For these aims the powerful Shapiro-Wilk test, hereafter *SW test*, was applied (Shapiro and Wilk 1965) as in the studies of Kovacs (2010) and Vaupotic and Kávási (2010). The null hypothesis is that the data come from a normal distribution or lognormal when natural logarithm is taken (P-value ≥ 0.05) against the alternative hypothesis that it is not (P-value < 0.05).

4.3.3. Correlation analysis

Statistically significant *non-zero relationships* among any meaningful pairs of independently measured parameters were studied by the help of Pearson's linear correlation coefficient (r). This is a measure of the dependence between two variables giving a value between +1 and -1. Its statistical significance can be given by rejecting the null hypothesis (P-value < 0.05) that the true correlation coefficient (ρ) is equal to 0, based on the value of the sample correlation coefficient (r). The lowest r accepted to be statistically significant is decreasing by the increase of sample number.

5. METHODOLOGY ACHIEVEMENTS IN RADON AND THORON EMANATION DETERMINATION

5.1. Radon: testing the equilibrium method by a comparison to the growth curve method

An appropriate radon emanation measurement method (growth curve method, measurement duration by RAD7 is in the 10 days of order of magnitude), which takes into account the radon leakage (Chapter 4.1.2.3.1.) is already available. However, it is a time consuming technique for large number of samples. One of the specific aims of this work is to *test an already existing, less time consuming method* (equilibrium method, measurement time by RAD7 is in the some hours of order of magnitude, Chapter 4.1.2.3.2.) for further consideration to use (**PV6.** and partially in **7.**).

5.1.1. Experimental – materials and measurement strategies

For the comparison of the equilibrium method (Chapter 4.1.2.3.2.) to the growth curve method (Chapter 4.1.2.3.1.), 27 adobe building material samples were analyzed using both measurement strategies and calculations. These samples were in the form of routine measurement samples, i.e. cut to about 200 g cubic bodies with widths of about 5 cm. After placing and sealing a sample into the sample container (*Fig.7.*), the radon activity concentration growth curve measurement was started and continued for 10 days. The sample container was then disconnected from the experimental setup and kept closed for about 19 days to make sure that the secular equilibrium was reached. Then the sample container was again connected to the experimental setup (i.e. same plastic tubes and RAD7 device) and the assumed equilibrium radon activity concentration was measured for about four hours.

5.1.2. Results and discussion – comparison of the radon emanation results of the two methods

The radon activity concentration measurement results from the two methods (growth curve method and equilibrium method) were evaluated as described in Chapter 4.1.2.3. with the application of *Eq.3.*, *4.* and of *Eq.5.*

On *Fig.8.* the radon emanation results of these calculations from the two applied methods are plotted vs. each other. Since the less time consuming equilibrium method (only four hours

measurement time by the RAD7 device) does not allow considering the leakage, which produce radon loss from the experimental setup (*Fig.7.*), it is obvious why it shows less radon emanation results than the growth curve method (*Fig.8.*, **PV6.**). It is also a remarkable observation that the determined statistical uncertainty is always higher in the growth curve method than in the equilibrium method (*Fig.8.*). However, the growth curve method results are not affected by the systematic error of possible radon leakage since it takes it into account by the value of α (*Eq.3.*, *4.*, Chapter 4.1.2.3.1.).

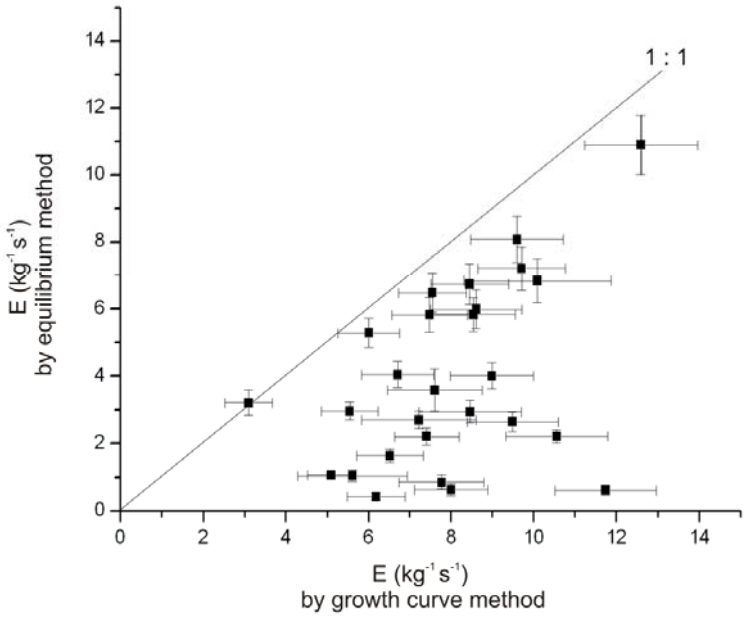

*Fig.8.: The radon emanation results of 27 adobe samples given by equilibrium method vs. growth curve method. Line 1:1 presents the perfect fitting of results. The data below this line show that equilibrium method measures lower values than growth curve method (**PV6.**).*

Plotting the ratio of results of equilibrium and growth curve methods, which is 1 (unit) in the ideal case, vs. α (defined in *Eq.2.*) of each experimental setup with a given sample holder, plastic tubes and RAD7 device, it was observed that neither of the growth curve nor the equilibrium radon emanation measurement methods can provide reliable results when the leakage is prevailing. Therefore, the data points with α higher than 0.02 h^{-1} were ignored together with those, in which one of the emanation results of the two methods, in the calculation of the ratio, had elevated statistical uncertainty (**PV6.**). Overall, the ratio vs. α results of 20 adobe building material samples are considered and presented on *Fig.9*.

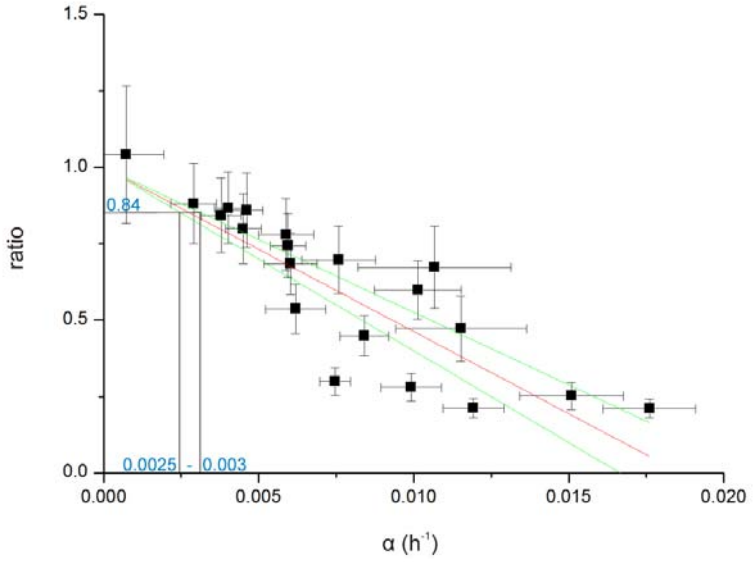

*Fig.9.: The ratio of emanation results of equilibrium and growth curve methods vs. the value of α representing the radon leakage of each experimental setup. The red line shows the observed connection between the plotted values. The green lines represent the 95 % confidence intervals. The black lines and blue numbers mark the acceptable level of radon leakage for the usage of equilibrium method (see more explanation in the text above and **PV6.**).*

The ratio of results of equilibrium and growth curve methods is observed to show an inverse linear connection with α of each measurement set up and approaches 1 (unit) when α is around 0 (zero) (*Fig.9.*, red line with green 95 % confidence intervals, fixed intercept: 1). In this case the radon emanation results of different methods are the same. This indicates that the less time consuming equilibrium method also can provide a good estimation of radon emanation below a certain, controlled degree of radon loss (**PV6.**)

It is important to determine the maximum level of acceptable radon leakage, below which the results of the two methods do not show any significant difference. The relative statistical uncertainty of the ratio of results of equilibrium and growth curve methods is considered, which has an average value of 16 %. Hence, if the ratio is reduced by 16 %[12] due to the not considered leakage in the equilibrium method, its error bar still reaches the value of 1 (unit). In this case, the difference between the radon emanation results is not significant. This 16 %

[12]The radon emanation result of the equilibrium method is 16% lower than that of the growth curve method.

reduction is presented on *Fig.9.* by the ratio value of 0.84[13] which signs out a 0.0025-0.003 h^{-1} maximum acceptable α of the experimental setup for the usage of the less time consuming equilibrium method (*Fig.9.*). This value is equal to 0.25-0.3 % h^{-1}, which means that 0.25-0.3 % of the actually accumulated radon atoms are leaving the experimental setup in one hour. This is about the 30-40 % of the value of radon decay constant for a comparison of the value of 2 % in **SJ5**. If the radon leakage is proven to vary only below this level the equilibrium method provides correct, comparable radon emanation results. If the leakage is higher, but can be kept below an α value of for example 0.009 h^{-1} (0.9 % h^{-1}), the results are only an order of magnitude estimation for the possible aim of finding hazardous samples for a more detailed study.

5.1.3. Conclusions and further applications

The measurement results above allow getting known the limits of the two radon emanation determination methods and sign out the degree of needed leakage control of the experimental setup (**PV6.**, **7.**). For the usage of the less time consuming equilibrium method (for large number of samples), a proven maximum 0.0025-0.003 h^{-1} α is acceptable, otherwise it most probably provides only an order of magnitude estimation of radon emanation. This acceptable α value is one order of magnitude higher (0.02 h^{-1}) for the growth curve method.

Since the results show that the available experimental setup tends to have varying and more significant radon leakage than 0.0025-0.003 h^{-1}, the growth curve method was applied, and only its results are considered in the evaluation of adobe building materials of this study. The radon emanations were remeasured by this method if α was determined to be above 0.02 h^{-1} in the first measurement.

For future consideration, note that the author and her coauthors have already designed, tested and used a radon leakage free High Density Polyethilene (HDPE) sample container for γ-ray spectrometry measurements (**SJ5.**). This design is suggested to improve for less time consuming radon emanation measurement purposes with the equilibrium method.

Possible errors and uncertainties

In the accepted radon emanation measurement results the statistical uncertainty is originated from the radon activity concentration determination uncertainty of RAD7, the uncertainty of the determined C_{max} and α in the *Eq.3.* fit to the measurement results and the uncertainty of experimental setup volumes. No systematic error is expected from any sources.

[13] I.e. $1 - 0.16 = 0.84$

5.2. Thoron: improving the data analysis method taking into account the sample geometry and the thoron attenuation in the sample holder

There was not an appropriate thoron emanation measurement/determination method available in the literature for the given experimental setup (*Fig.7.*). A *new data analysis method* was required with the regular measurement strategy (Chapter 4.1.2.3.2.). *Making this available* (**SJ4.**) got to be another specific aim of this work.

For the aim of efficiently analyze the thoron emanation of adobe building materials, the author considers first a cylindrical sample geometry both via measurements and model calculation (**SJ4.**) and then a cubical sample geometry via an improved model calculation (Csige, personal communication, 2013). Like this, an appropriate thoron emanation estimation method gets available for easily prepared cubical samples based on thoron activity concentration measurements in the available experimental setup (RAD7, *Fig.7.*) only with a single sample width. The need is proven by several similarly improved methods, which were discussed by Cozmuta and van der Graaf (2001), Tan and Xiao (2013) and Ujić et al. (2008). However, these methods use RAD7 detector for soil surface thoron exhalation determination or different measurement devices for sample thoron diffusion coefficient and emanation determination.

Note that the thoron emanation, due to the significant geometry sensitivity, is more meaningful to model as the thoron activity leaving a unit sample volume, which is named as the thoron generation rate (Bq m^{-3} s^{-1}). Therefore, this value is applied in this subsection. However, in the application of the new analysis method and in the presentation of the results, it is better to calculate to the thoron emanation on the following way (*Eq.13.*).

$$E = \frac{G}{\lambda \rho} \qquad (Eq.13.)$$

where G is the thoron generation rate (Bq m^{-3} s^{-1}) determined by the method built up below and ρ is the density of the sample (kg m^{-3}).

5.2.1. Cylindrical sample geometry

When a cylindrical sample is placed into the cylindrical sample holder, theoretically it has only one surface, on which thoron can be exhaled. In this case, the thoron activity concentration in the pore space of the sample depends only on one coordinate, which is the elevation. This fact reduces the complexity of the system, therefore, it can be understood better. An experiment was carried out detailed below and then a described model was fitted to its results for the determination of different sample parameters. This part of the work was published in **SJ4.**

5.2.1.1. Experimental – material and measurement strategy

A representative adobe building material sample from Gyomaendrőd, Békés County was selected which has a comparably hard, stable structure to cut and rasp to the cylindrical shape of the sample holder. The sample thickness was reduced in 19 different steps, from 8.35 cm to 0.85 cm. The free volume between the uneven surface of the sample side and the inner part of the sample holder was filled up with the powder of the same sample. The contribution of the powder to the mass was always between only 4 and 7 %. Due to this careful sample preparation process, the thoron could only escape through the top surfaces of the different thicknesses of the sample. The 19 thoron activity concentration measurements were carried out by RAD7 detector (*Fig.7.*) with 15 minutes measurement cycles, each measurement for at least four hours.

5.2.1.2. Measurement results – measured thoron activity concentrations vs. sample thicknesses

Experimental results show a non-linear dependence of measured thoron activity concentration on the sample thickness. Although the thoron activity concentration, first, is increasing linearly with the sample thickness (i.e. the sample amount until it is still significantly thinner than the diffusion length of thoron in the sample) for thicker samples the measurable thoron activity concentrations are decreased (below the linear trend) and the curve breaks forming a plateau (**SJ4.**). The measured values are presented on *Fig.11.* below in the Chapter 5.2.1.4. together with the fit of the appropriate model described here.

5.2.1.3. Model for cylindrical samples

In this subsection the RAD7 displayed (measurable) thoron activity concentrations are described by model calculations as a function of cylindrical sample thickness (**SJ4.**). Beside the geometry of the sample, the model also considers the thoron decay in RAD7 and the resulted thoron activity concentration attenuation in the V_{net} volume of the sample container (*Fig.7.*) (Chapter 4.1.2.2.2.).

An important factor to consider in this model is the diffusion of thoron along the z coordinate in the sample, which can be described by *Eq.14*.

$$\frac{d^2C(z)}{dz^2} = -\frac{G}{D} + \frac{\lambda\beta}{D}C(z) \qquad (Eq.14.)$$

where $C(z)$ is the actual thoron activity concentration (Bq m^{-3}) depending on the elevation in the sample, D is the thoron diffusion coefficient in the sample (m^2 s^{-1}) and β is the partition corrected porosity of the sample expressed as $\beta = (1 - m + Lm)\varepsilon$ taking into account the water saturation (m), the partition coefficient of thoron between water and air phase (L) and the porosity (ε) (Andersen 2001). The definitions of G and λ[14] are given earlier in the text; they are the thoron generation rate and the decay constant of thoron, respectively.

Zero flux boundary condition on the bottom of the sample container has to be applied ($dC(z)/dz|_{z=0} = 0$) and the one on the top surface of the sample has to state that the thoron activity concentration in the sample pore volume equals to that in V_{net} ($C(z = h) = C_{meas}$). Perfect mixing is assumed in V_{net} and also, due to the decay of thoron, that the value of thoron activity concentration drops to its half in the RAD7 radon-thoron detector with the given calibrated induced air flow rate of q = 11 cm^3 s^{-1} (*Fig.7.*, Durridge Co. 2013). This last process is causing the attenuation in V_{net}. The rate of change of thoron activity concentration in V_{net} hence can be described by the following differential equations (*Eq.15.*) consisting the terms of (1) thoron leaving the sample to V_{net}, (2) thoron decay, (3) thoron leaving V_{net} towards RAD7 and (4) thoron arriving back to V_{net} from RAD7. This reduces to an algebraic equation under steady state conditions.

[14]The author notes that using the λ of radon, the model (*Eq.16.*) describes a linear dependence for this isotope. Therefore, it proves that all radon atoms can leave the sample in the given experimental setup.

$$\frac{dC_{meas}(t)}{dt} = j\frac{1}{H-h} - \lambda C_{meas} - \frac{q}{V_{net}}C_{meas} + \frac{q}{2V_{net}}C_{meas} = 0 \qquad (Eq.15.)$$

where $C_{meas}(t)$ is the measurable thoron activity concentration (Bq m^{-3}) depending on the time elapsed since the sealing of the sample container, j is the diffusion flux of thoron on the top surface of the sample (Bq m^{-2} s^{-1}) expressed as $j = -D\,(dC(z)/dz)|_{z=h}$ and H and h are defined in Chapter 4.1.2.1. (*Fig.7.*, the height of the sample holder and the sample thickness, respectively).

Solving the equation system described above provides the final form[15] of the model (**SJ4.**), which is expressed here as the RAD7 displayed thoron activity concentration function of the sample thickness (*Eq.16.*).

$$C_{meas}(h) = \frac{G}{\lambda\beta + \frac{\gamma\{\lambda(H-h)+q/(2A)\}}{\tanh(\gamma h)}} \qquad (Eq.16.)$$

where $C_{meas}(h)$ is the measurable thoron activity concentration (Bq m^{-3}) depending the sample thickness and γ is a sample parameter, which is reciprocating z_d, the diffusion length of thoron in the sample (m) and it is expressed as $\gamma = \sqrt{\lambda\beta/D}$ (m^{-1}).

The final form of the model (*Eq.16.*) also describes a non-linear dependence of thoron activity concentration on the sample thickness similar to the experimental results. Some calculation scenarios with different sample parameters (G, β, γ) are presented on *Fig.10*. It is observed that C_{meas} and the curve shape highly depend on the values of G and γ. However, constraining the value of β in a meaningful range ($0 < L\varepsilon < \beta < \varepsilon < 1$) has an insignificant effect on the gained curves.

[15]The model was modified several times with the help of the measurement results.

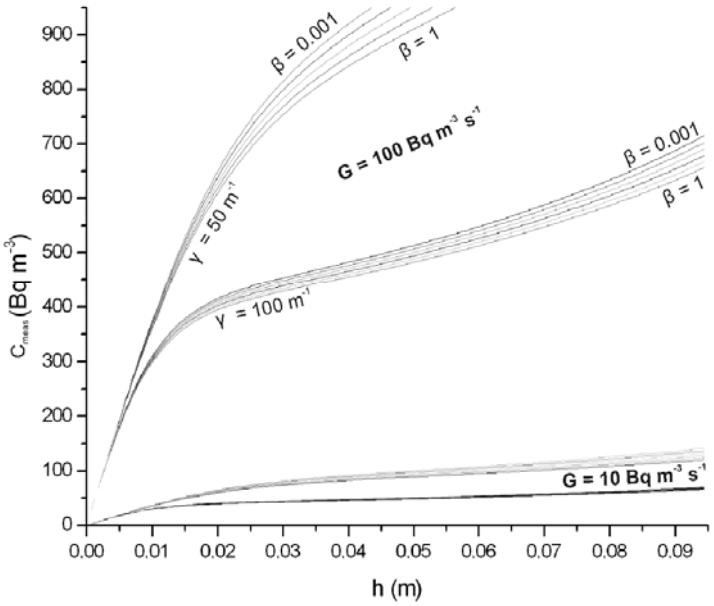

Fig.10.: Model (Eq.16.) predicted non-linear RAD7 displayed thoron activity concentrations vs. the thickness of the cylindrical sample in the experimental setup (Fig.7.). The maximum value of h is set to be H (0.095 m). The figure also presents the high curve shape sensitivity to thoron generation rate (G = 10 or 100 Bq m^{-3} s^{-1}) and γ parameter (γ = 50 or 100 m^{-1}) and the low sensitivity to partition corrected porosity (0 < β ≤ 1).

5.2.1.4. Discussion – the fit of model to the measurement results

Fitting the model (*Eq.16.*) to the measurement results (Chapter 5.2.1.2.) aims to determine the thoron generation rate of the sample and also provides a value for γ sample parameter. Determined value of γ can also be accepted as a good estimate for other samples (**SJ4.**) and, therefore, a general thoron diffusion coefficient in adobe building material can be estimated.

To fit the model (*Fig.11.*, red line) to the measurement results (*Fig.11.*, black quadrates), Microcal Origin software was used. The A, H and q of the experimental setup and the λ of thoron are obviously fix parameters with the given values on *Fig.11.* Considering β as a free fitting sample parameter resulted in meaningless results, which is not surprising due to the low curve sensitivity to its value (*Fig.10.*). Hence, fix partition corrected porosity has to be applied either from estimating its value or by obtaining it from independent measurements of sample porosity and water saturation. In the case of adobe building material samples its value is estimated to be 0.56±0.10 based on the estimated values m = 0.1±0.05, L = 0.25±0.1 and

ε = 0.6±0.1 and the definition of partition corrected porosity (Andersen 2001). *Fig.11.* presents the measurement results of the experiment and the fit of model by using β = 0.56.

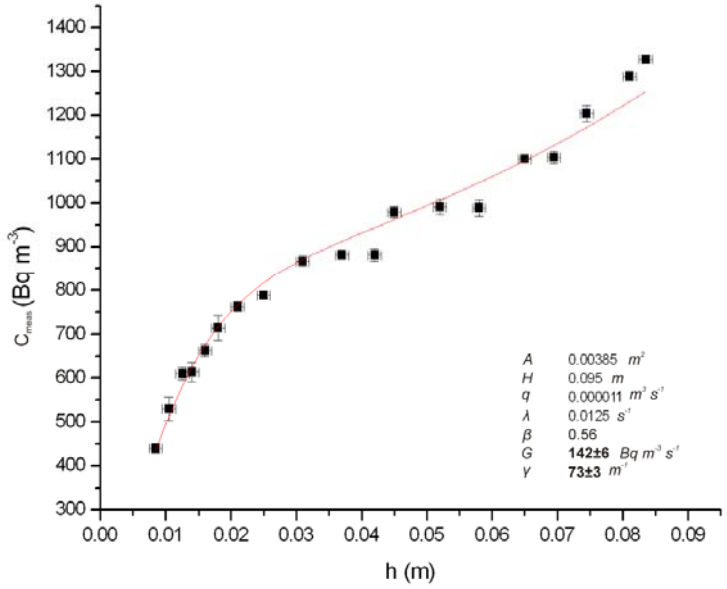

*Fig.11.: The measured thoron activity concentrations (black quadrates) as a function of the sample thickness in the experiment (Chapter 5.2.1.2.) and the best fit of the model (Eq.16., red line) (**SJ4.**). The fixed parameters and the results of the fit, indicated by bold numbers, are presented in the right bottom corner. Note that the Y axis starts at 300 Bq m^{-3}.*

The developed final model (*Eq.16.*) describes very well the experimental results and its fit provides the value (*Fig.11.*) of thoron generation rate of the selected sample from Gyomaendrőd (Békés County) and most importantly[16] γ parameter as an estimate for all adobe building material samples in this study. The uncertainties of G and γ on *Fig.11.* are the uncertainties of the non-linear curve fit. Repeating the fit in the range of estimated partition corrected porosity (β = 0.56±0.10) the results are given as G = 142±6 Bq m^{-3} s^{-1} and γ = 73±5 m^{-1} (**SJ4.**). Using this value of γ parameter, the thoron diffusion length is found to be z_d = 1.4±0.2 cm. For the analysis of other adobe samples (Chapter 5.2.2.), D is determined in the range of 1 to 3×10^{-6} m^2 s^{-1} ($D = \lambda\beta/\gamma^2$ and $D = \varepsilon\beta D_a \mathrm{e}^{-6m\varepsilon-6m^{14\varepsilon}}$ where $D_a \approx 1.1\times10^{-5}$ m^2 s^{-1} is the diffusion coefficient of thoron in air, **SJ4.**, Rogers and Nielson 1991). As a comparison, the radon bulk diffusion coefficient for a concrete sample was determined 4.6±0.4×10^{-10} m^2 s^{-1} (Cozmuta and van der Graaf 2001), which is four orders of magnitude

[16]Because it can be used in the simpler analysis method of the 45 other adobe samples.

lower than that for thoron in adobe building material determined in this study. This is considered to be a proof of high radon and also thoron exhalation potential of Hungarian adobe building materials and consequently indoor accumulation.

5.2.2. Cubical sample geometry – further application

When the partition corrected porosity of the sample and its thoron diffusion coefficient are known, thoron generation rate and consequently thoron emanation can be obtained from a single thoron activity concentration measurement with one given sample height. For this, the optimum sample thickness would be at around 5 cm (**SJ4.**). Not only measuring with many sample thicknesses requires a long laboratory work for only one sample, but also to form these well sample container fitting cylindrical shapes. The new analysis method is based on an improved version of the model described above. It is for a single thoron activity concentration data with easily formable cubical sample geometry.

For the thoron generation rate analysis of the other 5 cm width cubical adobe samples in this study, the new analysis method was applied, which is contained in the following equation (*Eq.17.*, provided by Csige, personal communication, 2013).

$$G = \frac{C_{meas}((AH-d^3)\lambda+q/2-a)}{b} \qquad (Eq.17.)$$

where a and b are constants with one specific cubical model provided values of $-7.0\pm2.4\times10^{-7}$ m^3 s^{-1} and $10\pm1.7\times10^{-5}$ m^3, respectively. Their values depend on the partition corrected porosity, the thoron diffusion coefficient in the sample and the width of the cubical sample. The used a and b values were determined for adobe samples by the most probable mean values of $\beta = 0.56$, $D = 2\times10^{-6}$ m^2 s^{-1} and $d = 5$ cm. Note that $AH\text{-}d^3$ is V_{net} and that q is the calibrated induced air flow rate of RAD7 radon-thoron detector. The thoron emanation, E, is then calculated from G based on *Eq.13.*

Possible errors and uncertainties

The uncertainty of thoron emanation results in this study is mostly due to the uncertainty of b constant. Its uncertainty was determined for $\beta = 0.46$ to 0.66 estimated range, $D = 1$ to 3×10^{-6} m^2 s^{-1} determined range and a certain d value of 5 cm. The sample size deviations, the measured thoron activity concentration uncertainty and the determined sample density uncertainty would further increase the overall uncertainties; however, these are not taken into account in the analysis process. Systematic errors might occur due to β and D estimates.

6. STATISTICS OF MEASUREMENT RESULTS OF ADOBE BUILDING MATERIAL AND DWELLINGS

In the presentation of the measurement results different meaningful data groups are statistically analyzed and compared. The analyzed data groups form a complicated system based on the studied parameter, time and location-geological information. Therefore, a notation system is defined here answering the ***what-when-where*** questions and helping to follow this part of the manuscript.

The *Tab.1.* defines the first part of the notation showing which measured parameter is considered in the given statistics (***what****, parameter code*). Each of these is analyzed in separate subchapter.

what	**studied parameter**
RnE	**radon emanation**
TnE	**thoron emanation**
Ra	**^{226}Ra activity concentration**
Th	**^{232}Th activity concentration**
K	**^{40}K activity concentration**
ED_{RaThK}	**estimated annual external effective dose**
f_{RnE}	**radon emanation fraction**
f_{TnE}	**thoron emanation fraction**
SSA	**estimated specific surface area**
RnC	**indoor radon activity concentration**
TnC	**indoor thoron activity concentration**
ID_{Rn}	**estimated annual radon inhalation dose**
γDR	**measured γ dose rate**

*Tab.1.: The possibilities for the first part of the notation describing the studied parameter (**what**). The dashed line marks the border of statistically analyzed parameters: measured in laboratory (above) or in-situ (below).*

The following table (*Tab.2.*) defines the second part of the notation providing information about the considered grouping interval length (***when****, interval length code*). ***C*** (constant, *Tab.2.*) is given in the second part of the notation in case of parameters of adobe building material samples measured in laboratory (above dashed line in *Tab.1.*, except $\boldsymbol{ED_{RaThK}}$) not changing in time. In case of any estimated or measured effective doses ($\boldsymbol{ED_{RaThK}}$, $\boldsymbol{ID_{Rn}}$ and ***γDR***, *Tab.1.*) the notation of ***Y*** (one year, *Tab.2.*) can only be paired because the end result is always an annual effective dose. In case of in-situ measured indoor radon and thoron activity concentrations (***RnC*** and ***TnC***, *Tab.1.*) the ***Y*** and ***S*** (one year and one season, *Tab.2.*) are both possible referring to datasets of annual average or seasonal values. When more possible

values are given for one notation (e.g. ***S***, *Tab.2.* and also valid for *Tab.3.*), all of them are considered separately in the statistical analysis and compared to each other.

when	grouping interval length	possible values
C	**constant**	**constant**
Y	**one year**	**one year**
S	**one season**	**winter, spring, summer, autumn**

*Tab.2.: The possibilities for the second part of the notation describing the grouping interval length and giving its possible values (**when**).*

The third part of the notation defined in *Tab.3.* provides information about the considered grouping location size or geological information (***where**, location size or geological information code*). The results are discussed in separate paragraphs going from ***G*** to ***H*** or from ***H*** to ***KH***, in case of laboratory and in-situ measurements, respectively. In case of laboratory measurements, ***JH*** and ***KH*** grouping options are not considered because of the lack of clear geological grouping of settlements at E-Mecsek Mts. and Sajó and Hernád Rivers Valleys and also the low sample numbers. ***G*** option (*Tab.3.*) is not possible in case of in-situ measurements of this study because the measurements were limited to only one of the studied areas, Békés County.

where	grouping location size or geological information	possible values
G	**all studied areas**	**all studied areas**
H	**one studied area**	**Békés County** **E-Mecsek Mts.** **Sajó and Hernád Rivers Valleys**
JH	**geological type at Békés County**	**clay** **loess** **turf**
KH	**geological age at Békés County**	**Pleistocene** **Holocene**

*Tab.3.: The possibilities for the third part of the notation describing the grouping location size or geological information and giving its possible values (**where**).*

6.1. Results of laboratory measurements on samples

6.1.1. Radon and thoron emanations of samples

In the closed chamber technique measurements the radon emanations (**PV6.**) are provided directly (*Eq.3., 4.*). However, in case of thoron the so-called thoron generation rates are gained first (*Eq.17.*) and the thoron emanation results are then calculated based on *Eq.13.*

(**SJ4.**). Altogether 92 radon and thoron emanation results are available for the 46 adobe building material samples. The relative uncertainties of the data were always estimated to be around 13 % and 20 % (consider the information provided in Chapter 5.2.2.), respectively, for radon and thoron emanations. Individual thoron emanation data should be handled carefully. However, statistics of sample groups presented below is useful and provide real information.

The statistics for all radon and thoron emanation data (***RnE-C-G*** and ***TnE-C-G***) of samples originated from either of the studied areas are summarized in *Tab.4.* and visualized in *Fig.12.* The median values are 7.9 and 5.7 kg^{-1} s^{-1} for radon and thoron emanations, respectively.

Emanation

	Count	Min.	L. quartile	Median	U. quartile	Max.	Average	St. dev.	St. skewness	St. kurtosis	MAD/Median
Radon	**46**	**3.1**	**6.7**	**7.9**	**9.6**	**13.8**	**8.2**	**2.3**	**0.86**	**0.30**	**0.20**
Thoron	**46**	**1.9**	**3.9**	**5.7**	**7.3**	**11.9**	**5.8**	**2.4**	**1.67**	**0.06**	**0.28**

*Tab.4.: Count (sample number), minimum, lower quartile, median, upper quartile, maximum, average, st. deviation (kg^{-1} s^{-1}), st. skewness, st. kurtosis and MAD/median for all radon and thoron emanation results (**RnE-C-G** and **TnE-C-G**).*

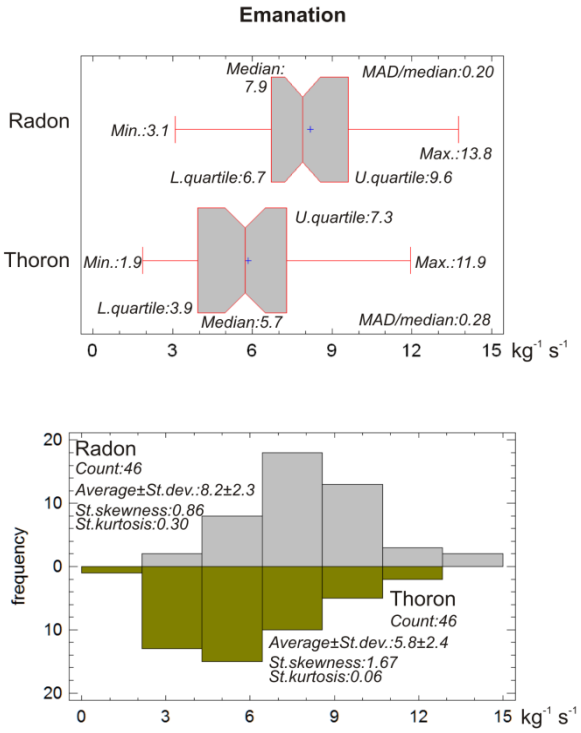

*Fig.12.: Box-whisker plots and frequency histograms of all radon and thoron emanation results (**RnE-C-G** and **TnE-C-G**).*

The adobe sample statistics for the three studied areas separately (***RnE-C-H*** and ***TnE-C-H***) are summarized in *Tab.5.* and visualized in *Fig.13.* The radon emanation median

values are 7.6, 8.1 and 8.6 kg^{-1} s^{-1}, whereas the thoron emanation medians are 5.7, 6.7 and 4.5 kg^{-1} s^{-1} for Békés County, E-Mecsek Mts. and Sajó and Hernád Rivers Valleys (presented as S-H Rivers Valleys in all tables), respectively. MW tests did not show any statistically significant differences among the three studied areas neither regarding the radon nor the thoron emanation medians (*Fig.13.*).

Emanation

		Count	Min.	L. quartile	Median	U. quartile	Max.	Average	St. dev.	St. skewness	St. kurtosis	MAD/Median
Radon	**Békés County**	**18**	**3.1**	**6.5**	**7.6**	**8.6**	**10.1**	**7.4**	**1.9**	**-1.38**	**0.42**	**0.14**
	E-Mecsek Mts.	**18**	**5.6**	**7.1**	**8.1**	**10.0**	**13.1**	**8.7**	**2.3**	**0.78**	**-0.66**	**0.21**
	S-H Rivers Valleys	**10**	**4.7**	**6.2**	**8.6**	**9.6**	**13.8**	**8.7**	**2.7**	**0.50**	**0.05**	**0.20**
Thoron	**Békés County**	**18**	**2.2**	**3.9**	**5.7**	**6.0**	**8.8**	**5.3**	**1.6**	**0.28**	**0.11**	**0.20**
	E-Mecsek Mts.	**18**	**2.5**	**4.8**	**6.7**	**7.6**	**10.8**	**6.5**	**2.5**	**0.36**	**-0.55**	**0.28**
	S-H Rivers Valleys	**10**	**1.9**	**3.8**	**4.5**	**7.4**	**11.9**	**5.7**	**3.1**	**1.14**	**0.12**	**0.47**

*Tab.5.: Count (sample number), minimum, lower quartile, median, upper quartile, maximum, average, st. deviation (kg^{-1} s^{-1}), st. skewness, st. kurtosis and MAD/median for radon and thoron emanation results separately for the three studied areas (**RnE-C-H** and **TnE-C-H**).*

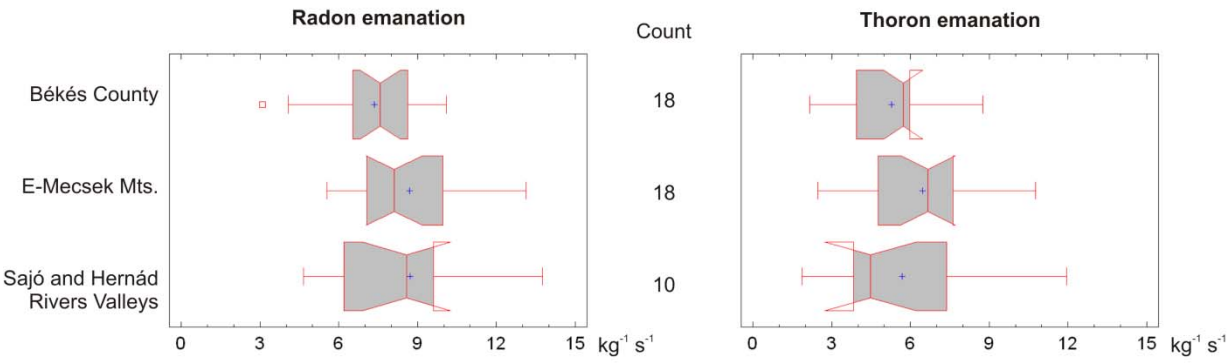

*Fig.13.: Box-whisker plots of radon and thoron emanation results separately for the three studied areas (**RnE-C-H** and **TnE-C-H**).*

6.1.2. ^{226}Ra, ^{232}Th and ^{40}K activity concentrations of samples

Based on the gamma-ray spectroscopy analysis of the 46 adobe building material samples altogether 138 ^{226}Ra, ^{232}Th and ^{40}K activity concentrations measurement data became available. This part of the work was partially published in **SJ2.** The relative uncertainties of the data were always around 13, 9 and 7 %, respectively for the three parameters.

The statistics for all ^{226}Ra, ^{232}Th and ^{40}K activity concentration data (***Ra-C-G***, ***Th-C-G*** and ***K-C-G***) of samples originated from either of the studied areas are summarized in *Tab.6.* and visualized in *Fig.14.* It is seen the median values are 28, 32 and 364 Bq kg^{-1} for ^{226}Ra, ^{232}Th and ^{40}K, respectively. The linear correlation coefficient between ^{226}Ra and ^{232}Th activity concentrations (r = 0.64) indicate a statistically significant, moderately strong relationship. The values of r for ^{40}K are lower (0.34 and 0.31) however, still indicate statistically significant, weak but non-zero relationships.

Activity concentration

	Count	Min.	L. quartile	Median	U. quartile	Max.	Average	St. dev.	St. skewness	St. kurtosis	MAD/Median
^{226}Ra	**46**	**18**	**26**	**28**	**31**	**41**	**29**	**5**	**1.01**	**0.74**	**0.09**
^{232}Th	**46**	**19**	**28**	**32**	**36**	**50**	**32**	**6**	**1.05**	**1.01**	**0.13**
^{40}K	**46**	**281**	**330**	**364**	**384**	**488**	**366**	**51**	**1.68**	**-0.08**	**0.09**

*Tab.6.: Count (sample number), minimum, lower quartile, median, upper quartile, maximum, average, st. deviation (Bq kg^{-1}), st. skewness, st. kurtosis and MAD/median for all ^{226}Ra, ^{232}Th and ^{40}K activity concentration results (**Ra-C-G**, **Th-C-G** and **K-C-G**).*

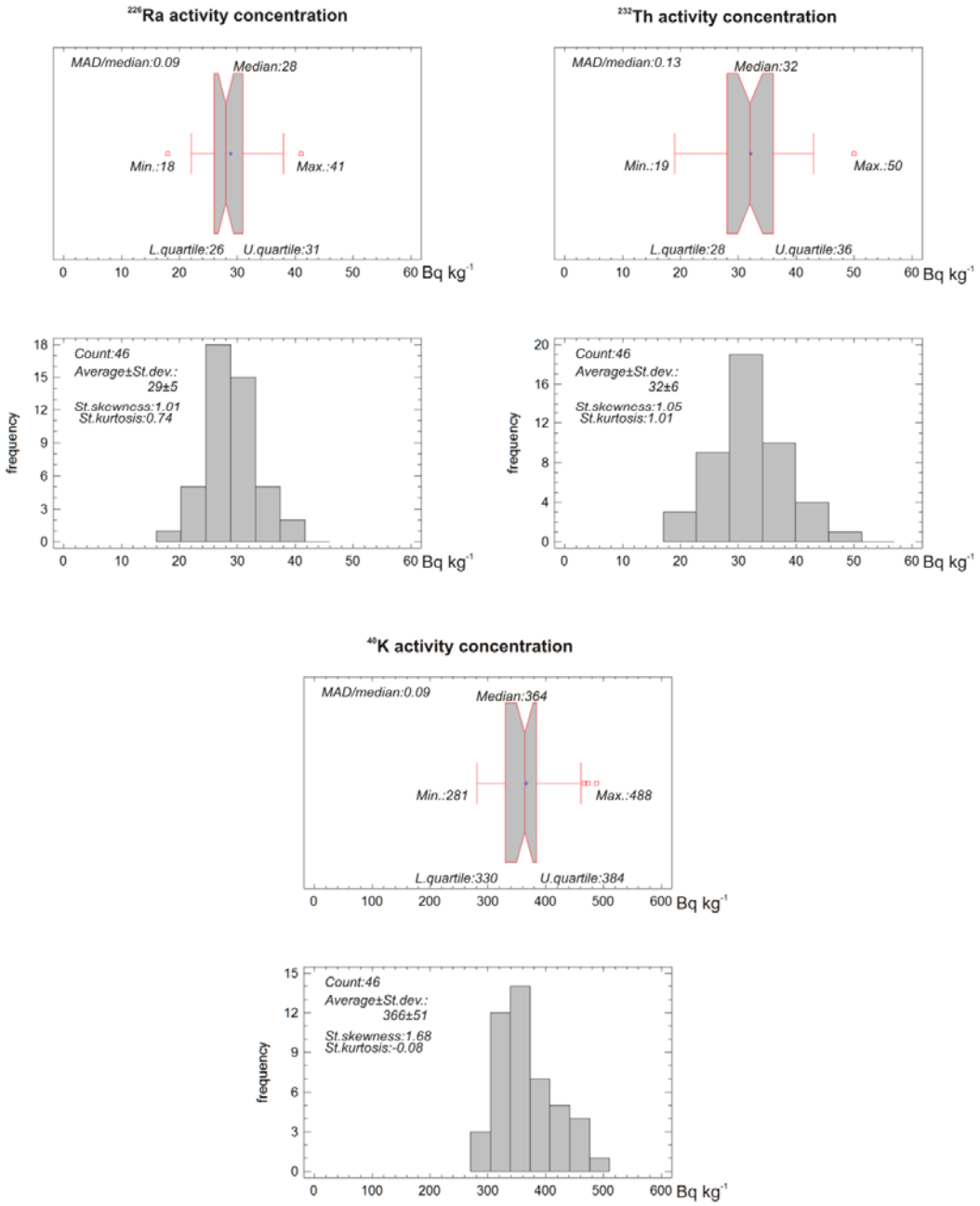

*Fig.14.: Box-whisker plots and frequency histograms of all ^{226}Ra, ^{232}Th and ^{40}K activity concentration results (**Ra-C-G**, **Th-C-G** and **K-C-G**).*

The adobe sample statistics for the three studied areas separately (***Ra-C-H***, ***Th-C-H*** and ***K-C-H***) are summarized in *Tab.7.* and visualized in *Fig.15.* The ^{226}Ra activity concentration median values are 28, 31 and 26 Bq kg^{-1}, the ^{232}Th medians are 29, 37 and 29 Bq kg^{-1} and the ^{40}K medians are 367, 360 and 365 Bq kg^{-1} for Békés County, E-Mecsek Mts. and Sajó and Hernád Rivers Valleys, respectively. MW tests show statistically significant differences among all three ^{226}Ra medians and satisfy that ^{232}Th activity concentrations of adobe samples originated from E-Mecsek Mts. are statistically significantly higher than that of other adobe

samples (*Fig.15.*). MW tests did not show any statistically significant differences among ^{40}K activity concentration medians at the three studied areas.

Activity concentration

		Count	Min.	L. quartile	Median	U. quartile	Max.	Average	St. dev.	St. skewness	St. kurtosis	MAD/Median
^{226}Ra	Békés County	18	23	27	28	30	38	29	4	2.09	1.55	0.07
	E-Mecsek Mts.	18	25	28	31	34	41	31	4	1.20	0.41	0.08
	S-H Rivers Valleys	10	18	22	26	27	32	25	4	0.16	-0.09	0.12
^{232}Th	Békés County	18	22	27	29	32	36	29	4	-0.22	-0.25	0.09
	E-Mecsek Mts.	18	29	35	37	40	50	38	5	1.56	1.89	0.07
	S-H Rivers Valleys	10	19	25	29	31	32	28	4	-1.36	0.05	0.09
^{40}K	Békés County	18	285	332	367	428	488	379	60	0.70	-0.74	0.12
	E-Mecsek Mts.	18	281	330	360	375	473	360	46	1.46	0.94	0.08
	S-H Rivers Valleys	10	286	317	365	382	413	356	41	-0.45	-0.49	0.08

*Tab.7.: Count (sample number), minimum, lower quartile, median, upper quartile, maximum, average, st. deviation (Bq kg^{-1}), st. skewness, st. kurtosis and MAD/median for ^{226}Ra, ^{232}Th and ^{40}K activity concentration results separately for the three studied areas (**Ra-C-H**, **Th-C-H** and **K-C-H**).*

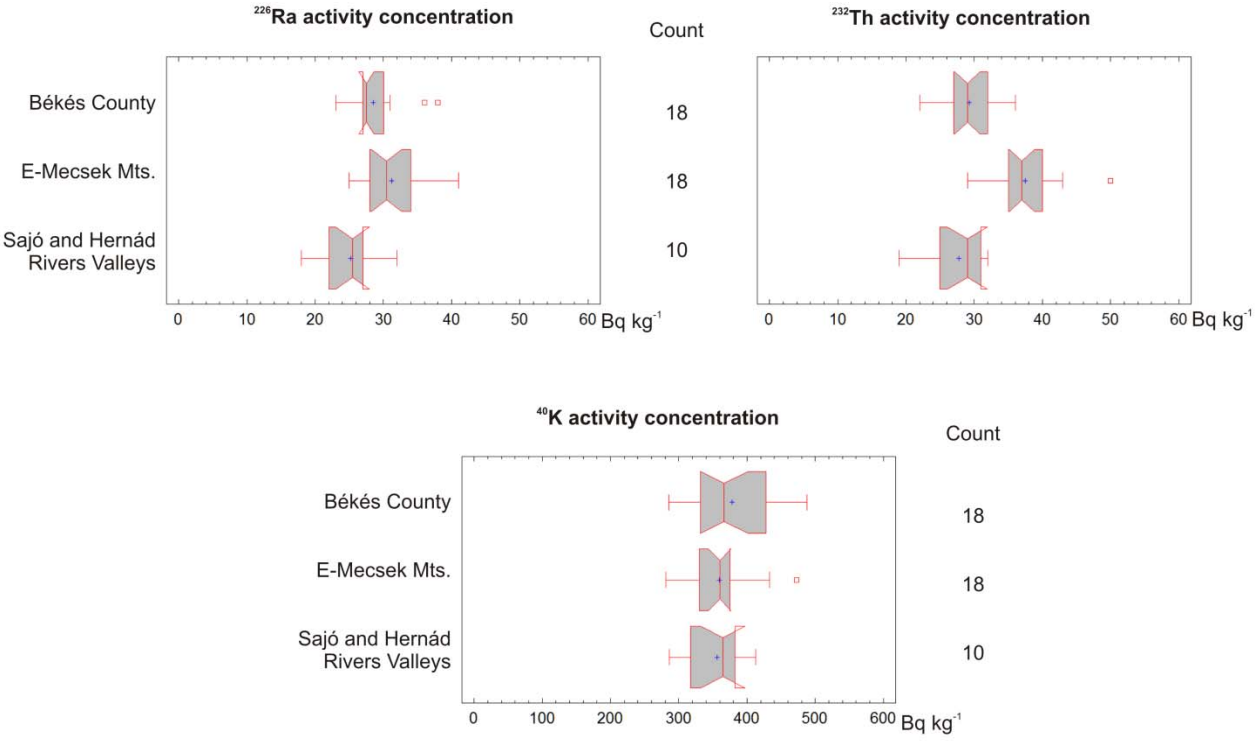

*Fig.15.: Box-whisker plots of ^{226}Ra, ^{232}Th and ^{40}K activity concentration results separately for the three studied areas (**Ra-C-H**, **Th-C-H** and **K-C-H**).*

6.1.2.1. *Hazard indices of samples*

As the statistics of hazard indices directly depend on the previously shown ^{226}Ra, ^{232}Th and ^{40}K activity concentration data it is not informative to present them in details in tables. However, they can be seen on *Fig.16*. The median and maximum are meaningful to compare to threshold values. The Ra_{eq}, I, H_{ex} and H_{in} hazard indices calculations (*Eq.6., 7., 8., 9.*) show medians of 105 Bq kg^{-1}, 0.39, 0.28 and 0.36, respectively. Even the maximum values of 141 Bq kg^{-1}, 0.52, 0.38 and 0.47 for the same indices, respectively are far below all the usually applied threshold values of 370 Bq kg^{-1} and 1 (*Fig.16.*, **SJ2.**).

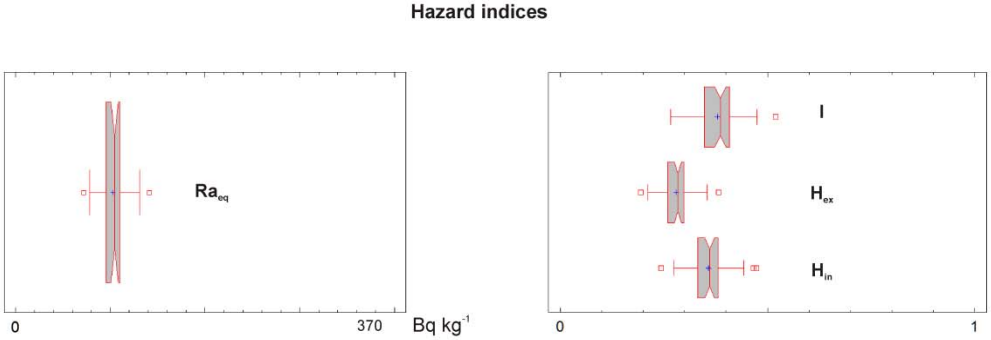

Fig.16.: Box-whisker plots of Ra_{eq} and I, H_{ex} and H_{in} hazard indices (Eq.6., 7., 8., 9.) of the 46 adobe samples. The Ra_{eq} threshold of 370 Bq kg^{-1} and the I, H_{ex} and H_{in} thresholds of 1 are marked on the scales.

6.1.2.2. *Estimated annual external effective doses in dwellings*

The statistics of annual external effective dose estimation results from ^{226}Ra, ^{232}Th and ^{40}K activity concentrations of adobe samples (*Eq.10.*, *11.*, $\boldsymbol{ED_{RaThK}\text{-}Y\text{-}G}$) are summarized in *Tab.8.* and visualized in *Fig.17.* The estimated annual effective dose has a median of 0.45 mSv y^{-1}. For other measures see *Fig.17.*

Estimated annual external effective dose

Count	Min.	L. quartile	Median	U. quartile	Max.	Average	St. dev.	St. skewness	St. kurtosis	MAD/Median
46	0.31	0.41	0.45	0.48	0.61	0.45	0.06	0.64	0.90	0.07

Tab.8.: Count (sample number), minimum, lower quartile, median, upper quartile, maximum, average, st. deviation (mSv y^{-1}), st. skewness, st. kurtosis and MAD/median for all estimated annual external effective doses from ^{226}Ra, ^{232}Th and ^{40}K activity concentrations of adobe samples ($\boldsymbol{ED_{RaThK}\text{-}Y\text{-}G}$).

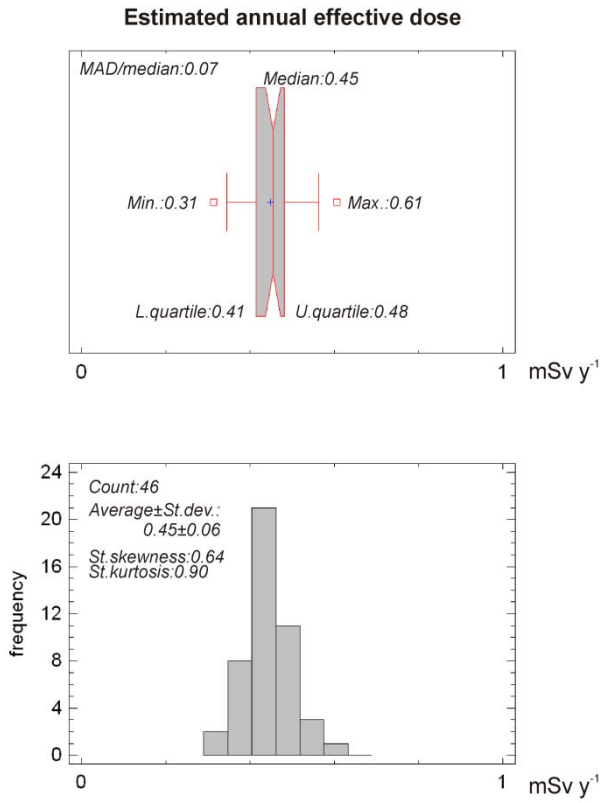

*Fig.17.: Box-whisker plot and frequency histogram of all estimated annual external effective doses from ^{226}Ra, ^{232}Th and ^{40}K activity concentrations of adobe samples (**ED_{RaThK}-Y-G**).*

6.1.3. Radon and thoron emanation fractions of samples

Dividing the radon and thoron emanation results by the measured ^{226}Ra and ^{232}Th activity concentrations, the radon and thoron emanation fractions are gained for the purposes described in Chapter 2.3.1. Hence, altogether 92 radon and thoron emanation fraction data are available for the 46 adobe samples. The relative uncertainties were around 19 and 20 % for radon and thoron emanation fractions, respectively. Here it is noted again that any individual thoron emanation fraction data should be handled carefully. However, statistics of sample groups presented below provide real information about the general levels.

The statistics for all radon and thoron emanation fraction data (***f_{RnE}-C-G*** and ***f_{TnE}-C-G***) of samples originated from either of the studied areas are summarized in *Tab.9.* and visualized in *Fig.18*. It is seen that the median values are 27 and 18 % for radon and thoron emanation fractions, respectively. Based on the MW test, the 18 % thoron emanation fraction median is statistically significantly lower than the 27 % of radon. The linear correlation coefficient between radon and thoron emanation fractions (r = 0.31) indicate a statistically significant but weak relationship.

Emanation fraction

	Count	Min.	L. quartile	Median	U. quartile	Max.	Average	St. dev.	St. skewness	St. kurtosis	MAD/Median
Radon	**46**	**12**	**24**	**27**	**32**	**53**	**28**	**7**	**1.67**	**2.23**	**0.17**
Thoron	**46**	**7**	**13**	**18**	**22**	**38**	**18**	**7**	**1.51**	**0.90**	**0.24**

*Tab.9.: Count (sample number), minimum, lower quartile, median, upper quartile, maximum, average, st. deviation (%), st. skewness, st. kurtosis and MAD/median for all radon and thoron emanation fraction results (**f_{RnE}-C-G** and **f_{TnE}-C-G**).*

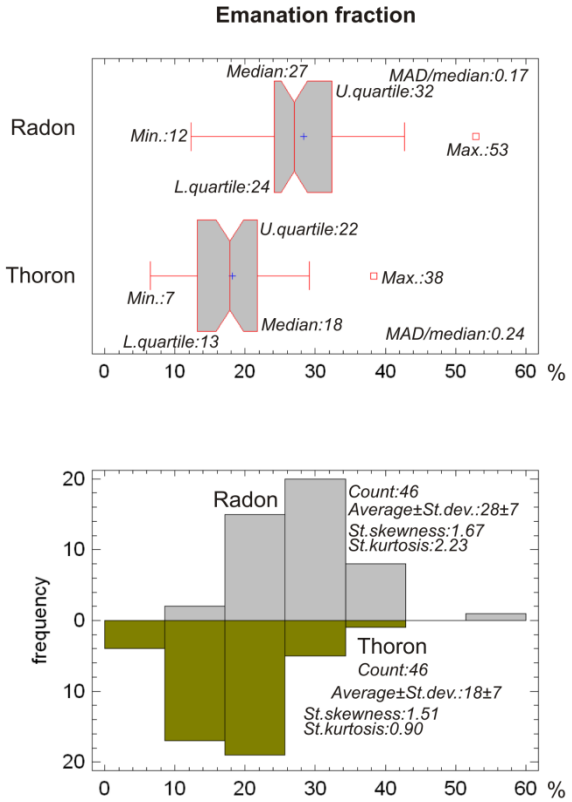

*Fig.18.: Box-whisker plots and frequency histograms of all radon and thoron emanation fraction results (**f_{RnE}-C-G** and **f_{TnE}-C-G**).*

The adobe sample statistics for the three studied areas separately (**f_{RnE}-C-H** and **f_{TnE}-C-H**) are summarized in *Tab.10.* and visualized in *Fig.19.* The radon emanation fraction median values are 26, 27 and 34 %, whereas those of thoron are 18, 17 and 20 % for Békés County, E-Mecsek Mts. and Sajó and Hernád Rivers Valleys, respectively. The MW tests carried out show that the radon emanation fraction median of adobe samples from Sajó and Hernád Rivers Valleys is statistically significantly higher than that of adobe samples from the other two studied areas (*Fig.19.*). The thoron emanation fractions also tend to be higher at Sajó and

Hernád Rivers Valleys than at Békés County and E-Mecsek Mts. (*Fig.19.*). However, the MW tests did not show any statistically significant differences among the medians.

Emanation fraction

		Count	Min.	L. quartile	Median	U. quartile	Max.	Average	St. dev.	St. skewness	St. kurtosis	MAD/Median
Radon	Békés County	18	12	23	26	31	33	26	6	-1.37	0.05	0.18
	E-Mecsek Mts.	18	16	24	27	33	35	28	6	-0.34	-0.63	0.16
	S-H Rivers Valleys	10	19	26	34	40	53	35	10	0.38	0.16	0.19
Thoron	Békés County	18	8	14	19	21	28	18	5	0.30	-0.34	0.22
	E-Mecsek Mts.	18	7	13	17	21	27	17	6	-0.11	-0.49	0.25
	S-H Rivers Valleys	10	7	13	20	28	38	20	10	0.61	-0.23	0.36

*Tab.10.: Count (sample number), minimum, lower quartile, median, upper quartile, maximum, average, st. deviation (%), st. skewness, st. kurtosis and MAD/median for radon and thoron emanation fraction results separately for the three studied areas (**f_{RnE}-C-H** and **f_{TnE}-C-H**).*

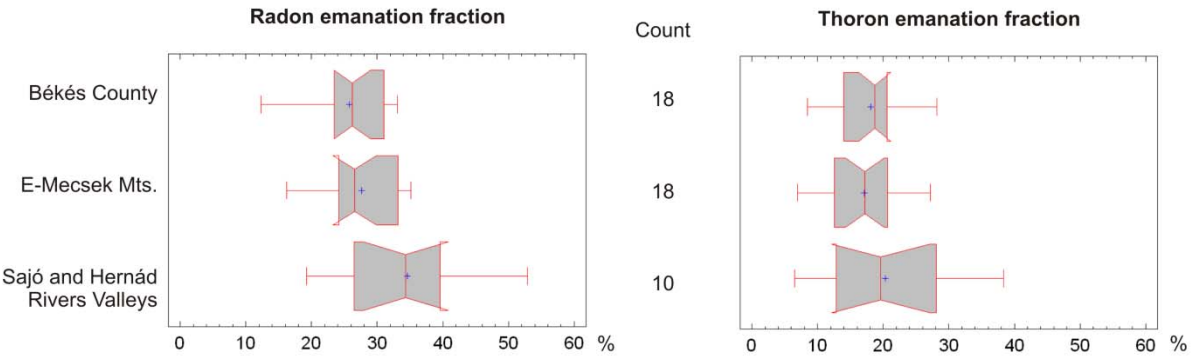

*Fig.19.: Box-whisker plots of radon and thoron emanation fraction results separately for the three studied areas (**f_{RnE}-C-H** and **f_{TnE}-C-H**).*

6.1.4. Grain size distributions of samples

The results of grain size distribution measurements are presented in a different structure than other results. First the inorganic raw material of adobe is classified into soil texture classes, then the characteristic peaks in clay and silt fractions are observed (**PV5., 6. and 7.**), and finally the statistics of estimated specific surface area results (SSA) are presented. At the end of this subchapter a correlation analysis is carried out for carefully selected grain size fractions vs. ^{226}Ra, ^{232}Th, ^{40}K activity concentrations and radon, thoron emanation fractions.

6.1.4.1. Soil texture classification of inorganic raw materials in adobe – clay, silt and sand

After carefully coupling the mass% and the volume% data of wet sieving and laser grain size analysis, the following results are gained. The proportions of clay (< 2 μm), silt (2-50 μm) and sand (0.05-2 mm) show medians of 15, 73 and 9 mass%, respectively. The individual data points are shown in *Fig.20.* Based on these results, the USDA soil texture classification of the inorganic raw material of adobes show a homogeneous sample group: almost all samples fall into the *silt loam* class. Only one significant exception is observed from Sajó and Hernád Rivers Valleys (*Fig.20.*).

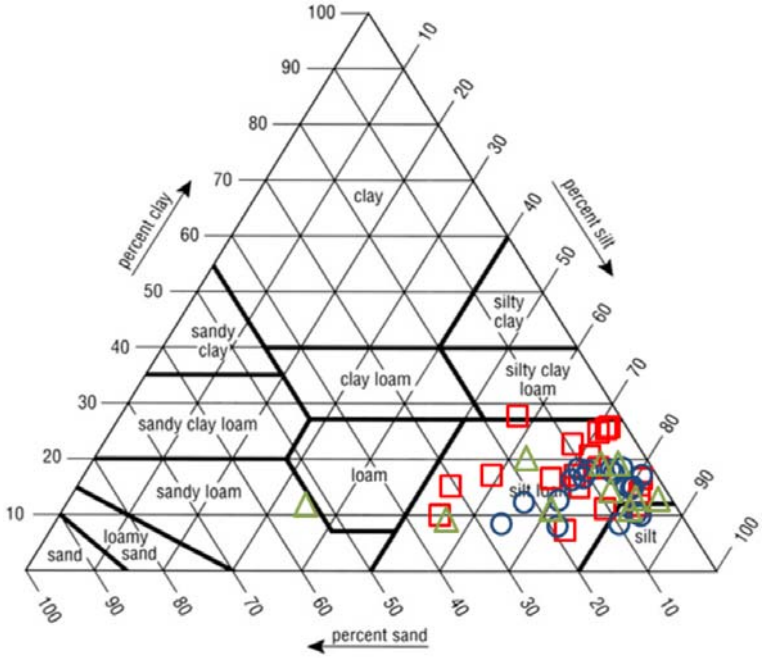

Fig.20.: Classification of inorganic raw materials in the 46 adobe building material samples by the USDA soil texture triangle (Wunsch 2009): silt loam. The red quadrates, blue circles and green triangles represent the adobe samples from Békés County, E-Mecsek Mts. and Sajó and Hernád Rivers Valleys, respectively.

6.1.4.2. Characteristic peaks in clay and silt fractions

The representative detailed results of laser grain size analysis in clay and silt fractions (0-50 μm) are presented in *Fig.21.* (up to 63 μm grain size already in the sand fraction). On these graphs three characteristic peaks, always at the same grain size positions are observed in most of the adobe samples: at 2-3, 10 and 30 μm grain sizes[17] (*Fig.21.*). Only two samples from Békés County did not show all of these peaks: the one at 30 μm is lacking. However, more significant differences can be observed in the amplitudes than in positions. This variation is described by the maximum volume% values (proportion among other size grains, *Fig.21.*). The 2-3 μm peak shows maximum volume% values of 2.5, 2 and 2 volume%, the 10 μm peak of 4, 3.5 and 3.5 volume% and the 30 μm peak of 2.5, 5 and 3.5 volume% at Békés County, E-Mecsek Mts. and Sajó and Hernád Rivers Valleys, respectively (*Fig.21.*). The proportion of grains with 30 μm grain size varies the most significantly among studied areas.

[17]These are the better grain size (diameter) resolution graphs of 27 adobe samples which were measured by the instrument of Research Centre for Astronomy and Earth Sciences, Hungarian Academy of Sciences. On the weaker resolution graphs measured by the instrument of Lithosphere Fluid Research Lab, the 10 and 30 μm peaks overlap.

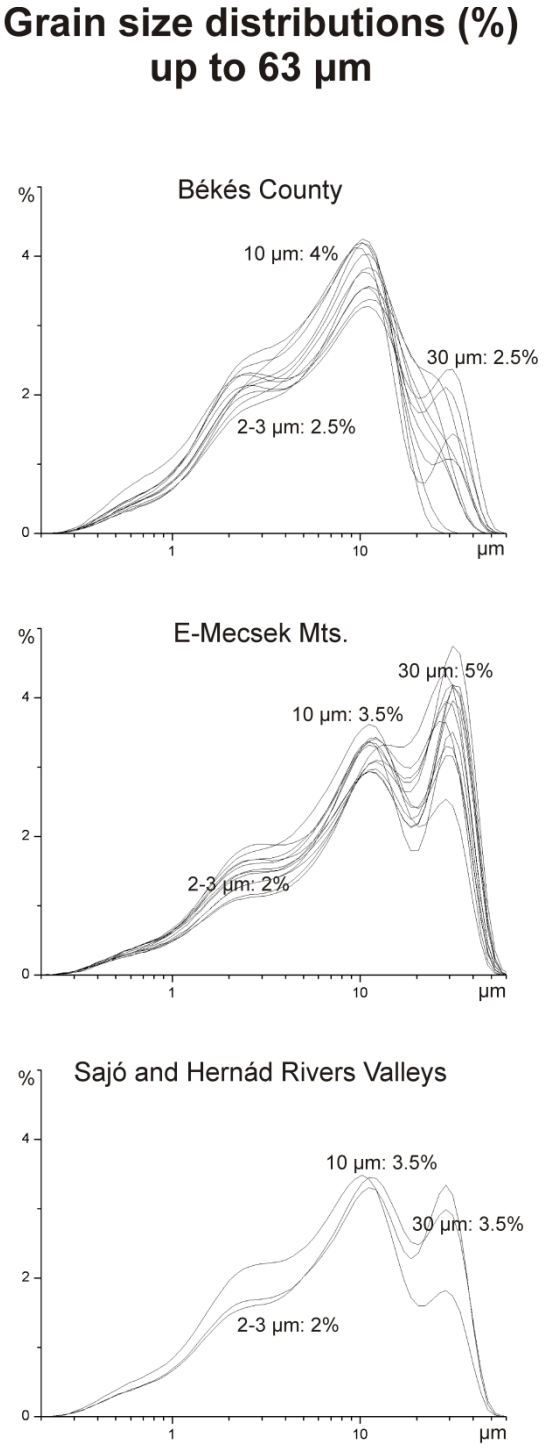

Fig.21.: Characteristic peaks at 2-3, 10 and 30 µm grain sizes in adobe samples from the three studied areas of Békés County, E-Mecsek Mts. and Sajó and Hernád Rivers Valleys. The figure presents the maximum volume% results at the characteristic peaks based on the better grain size resolution measurements of 27 adobe samples.

6.1.4.3. Estimated specific surface areas of samples

Altogether 46 specific surface area data were estimated for all of the adobe samples. The uncertainty of the estimation is high due to reasons described in Chapter 4.1.4.3. However, statistics of sample groups presented below provide real information about the general levels.

The statistics for all specific surface area data (***SSA-C-G***) of samples originated from either of the studied areas are summarized in *Tab.11.* and visualized in *Fig.22.* The median value is given to be 0.51 m^2 g^{-1}.

Estimated specific surface area

Count	Min.	L. quartile	Median	U. quartile	Max.	Average	St. dev.	St. skewness	St. kurtosis	MAD/Median
46	0.32	0.43	0.51	0.54	0.72	0.49	0.10	0.71	-0.29	0.12

*Tab.11.: Count (sample number), minimum, lower quartile, median, upper quartile, maximum, average, st. deviation (m^2 g^{-1}), st. skewness, st. kurtosis and MAD/median for all estimated specific surface areas of adobe samples (**SSA-C-G**).*

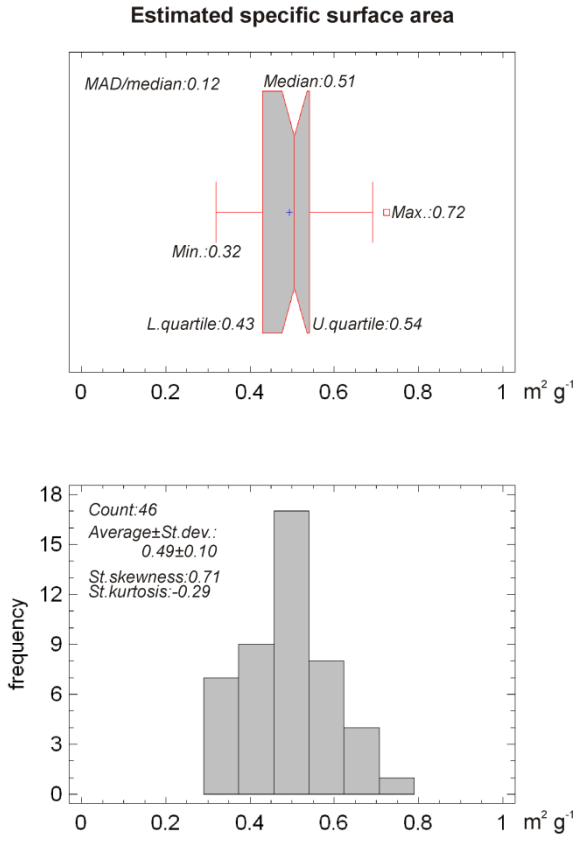

*Fig.22.: Box-whisker plot and frequency histogram of all estimated specific surface areas of adobe samples (**SSA-C-G**).*

The adobe sample statistics for the three studied areas separately (***SSA-C-H***) are summarized in *Tab.12.* and visualized on *Fig.23.* The median values are 0.54, 0.46 and 0.51 m^2 g^{-1} for Békés County, E-Mecsek Mts. and Sajó and Hernád Rivers Valleys, respectively. These medians all fall into the same order of magnitude, however, the MW tests carried out reveal that the specific surface area median of adobe samples from Békés County is statistically significantly higher than that of adobe samples from E-Mecsek Mts. (*Fig.23.*).

Estimated specific surface area

	Count	Min.	L. quartile	Median	U. quartile	Max.	Average	St. dev.	St. skewness	St. kurtosis	MAD/Median
Békés County	**18**	**0.32**	**0.47**	**0.54**	**0.66**	**0.72**	**0.55**	**0.11**	**-0.42**	**-0.58**	**0.17**
E-Mecsek Mts.	**18**	**0.33**	**0.38**	**0.46**	**0.51**	**0.54**	**0.45**	**0.07**	**-0.76**	**-1.06**	**0.10**
S-H Rivers Valleys	**10**	**0.32**	**0.44**	**0.51**	**0.54**	**0.56**	**0.48**	**0.08**	**-1.23**	**-0.22**	**0.09**

*Tab.12.: Count (sample number), minimum, lower quartile, median, upper quartile, maximum, average, st. deviation (m^2 g^{-1}), st. skewness, st. kurtosis and MAD/median for estimated specific surface areas of adobe samples separately for the three studied areas (**SSA-C-H**).*

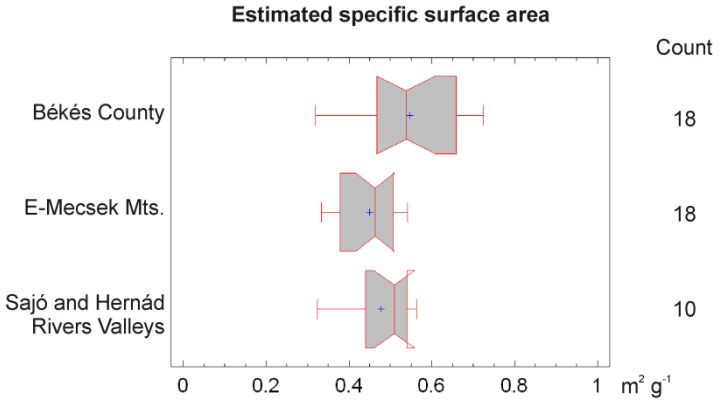

*Fig.23.: Box-whisker plots of estimated specific surface areas of adobe samples separately for the three studied areas (**SSA-C-H**).*

6.1.4.4. Correlation analysis: percentage of grain size fractions vs. ^{226}Ra, ^{232}Th, ^{40}K activity concentrations, radon, thoron emanation fractions

The correlation analysis was carried out in two parallel steps: sample parameters (^{226}Ra, ^{232}Th, ^{40}K activity concentrations, radon, thoron emanation fractions) vs. (1) clay, silt and sand fractions and vs. (2) observed peaks in clay and silt fractions, such as ranges of 0-1, 1-4, 4-20 and 20-63 μm (*Fig.21.*). The correlation coefficients are given here for the three studied areas separately because of their observed significant differences. These are highlighted by frames in tables when they are shown to be statistically significant.

6.1.4.4.1. Correlations with clay, silt and sand fractions

Correlation coefficients among ^{226}Ra, ^{232}Th, ^{40}K activity concentrations, radon, thoron emanation fractions (***Ra-C-H***, ***Th-C-H***, ***K-C-H***, ***f_{RnE}-C-H***, ***f_{TnE}-C-H***) and proportions of clay, silt and sand in the grain size distributions for adobe samples of the three studied areas are shown in *Tab.13.* At Békés County and Sajó and Hernád Rivers Valleys the ^{226}Ra, ^{232}Th, ^{40}K activity concentrations generally show positive correlation coefficients with silt and clay fractions. However, at E-Mecsek Mts. the results show statistically significant, but inverse relationships with silt fraction. The radon emanation fraction seems to be connected the most to the proportion of silt fraction.

	Békés County					E-Mecsek Mts.					Sajó and Hernád Rivers Valleys				
r	**Ra**	**Th**	**K**	**f_{RnE}**	**f_{TnE}**	**Ra**	**Th**	**K**	**f_{RnE}**	**f_{TnE}**	**Ra**	**Th**	**K**	**f_{RnE}**	**f_{TnE}**
clay	0.25	0.19	0.43	-0.09	0.09	0.17	0.16	0.13	0.09	0.23	0.22	0.47	0.00	0.29	-0.15
silt	0.34	0.11	-0.08	0.49	-0.19	-0.22	-0.59	-0.54	0.12	-0.10	0.68	0.64	0.88	0.20	0.27
sand	-0.47	-0.24	-0.19	-0.40	0.11	0.08	0.43	0.39	-0.15	-0.02	-0.69	-0.71	-0.83	-0.25	-0.21

*Tab.13.: Correlation coefficients for the three studied areas among ^{226}Ra, ^{232}Th, ^{40}K activity concentrations, radon, thoron emanation fractions (**Ra-C-H**, **Th-C-H**, **K-C-H**, **f_{RnE}-C-H**, **f_{TnE}-C-H**) and the estimated proportions of clay, silt and sand in the grain size distributions. The colors from blue to red indicate increasing correlation coefficients among which the ones referring to statistically significant relationships are highlighted by frames.*

6.1.4.4.2. Correlations with characteristic peaks in clay and silt fractions

The correlation coefficients among ^{226}Ra, ^{232}Th, ^{40}K activity concentrations, radon, thoron emanation fractions (***Ra-C-H***, ***Th-C-H***, ***K-C-H***, ***f_{RnE}-C-H***, ***f_{TnE}-C-H***) and 2-3, 10 and 30 μm characteristic peaks in clay and silt fractions, i.e. 0-1, 1-4, 4-20 and 20-63 μm grain size

ranges, are shown in *Tab.14.* In this case, Békés County and E-Mecsek Mts. seem to be similar: for ^{226}Ra, ^{232}Th, ^{40}K activity concentrations positive correlation coefficients are observed with 1-4 and 4-20 µm ranges. Whereas, in case of Sajó and Hernád Rivers Valleys the positive correlation coefficients are observed with the 20-63 µm range. The radon emanation fraction is the most connected to the presence of 10 µm peak.

	Békés County					E-Mecsek Mts.					Sajó and Hernád Rivers Valleys				
r	Ra	Th	K	f_{RnE}	f_{TnE}	Ra	Th	K	f_{RnE}	f_{TnE}	Ra	Th	K	f_{RnE}	f_{TnE}
0-1 µm	-0.01	0.11	0.30	-0.25	0.07	-0.09	-0.21	-0.12	0.11	0.03	-0.21	-0.43	-0.56	-0.53	-0.48
1-4 µm	0.25	0.27	0.58	-0.23	0.06	0.10	0.27	0.25	0.03	0.42	-0.42	-0.27	-0.81	-0.08	-0.40
4-20 µm	0.43	0.26	0.62	-0.05	-0.12	0.34	-0.03	0.31	0.67	-0.07	-0.12	0.20	-0.06	0.37	0.15
20-63 µm	-0.29	-0.26	-0.64	0.16	-0.01	-0.23	-0.08	-0.30	-0.43	-0.22	0.41	0.21	0.76	-0.01	0.33

*Tab.14.: Correlation coefficients for the three studied areas among ^{226}Ra, ^{232}Th, ^{40}K activity concentrations, radon, thoron emanation fractions (**Ra-C-H**, **Th-C-H**, **K-C-H**, **f_{RnE}-C-H**, **f_{TnE}-C-H**) and the proportions of characteristic peaks in clay and silt fractions. The colors from blue to red indicate increasing correlation coefficients among which the ones referring to statistically significant relationships are highlighted by frames.*

6.1.4.4.3. Correlations with specific surface area

The correlation coefficients among ^{226}Ra, ^{232}Th, ^{40}K activity concentrations, radon, thoron emanation fractions (***Ra-C-H***, ***Th-C-H***, ***K-C-H***, ***f_{RnE}-C-H***, ***f_{TnE}-C-H***) and specific surface areas (***SSA-C-H***) are shown in *Tab.15.* At Békés County and Sajó and Hernád Rivers Valleys the ^{40}K activity concentrations show statistically significant positive correlation coefficients with the specific surface area. The values with ^{226}Ra and ^{232}Th activity concentrations are also positive, but statistically insignificant. At E-Mecsek Mts. the same results show no relationship. The correlation coefficients of specific surface area with thoron emanation fraction are more positive than that with radon emanation fraction in case of E-Mecsek Mts. and Sajó and Hernád Rivers Valleys.

	Békés County					E-Mecsek Mts.					Sajó and Hernád Rivers Valleys				
	Ra	Th	K	f_{RnE}	f_{TnE}	Ra	Th	K	f_{RnE}	f_{TnE}	Ra	Th	K	f_{RnE}	f_{TnE}
SSA	0.37	0.29	0.52	0.06	-0.01	0.01	-0.08	-0.03	0.10	0.27	0.50	0.29	0.70	0.09	0.24

*Tab.15.: Correlation coefficients for the three studied areas among ^{226}Ra, ^{232}Th, ^{40}K activity concentrations, radon, thoron emanation fractions (**Ra-C-H**, **Th-C-H**, **K-C-H**, **f_{RnE}-C-H**, **f_{TnE}-C-H**) and the estimated specific surface areas (**SSA-C-H**). The colors from blue to red indicate increasing correlation coefficients among which the ones referring to statistically significant relationships are highlighted by frames.*

6.2. Results of in-situ measurements in dwellings

6.2.1. Indoor radon and thoron activity concentrations in dwellings

In the 53 adobe dwellings of Békés County 190 radon and 189 thoron measurement data are available for the four seasons in the measurement period from December 2010 to November 2011 (**SJ6.**). For radon and thoron activity concentrations, the overall uncertainties are determined to be 20 and 30 % and the lowest accepted LLDs to be around 15 and 80 Bq m^{-3}, respectively[18]. As already noted above (Chapter 4.2.2.), to represent low values in the statistics, all measurement data were used in the statistical evaluation even though a part of them were below their LLDs (AMC 2001, Reimann et al. 2008). The annual average radon and thoron activity concentrations were determined in 43 and 42 adobe dwellings, respectively, only where measurement data were available in all seasons. These annual average radon and thoron activity concentrations were used for inhalation dose estimations in dwellings.

6.2.1.1. Annual activity concentrations

The statistics of annual average activity concentrations at Békés County (***RnC-Y-H*** and ***TnC-Y-H***) are summarized in *Tab.16.* and visualized on *Fig.24.* It is shown that annual radon activity concentration has a median of 188 Bq m^{-3}, and it is 232 Bq m^{-3} for thoron. The geometric means of the results are also presented for comparison purposes in the discussion, they are 166 and 211 Bq m^{-3}, respectively for radon and thoron.

Being consequent with the standardized skewness and the standardized kurtosis values (*Tab.16.*, *Fig.24.*), SW tests reject the normality, but do not reject the lognormality for annual average radon data and for thoron, it cannot reject the idea of neither normal nor lognormal distributions[19]. For radon the best fitting distribution is the lognormal distribution, and for thoron, normal distribution better fits than lognormal. Summarizing, during further analysis of the results it is accepted that annual radon data come from a lognormal and annual thoron data come from a normal distribution (**SJ6.**). No significant connection was found with the type of wall coating and the level of heating.

[18]These are given based on the calculation of the manufacturer (Kocsy 2012), however based on Stojanovska et al. (2013) the thoron LLD is calculated to be 7 Bq m^{-3}.

[19]However, taking the $\log_{10}$=lg instead of $\log_e$=ln of the data, the lognormal distribution is rejected.

Annual indoor activity concentration

	Count	Min.	L. quartile	Median	U. quartile	Max.	Average	St. dev.	St. skewness	St. kurtosis	MAD/Median
Radon	**43**	**45**	**116**	**188**	**232**	**609**	**194**	**113**	**4.24**	**4.90**	**0.29**
Thoron	**42**	**33**	**154**	**232**	**325**	**576**	**245**	**124**	**1.64**	**0.49**	**0.35**

*Tab.16.: Count (sample number), minimum, lower quartile, median, upper quartile, maximum, average, st. deviation (Bq m^{-3}), st. skewness, st. kurtosis and MAD/median for all annual indoor radon and thoron activity concentration results at Békés County (**RnC-Y-H** and **TnC-Y-H**).*

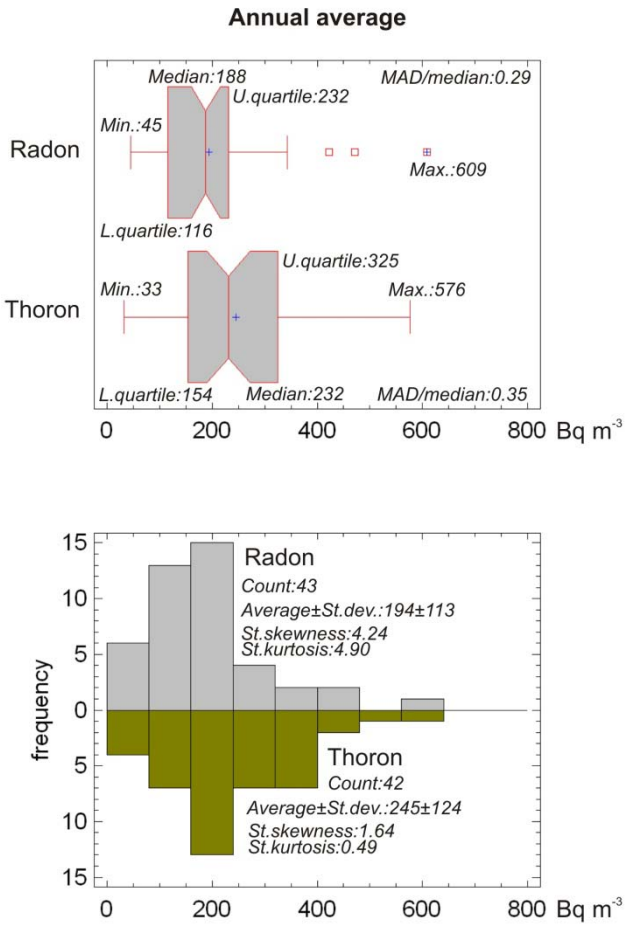

*Fig.24.: Box-whisker plots and frequency histograms of all annual indoor radon and thoron activity concentration results at Békés County (**RnC-Y-H** and **TnC-Y-H**, **SJ6.**).*

The statistics for the local clay, loess and turf geological formations (***RnC-Y-JH*** and ***TnC-Y-JH***) are summarized in *Tab.17.* and visualized on *Fig.25*. The radon activity concentration median values are 199, 175 and 102 Bq m^{-3}, whereas the thoron medians are 234, 211 and 320 Bq m^{-3} for clay, loess and turf, respectively. All distributions strongly overlap and the sample numbers are low (*Fig.25.*), but MW tests still indicate that radon annual average median on clay (199 Bq m^{-3}) is statistically significantly higher than on

turf (102 Bq m^{-3}) (**SJ6.**). The highest values in case of both radon and thoron are detected on clay formations (*Fig.25.*).

Annual indoor activity concentration

		Count	Min.	L. quartile	Median	U. quartile	Max.	Average	St. dev.	St. skewness	St. kurtosis	MAD/Median
Radon	Clay	26	68	124	199	242	609	215	126	3.40	3.16	0.28
	Loess	12	49	132	175	232	330	181	85	0.20	-0.35	0.30
	Turf	5	45	66	102	146	221	116	70	0.77	-0.01	0.43
Thoron	Clay	26	33	165	234	331	576	253	134	1.47	0.53	0.34
	Loess	12	69	140	211	273	389	210	97	0.42	-0.28	0.34
	Turf	4	116	209	320	382	425	295	130	-0.85	0.73	0.19

*Tab.17.: Count (sample number), minimum, lower quartile, median, upper quartile, maximum, average, st. deviation (Bq m^{-3}), st. skewness, st. kurtosis and MAD/median for annual indoor radon and thoron activity concentration results separately for different types of geological formations (clay, loess and turf) at Békés County (**RnC-Y-JH** and **TnC-Y-JH**).*

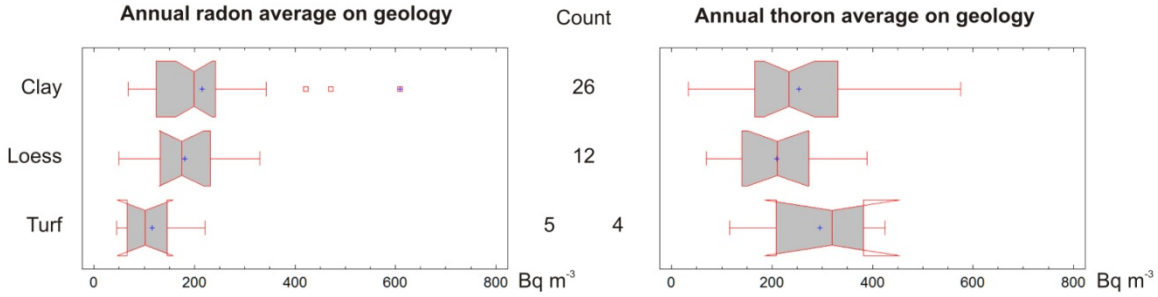

*Fig.25.: Box-whisker plots of annual indoor radon and thoron activity concentration results separately for different types of geological formations (clay, loess and turf) at Békés County (**RnC-Y-JH** and **TnC-Y-JH**, **SJ6.**).*

The statistics for Pleistocene and Holocene age formations (***RnC-Y-KH*** *and* ***TnC-Y-KH***) are summarized in *Tab.18.* and visualized on *Fig.26*. The radon activity concentration median values are 188 and 176 Bq m^{-3}, whereas the thoron medians are 206 and 263 Bq m^{-3} for Pleistocene and Holocene, respectively. The distributions strongly overlap (*Fig.26.*), MW tests do not show any significant differences for the two geological ages.

Annual indoor activity concentration

		Count	Min.	L. quartile	Median	U. quartile	Max.	Average	St. dev.	St. skewness	St. kurtosis	MAD/Median
Radon	**Pleistocene**	**17**	**49**	**139**	**188**	**232**	**330**	**188**	**75**	**-0.17**	**-0.16**	**0.26**
	Holocene	**26**	**45**	**104**	**176**	**224**	**609**	**198**	**134**	**3.33**	**2.80**	**0.36**
Thoron	**Pleistocene**	**17**	**69**	**146**	**206**	**236**	**389**	**202**	**88**	**0.60**	**-0.12**	**0.28**
	Holocene	**25**	**33**	**200**	**263**	**340**	**576**	**274**	**137**	**0.72**	**-0.07**	**0.29**

*Tab.18.: Count (sample number), minimum, lower quartile, median, upper quartile, maximum, average, st. deviation (Bq m^{-3}), st. skewness, st. kurtosis and MAD/median for annual indoor radon and thoron activity concentration results separately for different ages of geological formations (Pleistocene and Holocene) at Békés County (**RnC-Y-KH** and **TnC-Y-KH**).*

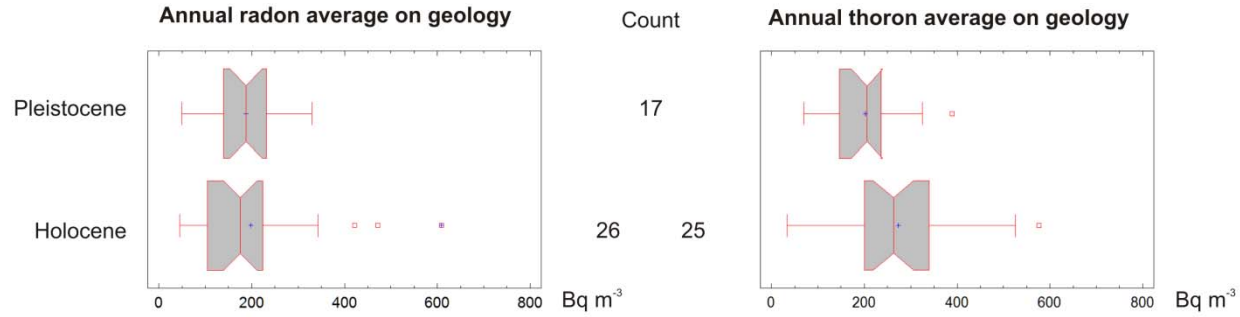

*Fig.26.: Box-whisker plots of annual indoor radon and thoron activity concentration results separately for different ages of geological formations (Pleistocene and Holocene) at Békés County (**RnC-Y-KH** and **TnC-Y-KH**).*

6.2.1.2. Estimated annual radon and thoron inhalation doses in dwellings

The statistics of estimated annual radon inhalation dose (***ID$_{Rn}$-Y-H***, *Eq.12.*) are summarized in *Tab.19.* and visualized on *Fig.27.* Separate detailed statistics is not meaningful to carry out because they are directly calculated from ***RnC-Y-H***. The MAD/median and the statistical distribution are equal. However, the median of all calculated radon inhalation doses is 4.74 mSv y^{-1} and the average is 4.90 mSv y^{-1} (*Fig.27.*). In three studied dwellings the inhalation dose exceeds 10 mSv y^{-1}.

Estimated radon inhalation dose

Count	Min.	L. quartile	Median	U. quartile	Max.	Average	St. dev.	St. skewness	St. kurtosis	MAD/Median
43	1.15	2.92	4.74	5.85	15.37	4.90	2.86	4.24	4.90	0.29

*Tab.19.: Count (sample number), minimum, lower quartile, median, upper quartile, maximum, average, st. deviation (mSv y^{-1}), st. skewness, st. kurtosis and MAD/median all estimated radon inhalation doses at Békés County (**ID_{Rn}-Y-H**).*

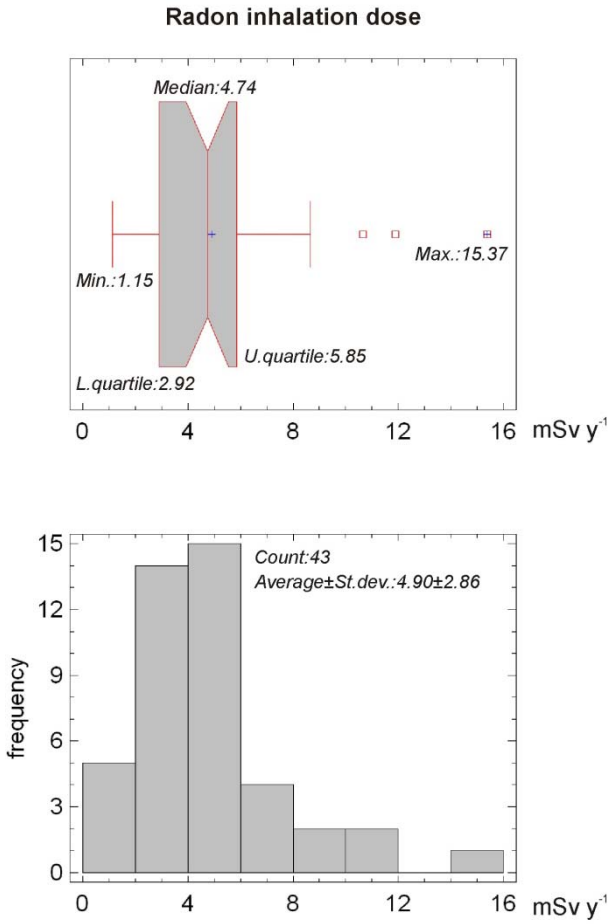

*Fig.27.: Box-whisker plot and frequency histogram of all estimated radon inhalation doses at Békés County (**ID_{Rn}-Y-H**, **SJ6.**).*

Since similar reliable dose estimation is not possible to carry out for thoron isotope with the obtained data (Chapter 4.2.2.1.) only a crude estimation, based on the thoron activity concentration data and international experiences, is available (it would be ***ID_{Tn}-Y-H***). This should be carefully accepted. The individual values might have 100-200 % uncertainty (Omori et al. 2013). However, the average value is probably close to the reality. It shows that thoron gives at least about 30 % of the total inhalation (internal effective) dose in the studied dwellings (**SJ6.**).

6.2.1.3. *Seasonal activity concentrations*

The statistics for the radon and thoron activity concentration measurement data in the four seasons (***RnC-S-H*** and ***TnC-S-H***) are summarized in *Tab.20.* and visualized by box-whisker plots on *Fig.28.* (**SJ6.**). The relevant measures and the linear correlation coefficients in *Tab.21.* are analyzed below.

Indoor activity concentration in seasons

		Count	Min.	L. quartile	Median	U. quartile	Max.	Average	St. dev.	St. skewness	St. kurtosis	MAD/Median
Radon	Winter	50	45	100	217	334	888	244	179	4.45	4.20	0.54
	Spring	48	22	92	159	222	634	171	108	4.91	8.30	0.40
	Summer	46	3	43	70	109	281	81	57	4.02	3.63	0.45
	Autumn	46	55	171	276	339	827	287	160	3.57	3.18	0.29
Thoron	Winter	50	75	203	372	491	2306	407	344	11.00	27.92	0.36
	Spring	47	8	139	228	388	1264	284	218	5.97	10.85	0.54
	Summer	46	11	78	156	266	914	212	210	5.15	4.92	0.65
	Autumn	46	14	79	174	225	340	163	86	-0.10	-1.21	0.35

*Tab.20.: Count (sample number), minimum, lower quartile, median, upper quartile, maximum, average, st. deviation (Bq m^{-3}), st. skewness, st. kurtosis and MAD/median for all seasonal radon and thoron activity concentration measurement results at Békés County (**RnC-S-H** and **TnC-S-H**, **SJ6.**).*

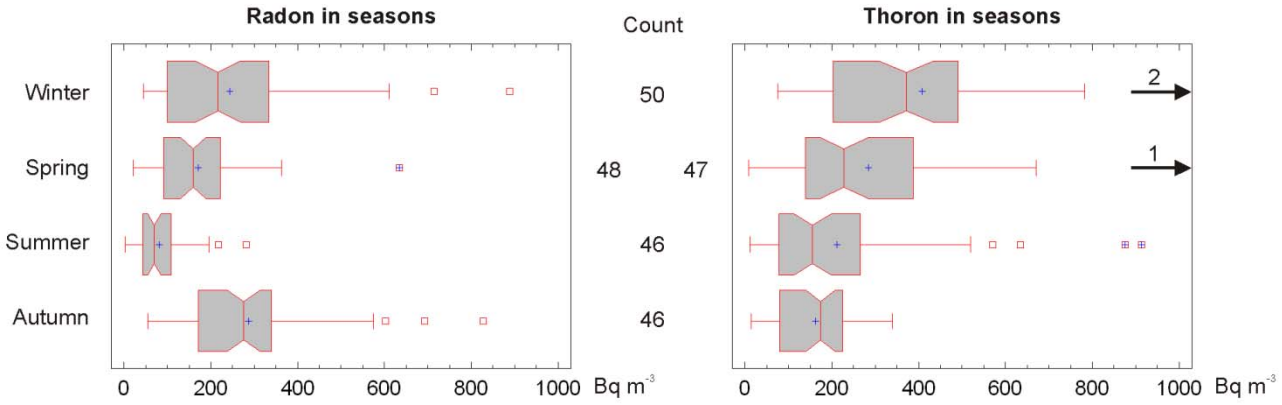

*Fig.28.: Box-whisker plots of all seasonal radon and thoron activity concentration measurement results at Békés County (**RnC-S-H** and **TnC-S-H**, **SJ6.**). In case of thoron, three outlier values are not shown on the figure for better visibility.*

r	Winter-Spring	Winter-Summer	Winter-Autumn	Spring-Summer	Spring-Autumn	Summer-Autumn
RnC	0.89	0.32	0.90	0.50	0.90	0.50
TnC	0.77	0.18	0.44	0.54	0.55	0.36

*Tab.21.: Correlation coefficients among radon and thoron activity concentrations measured in four seasons (**RnC-S-H** and **TnC-S-H**, **SJ6.**). The tones of red from light to deep indicate increasing correlation coefficients among which the ones referring to statistically significant relationships are highlighted by frames.*

6.2.1.3.1. Seasonal medians and MW tests

The radon activity concentration median values are 217, 159, 70 and 276 Bq m^{-3} for winter, spring, summer and autumn, respectively. *Tab.20.* and *Fig.28.* show that radon displays a close to typical seasonal variation with high values in winter and autumn, lower values in spring and low values in summer. Winter and autumn medians are three to four times higher than that of summer. The MW tests show that there are statistically significant differences among the seasonal median radon activity concentrations, except the winter-autumn pair (**SJ6.**).

At the same time thoron level is steadily decreasing during the measurement period (*Tab.20.*, *Fig.28.*). The medians are 372, 228, 156 and 174 Bq m^{-3} for winter, spring, summer and autumn, respectively. Winter median is more than twice higher than that of summer and autumn. MW tests show that there are statistically significant differences among the thoron activity concentration medians in seasons, except the summer-autumn pair (**SJ6.**).

Medians of thoron activity concentration data tend to exceed those of radon in winter, spring and summer. However, in autumn, radon exceeds almost twice the thoron median (*Tab.20.*, *Fig.28.*). Based on MW tests, there are statistically significant differences between the radon and thoron activity concentration medians in all seasons.

6.2.1.3.2. Seasonal statistical distributions and SW tests

The SW tests verify what standardized skewness and the standardized kurtosis values (*Tab.20.*) suggest, namely that only autumn thoron activity concentration come from a normal distribution and that winter, spring and autumn radon and winter thoron results are lognormally distributed. However, the SW tests reject both normality and lognormality in the cases of summer radon, as well as spring and summer thoron measurements (**SJ6.**).

6.2.1.3.3. Correlation analysis for seasons

Linear correlation coefficients among different seasons were studied for both radon and thoron (*Tab.21.*). Radon shows $r \approx 0.9$ among winter, spring and autumn seasons in different

dwellings, whereas summer has weaker *r* values between 0.32 and 0.50 (*Tab.21.*). All of these indicate statistically significant non-zero correlations, namely strong relationships among seasons.

Thoron generally shows lower correlation coefficients. Most of them fall between 0.36 and 0.55, whereas for winter and spring *r* is higher (0.77) and for winter and summer *r* is lower (0.18) (*Tab.21.*). These indicate statistically significant non-zero correlations, i.e. moderate relationships among seasons, except winter and summer.

The linear correlation coefficients between the two studied isotopes are r = 0.12, 0.00, -0.04 and 0.23 for winter, spring, summer and autumn seasons, respectively (**SJ6.**). These are all statistically insignificant.

6.2.2. Measured indoor γ dose rates in dwellings

In 48 adobe dwellings of Békés County 144 γ dose rate measurement data are available. These are dose rate values on wall surfaces, ground surfaces and also at one meter height in the middle of the chosen rooms. The relative uncertainties (in this case, relative standard deviations) of the data were always around 7 %. The statistics for the three detector positions do not show statistically significant differences (MW tests). Therefore, in the presentation of the results one data group is considered which is the average γ dose rate in a dwelling. This is representing the sum of γ-radiation of the cosmic background and the terrestrial radionuclide concentration of the soil and the building materials (Chapter 4.2.3.)

The statistics of all data from Békés County (***γDR-Y-H***) is summarized in *Tab.22.* and visualized on *Fig.29*. It is shown that the average γ dose rate has a median of 140 nSv h^{-1}. Taking into account the indoor occupancy time applied elsewhere (7012.8 h y^{-1}, *Eq.11.*) this 140 nSv h^{-1} value is leading to a 0.98 mSv y^{-1} external effective dose on the annual basis (*Tab.22.*).

The linear correlation coefficients with annual radon and thoron activity concentration data (***RnC-Y-H*** and ***TnC-Y-H***) are low and statistically insignificant (r = 0.23 and 0.08, respectively).

Average γ dose rate (nSv h^{-1}) and resulting annual external effective dose (mSv y^{-1})

	Count	Min.	L. quartile	Median	U. quartile	Max.	Average	St. dev.	St. skewness	St. kurtosis	MAD/Median
nSv h^{-1}	48	104	121	140	160	196	143	24	0.55	-1.22	0.14
mSv y^{-1}		0.73	0.85	0.98	1.12	1.37	1.00	0.17			

*Tab.22.: Count (sample number), minimum, lower quartile, median, upper quartile, maximum, average, st. deviation (nSv h^{-1}, mSv y^{-1}), st. skewness, st. kurtosis and MAD/median for all average γ dose rate measurement results at Békés County (**γDR-Y-H**) and the values of resulting annual external effective dose.*

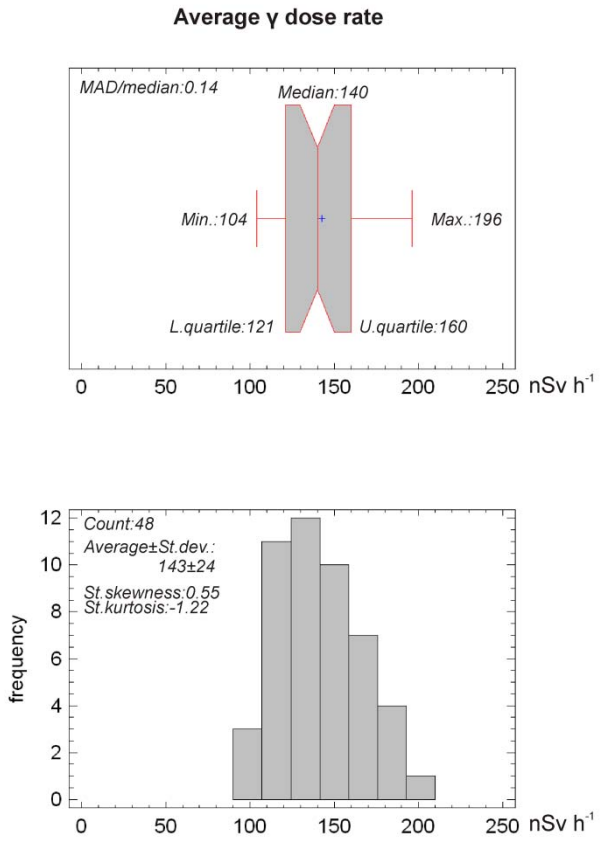

*Fig.29.: Box-whisker plot and frequency histogram of all γ dose rate measurement results at Békés County (**γDR-Y-H**).*

The statistics for local geological formations of clay, loess and turf (***γDR-Y-JH***) are summarized in *Tab.23.* and visualized on *Fig.30*. The average γ dose rate median values are 153, 131 and 139 nSv h^{-1} for clay, loess and turf, respectively. All distributions strongly overlap (*Fig.30.*). However, MW tests still show that average γ dose rate median on clay (153 nSv h^{-1}) is statistically significantly higher than on loess (131 nSv h^{-1}). Other pairs do not show statistically significant differences.

Average γ dose rate

	Count	Min.	L. quartile	Median	U. quartile	Max.	Average	St. dev.	St. skewness	St. kurtosis	MAD/Median
Clay	**25**	**106**	**133**	**153**	**171**	**196**	**150**	**25**	**-0.10**	**-0.85**	**0.12**
Loess	**18**	**104**	**116**	**131**	**154**	**177**	**133**	**23**	**0.83**	**-0.84**	**0.13**
Turf	**5**	**123**	**134**	**139**	**152**	**162**	**142**	**15**	**0.17**	**-0.47**	**0.09**

*Tab.23.: Count (sample number), minimum, lower quartile, median, upper quartile, maximum, average, st. deviation (nSv h^{-1}), st. skewness, st. kurtosis and MAD/median for γ dose rate measurement results separately for different types of geological formations (clay, loess and turf) at Békés County (**γDR-Y-JH**).*

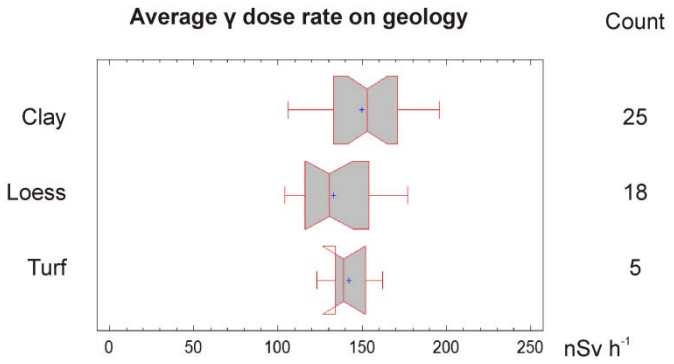

*Fig.30.: Box-whisker plots of γ dose rate measurement results separately for different types of geological formations (clay, loess and turf) at Békés County (**γDR-Y-JH**).*

The statistics for Pleistocene and Holocene age environments (***γDR-Y-KH***) are summarized in *Tab.24.* and visualized on *Fig.31*. The average γ dose rate median values are 138 and 152 nSv h^{-1} for Pleistocene and Holocene geological ages, respectively. The MW test does not show statistically significant difference between these medians.

Average γ dose rate

	Count	Min.	L. quartile	Median	U. quartile	Max.	Average	St. dev.	St. skewness	St. kurtosis	MAD/Median
Pleistocene	**21**	**104**	**116**	**138**	**154**	**177**	**135**	**22**	**0.50**	**-0.96**	**0.14**
Holocene	**27**	**106**	**127**	**152**	**171**	**196**	**149**	**25**	**0.06**	**-0.92**	**0.13**

*Tab.24.: Count (sample number), minimum, lower quartile, median, upper quartile, maximum, average, st. deviation (nSv h^{-1}), st. skewness, st. kurtosis and MAD/median for γ dose rate measurement results separately for different ages of geological formations (Pleistocene and Holocene) at Békés County (**γDR-Y-KH**).*

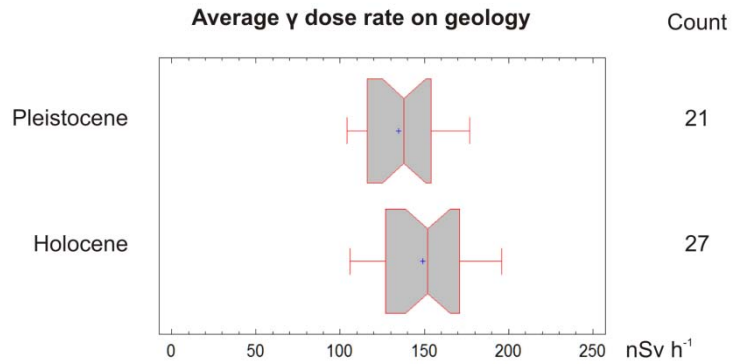

*Fig.31.: Box-whisker plots of γ dose rate measurement results separately for different ages of geological formations (Pleistocene and Holocene) at Békés County (**γDR-Y-KH**).*

7. DISCUSSION OF TERRESTRIAL RADIOCTIVITY IN ADOBE BUILDING MATERIAL AND DWELLINGS

7.1. Evaluation of the assumed elevated terrestrial radiation risk in Hungarian adobe dwellings

7.1.1. Hazard evaluation of adobe building material

7.1.1.1. Definition of the radon hazard portion and its role in building material qualification

This subchapter provides a theoretical evaluation of one of the building material hazard indices (Chapter 4.1.3.1.) supplied by the measurement results of adobe building materials (Chapter 6.1.2.1.). It is needed because many high quality papers on radiation hazard of building materials are now published without referring to the importance of direct radon (and thoron) emanation or exhalation measurements and use only the H_{in} index (*Eq.9.*) for "internal" qualification purposes. The author considers it too ambitious and has defined a new measure to point out some usually not recognized limitations of this index, H_{in}. The new measure is called the *radon hazard portion*, which was published in **PV8.** and **SJ2.** A simple calculation was used in *Eq.18.* to define this new measure, which is based on the difference between H_{ex} (*Eq.8.*) and H_{in} (*Eq.9.*).

$$H_{R\%} = 100\left(\frac{H_{in}}{H_{ex}} - 1\right) \qquad (Eq.18.)$$

where $H_{R\%}$ is the so-called radon hazard portion (%) (**SJ2.**).

The value of the $H_{R\%}$ is related only to the ^{226}Ra activity concentration of the building material and does not take into account the radon emanation factor, the gas diffusion coefficient, the density, porosity and permeability of the material. Therefore, despite the name of radon hazard portion, it has no correct information content about its radon hazard. $H_{R\%}$ calculated for adobe samples are used below to point on the limitations and the need for a less ambitious use of H_{in} index in the literature.

The $H_{R\%}$ results of the studied adobe samples have a median and average of 28 % with a standard deviation of ±3 %. These values suggest that less than a third of the radiation hazard

is from internal/inhalation dose in dwellings made of adobe. This seems to be a significant underestimate considering the results and their further evaluation below. Moreover, the correlation coefficient between $H_{R\%}$ and radon emanation results is statistically far from significant ($r = 0.02$).

Therefore, the author considers Ra_{eq} and I indices to be more effective than H_{ex} and H_{in} in building material qualification. Beside their correct information content, i.e. not trying to refer to internal radiation, these are the most frequently published values useful for comparison purposes. However, radon and thoron emanation values should not be neglected even if the hazard indices are low. Note that in some national regulations (e.g. Austria: ASI 2009, Netherlands: van der Graaf et al. 2001, Tuccimei et al. 2006) these properties are also involved in the qualification process.

7.1.1.2. Building material qualification based on Ra_{eq} and I indices and evaluation of their radon and thoron emanations

Whereas the ^{226}Ra, ^{232}Th and ^{40}K activity concentration averages are 33, 28 and 370 Bq kg^{-1} in Hungarian soils (UNSCEAR 2000), the measured results (***Ra-C-H***, ***Th-C-H*** and ***K-C-H***) show median values of 28, 32 and 364 Bq kg^{-1}, respectively in the studied adobe samples (*Tab.6.*, *Fig.14.*). These values indicate comparably low terrestrial radionuclide contents for Hungarian adobe building materials. The considered Ra_{eq} and I hazard indices calculated based on these ^{226}Ra, ^{232}Th and ^{40}K activity concentrations (*Eq.6.* and *Eq.7.*) are always below their given thresholds of 370 Bq kg^{-1} and 1 (unit) (*Fig.16.*). Further evaluation was first carried out by comparing the Ra_{eq} average to international references and other types of building materials studied by the author in **SJ2.** (*Tab.25.*).

In the comparison of radium equivalent indices (Ra_{eq}, *Tab.25.*), the adobe samples were considered together with Hungarian brick samples and their averages were both compared to the clay brick (unfired and fired) building materials in the cited references (Beretka and Mathew 1985 and references therein). The Hungarian adobe samples show a Ra_{eq} average of 103 Bq kg^{-1}, whereas in the international studies those values range between 170 and 352 Bq kg^{-1} for similar types of building materials. The adobe samples also show Ra_{eq} indices lower than or comparable to most of the other types of building materials studied in **SJ2.**, with the exception of the two samples of concrete (*Tab.25.*).

Building material type	This study and SJ2.	Beretka and Mathew (1985) and references therein					
	Hungary	Australia	Finland	Germany	Norway	Sweden	United Kingdom
adobe	103 (46)	218 (25)	241	204	274	352	170
brick	113 (2)						
concrete	31 (2)	85 (5)	-	155	133	-	-
coal slag concrete	138 (3)						
coal slag	621 (6)	340 (3)	215	422	-	-	-
gas silicate	107 (7)	-	-	-	-	-	-

*Tab.25.: The underlined average of determined adobe Ra_{eq} indices (Bq kg^{-1}) in this study in comparison with international references and other types of building materials studied by the author and her coauthors (**SJ2.**). The sample numbers are indicated in brackets following the activity concentration values.*

The other building material hazard index considered to limit external dose in this study is the activity concentration index, *I* (*Eq.7.*). The value of this index varies among 0.27 and 0.52 for the studied adobe samples (*Fig.16.*). All of these determined values are far below the accepted limit value of 1 (unit) responding to about 1 mSv y^{-1} external dose (EC 1999, limit value advised by Trevisi et al. 2012). It is noted that comparing to another, generally too ambitious (Trevisi et al. 2012) possible limit value of 0.5 corresponding to about 0.3 mSv y^{-1} (EC 1999), one adobe sample exceeds it from E-Mecsek Mts., where all other results are also slightly elevated (for explanation see below in Chapter 7.2.1.1.). Overall, based on any building material indices, adobe samples cannot be considered hazardous.

However, it is already mentioned above (Chapter 7.1.1.1.) that the radon and thoron emanation (***RnE-C-G*** and ***TnE-C-G***) properties should not be neglected even if the presented hazard indices are low. The median values were given among the results (*Tab.4.*, *Fig.12.*) as 7.9 and 5.7 kg^{-1} s^{-1} for Hungarian adobe radon and thoron emanations, respectively. In the evaluation of these values difficulties occur due to the possibly different measurement conditions applied in different publications such as the moisture content (e.g. Hassan et al. 2011, Hosoda et al. 2007, Porstendörfer 1994, Sas 2012, Strong and Levins 1982, Tanner 1980), the sample geometry and the inconsequences and diversity of applied emanation and/or exhalations units. However, the emanation results are elevated compared to most of the other types of building materials used in bulk amounts studied at Lithosphere Fluid Research Lab, Eötvös University (Völgyesi et al. 2011). Further evaluation of radon and thoron hazard of the

adobe building material is carried out by the help of the consequent indoor radon and thoron activity concentration results (Chapter 7.1.2.1).

7.1.2. Evaluation of annual indoor radon and thoron activity concentration levels at Békés County

7.1.2.1. International comparison

An international comparison of some selected measures of annual indoor radon and thoron activity concentrations (*Tab.16.*, *Fig.24.*) is summarized in *Tab.26.* (**SJ6.**) and shows the types of building materials and the measurement distances from the walls. The average, minimum and maximum values and geometric means of the results are presented covering the information found most frequently in the literature.

Only three studies show high radon activity concentrations comparable to our results (*Tab.16.*, *Fig.24.*, *Tab.26.*). These were performed at Kővágószőlős, Hungary (Kávási et al. 2007, Kovács 2010) known by its former uranium mine and in Kosovo and Metohija, Serbia (Milić et al. 2010). Thoron generally has low activity concentrations (<50 Bq m^{-3}) (Chougaonkar et al. 2004, Deka et al. 2003, Kávási et al. 2007, Khokhar et al. 2008, Kovács 2010, Milić et al. 2010, Sreenath Reddy et al. 2004, Stojanovska et al. 2011 and 2013, *Tab.26.*). However, elevated thoron activity concentrations were detected in Indian mud dwellings (Sreenath Reddy et al. 2004) and rural dwellings of Balkans (Zunić et al. 2010). Only in Chinese cave dwellings (Luo et al. 2005, Yamada et al. 2005) were thoron levels measured to be as high as in Hungarian adobe dwellings. It is seen that the annual radon and thoron activity concentrations measured in adobe dwellings at Békés County show elevated levels compared to results in other studies (*Tab.26.*, **SJ6.**).

	Country	Building material	Distance	Measure	Radon	Thoron
This study	Hungary - Békés County	adobe	10 cm	Av. Min.-Max. GM	194 (43) 45-609 (43) 166 (43)	245 (42) 33-576 (42) 211 (42)
Kávási et al. 2007 Kovács 2010	Hungary - Kővágószőlős	various - summer	15-20 cm	Av. GM	154 (72) 107 (80)	98 (72) 53 (74)
Luo et al. 2005	China	various	10 cm	Av.	29 (100)	184 (100)
Yamada et al. 2005	China	cave dwelling (adobe)	5-30 cm	GM	81 (102)	261 (102)
Sreenath Reddy et al. 2004	India - Andhra Pradesh	mud (adobe) stone mosaic concrete	- - - -	- - - -	- - - -	143 (8) 34 (60) 31 (10) 33 (11)
Deka et al. 2003	India - Assam	various	10 cm	Min.-Max.	40-215 (46)	13-38 (46)
Khokhar et al. 2008	India - Chhattisgarh	various	20 cm	GM	26 (210)	18 (210)
Chougaonkar et al. 2004	India - Kerala	various	10 cm	GM	23 (200)	24 (200)
Milić et al. 2010	Serbia - Kosovo and Metohija	various	-	GM	224 (63)	43 (63)
Stojanovska et al. 2011 and 2013	Macedonia	various	50 cm	GM	82 (437)	28 (53-300)
Zunic et al. 2010	Serbia Bosnia-Hercegovina	rural dwellings	20 cm	GM	82 (183)	109 (183)

*Tab.26.: The underlined average (av.), minimum-maximum (min.-max.) and geometric mean (GM) (Bq m^{-3}) of determined annual indoor radon and thoron activity concentrations in this study (**RnC-Y-H** and **TnC-Y-H**, **SJ6.**) in comparison with international references. The sample numbers are indicated in brackets following the activity concentration values.*

7.1.2.2. Proportion of dwellings above reference levels

The measured annual indoor radon activity concentration follows a lognormal distribution, whereas the author accepted that the annual thoron data are normally distributed (Chapter 6.2.1.1., *Tab.16.*, *Fig.24.*, **SJ6.**). In *Fig.32.* the scales of X and Y axes is chosen in such a way so that the plotted annual activity concentration values (X axes) vs. the cumulative probability (Y axes[20]) describe closely linear functions. For this purpose, the activity concentrations are presented on a log scale for radon, but on a linear scale for thoron.

For radon, the 300 Bq m^{-3} as the highest reference level recommended by WHO (2009) was considered. Choosing a reference level for thoron is not as obvious as for radon

[20]It represents the inverse of a cumulative Gaussian distribution. Plotting a cumulative Gaussian distribution produces a sigmoidally-shaped curve. This curve, when displayed on a probability scale, appears as a straight line (Microcal Origin software, Help).

(Chapter 2.4.). In this study, for a comparison, the proportion of dwellings above the same activity concentration as for radon, 300 Bq m^{-3}, is determined. However, it is emphasized that the same thoron effective dose must originate from a much higher activity concentration due to the one order of magnitude lower equilibrium factor of thoron.

Based on *Fig.32.* and the fitted linear functions representing the lognormal (radon) and normal (thoron) distributions, the following four points are stated: (1) 14-17 % of the adobe dwellings at Békés County have higher radon activity concentration than the reference level of 300 Bq m^{-3} by 95 % probability, (2) in this study, 12 % of the dwellings were above this reference level (*Fig.32.*, left side). (3) 29-32 % of the adobe dwellings at Békés County have higher thoron activity concentration than 300 Bq m^{-3} by 95 % probability and (4) the empirical proportion for thoron in this study is determined to be 33 % (*Fig.32.*, right side) (**SJ6.**).

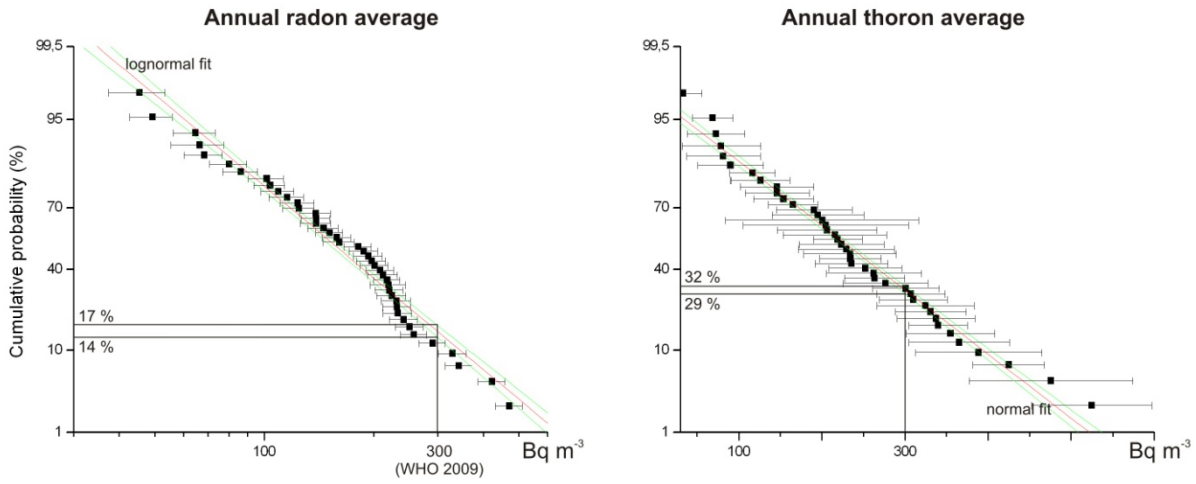

*Fig.32.: Cumulative probabilities of annual indoor radon and thoron activity concentrations (**RnC-Y-H** and **TnC-Y-H**, **SJ6.**). The activity concentrations are presented on a log scale for radon, and on a linear scale for thoron based on the results of SW tests. Red and green dashed lines show the fitted lognormal (radon) and normal (thoron) distribution functions with their 95 % confidence intervals.*

7.1.3. Evaluation of estimated and measured external and internal effective doses

In this study, three effective dose values affecting residents via two different pathways are given among the results. These are estimated annual external effective doses (***ED_{RaThK}-Y-G***)

in Chapter 6.1.2.2., in-situ measured γ dose rates (***γDR-Y-H***) in Chapter 6.2.2., and estimated radon inhalation doses (internal, $\boldsymbol{ID_{Rn}}$***-Y-H***) in Chapter 6.2.1.2. The evaluation of these results is described below.

The estimated annual external effective dose based on ^{226}Ra, ^{232}Th and ^{40}K activity concentrations in adobe samples ($\boldsymbol{ED_{RaThK}}$***-Y-G***, *Eq.10., 11.*) is given to have a median of 0.45 mSv y^{-1} in Hungarian adobe dwellings (*Tab.8.*, *Fig.17.*). By subtracting the assumed 50 nGy h^{-1} background radiation (EC 1999, Chapter 4.1.3.2.) from this result, the excess of building materials to the external dose received outdoors can be calculated. In this study the contribution of adobe to the received external dose is estimated to have a median of 0.2 mSv y^{-1} and a maximum of 0.36 mSv y^{-1}. These values are far below the accepted dose criterion of 1 mSv y^{-1} (EC 1999, Trevisi et al. 2012), explaining better the findings of the activity concentration index, *I* in Chapter 7.1.1.2. The actual, in-situ measured, γ dose rates (***γDR-Y-H***) indicate an annual effective dose median of 0.98 mSv y^{-1} (calculated from 140 nSv h^{-1}) and a maximum of 1.37 mSv y^{-1} (calculated from 196 nSv h^{-1}) (*Tab.22.*). These measurements do not give the possibility to distinguish the contribution of the building material from that of the ground or cosmic radiation. However, considering an average 0.4 mSv y^{-1} order of magnitude contribution of cosmic radiation (*Fig.1.*, Eisenbud and Gesell 1997, UNSCEAR 2000), and another significant contribution of the terrestrial radioactivity of the ground, these results also refer to a building material excess external dose far below the accepted criterion of 1 mSv y^{-1}, hence verifying $\boldsymbol{ED_{RaThK}}$***-Y-G*** results.

One-two orders of magnitude higher internal effective doses are indicated to originate from radon (and thoron) inhalation than from γ-radiation excess of adobe building material. However, regarding inhalation dose, also a much higher, about 10 mSv y^{-1} effective dose criterion (300 Bq m^{-3} radon activity concentration, ICRP 2007, 2009, WHO 2009, Chapter 2.4.) could be applicable. The median of all estimated radon inhalation doses in adobe dwellings ($\boldsymbol{ID_{Rn}}$***-Y-H*** calculated by *Eq.12.*) is given to be 4.74 mSv y^{-1} (*Tab.19.*, *Fig.27.*). As a comparison, the world average value is about 1.15 mSv y^{-1} (UNSCEAR 2006) which is equal to the minimum in the statistics. The estimated value exceeds 10 mSv y^{-1} in three studied dwellings which means the 7 % of the results. Additionally, thoron is estimated to contribute with at least about 30 % to the total inhalation dose (Chapter 6.2.1.2., **SJ6.**). Note the much lower contribution of thoron in an average environment, which was estimated to be between 13 % (Eisenbud and Gesell 1997) and 8 % (UNSCEAR 2000) (Chapter 2.1.). Therefore, thoron might be significantly further increasing the proportion of adobe dwellings

with not negligible inhalation dose values. Significance of the results is enlighten not only by international recommendations considering the LNT model, but also by already mentioned recent studies (Madas and Balásházy 2011, Chapter 2.3.3.), which describe a much higher local tissue dose resulted from the determined effective dose of radon inhalation because of its inhomogeneous distribution in the lungs.

7.2. Environmental factors affecting the spatial and seasonal variation of terrestrial radioactivity levels

7.2.1. Distribution of measurement results in different geological environments

7.2.1.1. Regional geology of the three studied areas

In this subchapter regional tendencies of radon and thoron emanations, ^{226}Ra, ^{232}Th and ^{40}K activity concentrations, radon and thoron emanation fractions (***RnE-C-H*** and ***TnE-C-H***, ***Ra-C-H***, ***Th-C-H*** and ***K-C-H***, f_{RnE}***-C-H*** and f_{TnE}***-C-H***) and grain size distributions (*Tab.5.*, *7.*, *10.*, *12.* and *Fig.13.*, *15.*, *19.*, *21.*, *23.*) are discussed. Békés County, E-Mecsek Mts. and Sajó and Hernád Rivers Valleys have different geological backgrounds as described in Chapter 3.2.3. Any significant difference of measured parameters of regionally grouped adobe building material samples is assumed to be its consequence due to the local origin of adobes. The actually observed differences detailed below strengthen these assumptions and understood by looking at geological backgrounds of the studied areas.

Adobe samples from *Békés County* are not characterized by many statistically significant observations, this area is the most moderate one. However, the highest ^{40}K activity concentration (*Tab.7.*, *Fig.15.*) and the lowest radon emanation fraction medians are connected to this area among the three and the thoron emanation fraction median is also low (*Tab.10.*, *Fig.19.*). The most significant presence of the smallest size, 2-3 and 10 μm peaks in grain size distributions is observed in adobe building materials from Békés County (*Fig.21.*) which is consequent with its fluvial, most frequently clay type origin. This causes the statistically significantly higher estimated specific surface area median of these samples (*Tab.12.*, *Fig.23.*), however, it does not result in elevated emanation fractions results as mentioned above and will be discussed in Chapter 7.2.2. Direct indoor radon and thoron activity concentration measurements were carried out at this studied area. These show high

central tendencies of 188 and 232 Bq m^{-3} median values (*Tab.16.*, *Fig.24.*) for radon and thoron, respectively, and analyzed in details in Chapter 7.1.2.

Adobe samples from *E-Mecsek Mts.* show significantly higher ^{226}Ra and ^{232}Th activity concentration medians than the other two areas (*Tab.7.*, *Fig.15.*). This seems to be consequent to the prevailing granite bedrock (Chapter 3.2.3.), which type of rock is usually considered to be enriched in terrestrial radionuclides. The adobe building materials of the area are also characterized by the highest thoron emanation median (*Tab.5.*, *Fig.13.*) as a result of the high ^{232}Th activity concentration, but not statistically significantly. The difference is mitigated by the reduced radon and thoron emanation fractions (*Tab.10.*, *Fig.19.*). These comparatively low emanation fractions and the also observed lowest ^{40}K activity concentration median are understood by observing the grain size distribution shift towards bigger grains, i.e. observing the most significant presence of the 30 μm size peak (*Fig.21.*). This shift is probably connected to the loess covering the bedrock instead of fluvial origin layers. The lowest estimated specific surface area median (*Tab.12.*, *Fig.23.*) is also connected to this area. Direct indoor radon and thoron activity concentration measurements were not carried out at E-Mecsek Mts. Radon concentrations cannot be predicted based on building material radon emanation results since it also originates from the soil below the buildings. However, the thoron emanation results (*Tab.5.*, *Fig.13.*) suggest that slightly higher indoor thoron activity concentrations might be present than what have been measured at Békés County (not statistically proven).

From *Sajó and Hernád Rivers Valleys* the lowest ^{226}Ra activity concentration median was detected in adobe samples. The same for ^{232}Th was also found to be as low as at Békés County (*Tab.7.*, *Fig.15.*). However, significantly higher median radon emanation fraction is determined and thoron emanation fraction is also elevated (*Tab.10.*, *Fig.19.*). The resulted radon and thoron emanations are unpredictable; the distributions are strongly overlapped, however, the maximum values are connected to this area (*Tab.5.*, *Fig.13.*). The grain size distributions (*Fig.21.*) and consequently the estimated specific surface areas (*Tab.12.*, *Fig.23.*) seem to be transitions between Békés County and E-Mecsek Mts., many different types of sediments are mixed at this area (Chapter 3.2.3.). Direct indoor radon and thoron activity concentration measurements have not been performed. However, the laboratory results of the adobe building material samples suggest that generally lower thoron activity concentrations are expected than at Békés County, but the outlier values can be even higher.

7.2.1.2. Local geology at Békés County

In this subsection the dependence of annual indoor radon and thoron activity concentrations (***RnC-Y-JH***, ***TnC-Y-JH***, ***RnC-Y-KH*** and ***TnC-Y-KH***) and γ dose rates (***γDR-Y-JH*** and ***γDR-Y-KH***) on the local geological formations at Békés County (*Fig.4.*) is discussed.

Minda et al. (2009) and other authors have already pointed out that indoor radon activity concentrations show dependence on geological formations in Hungary. This connection might be emphasized in case of adobe dwellings due to the local origin of building materials. In this study, three types of geological formations can be considered at Békés County. Among these, on clay the highest, on loess medium and on turf the lowest annual radon activity concentrations were detected. In case of thoron, the highest median was on turf although the maximum values were again on clay (*Tab.17.*, *Fig.25.*, **SJ6.**). Based on these results, the local geology seems to affect differently the radon and thoron levels resulting in different spatial variations. The insignificant linear correlation coefficients between radon and thoron isotopes are consistent with these observations. Radon and thoron data are generally not elevated in the same dwelling, however, for both isotopes the clay formations showed to be the highest risk localities at Békés County (**SJ6.**). Despite of the low correlation coefficients, the indoor measured average γ dose rate is consequent with these results, its determined median on clay is statistically significantly higher than on loess and also higher than on turf (*Tab.23.*, *Fig.30.*).

Considering the age of geological formations at Békés County, only statistically not significant differences were observed between Pleistocene and Holocene ages. However, it is seen (*Tab.18.*, *Fig.26.* and *Tab.24.*, *Fig.31.*) that the highest radon and thoron activity concentration and also γ dose rate values were measured on Holocene age formations.

7.2.2. The significance of the texture of adobe building material

It has been shown that almost all studied adobe building materials have similar bulk textural properties and are classified as *silt loam* (Wunsch 2009, *Fig.20.*). However, minor deviations are observed in their grain size distributions: proportions of clay, silt and sand fractions (*Fig.20.*), amplitude of observed peaks in clay and silt fractions (*Fig.21.*) and estimated specific surface areas (*Tab.11.*, *12.* and *Fig.22.*, *23.*, Chapter 6.1.4. and 7.2.1.1.). In this study, the significance of these minor differences might be in the different ^{226}Ra, ^{232}Th and also ^{40}K enrichment in different grain size fractions (Chapter 2.2.), and in influencing

radon and thoron emanation (and also exhalation) fractions as explained in Chapter 2.3.1.1. The actually important processes are aimed to observe by the help of correlation coefficients presented in *Tab.13.*, *14.* and *15.* (Chapter 4.3.3 and 6.1.4.4.).

Looking at these results, significant differences are seen among the three studied areas. Based on the correlation coefficients, the radionuclides of ^{226}Ra, ^{232}Th and ^{40}K correlate always with different grain size fractions. Békés County and Sajó and Hernád Rivers Valleys show the radionuclides to be enriched in clay and silt fractions; however, at E-Mecsek Mts. the sand fractions has a more important role (*Tab.13.*). This observation is considered to be connected to the elevated ^{226}Ra and ^{232}Th activity concentrations at this area (Chapter 7.2.1.1.) and also the prevailing granite bedrock and its weathering process. Also significant differences among the three studied areas are observed in relationships of characteristic peaks in clay and silt fractions to radionuclides: positive correlation coefficients are obtained with the 2-3 and 10 or with the 30 μm size peaks (*Tab.14.*). However, the radionuclide content never shows to be belonging to the 0-1 μm grain size range.

The radon emanation fraction is the most linearly connected to the silt fraction (*Tab.13.*) and more specifically to the 10 μm characteristic peak, except at Békés County (*Tab.14.*). Thoron emanation fraction show inexplicable variation in correlation coefficients. This can also be because of the high uncertainty of these thoron results (Chapter 6.1.3.). As the linear correlation coefficient between radon and thoron emanation fractions indicate a weak relationship (Chapter 6.1.3.) it might be also elevated when the silt fraction and the 10 μm characteristic peak is dominant.

E-Mecsek Mts. shows a shift to bigger grain sizes (30 μm peak, *Fig.21.*) and a connected low estimated specific surface area and hence also an understandable indication for decreased emanation fractions (*Tab.10.*, *Fig.19.*). This is mitigating the difference of emanation results (not statistically significant difference, *Tab.5.*, *Fig.13.*) originating from the elevated ^{226}Ra and ^{232}Th activity concentrations (*Tab.7.*, *Fig.15.*). However, adobe samples from Békés County show statistically significantly higher estimated specific surface area median (*Tab.12.*, *Fig.23.*) and it is clear that they do not have increased radon and thoron emanation fractions (*Tab.10.*, *Fig.19.*). Where the emanation fractions are elevated, Sajó and Hernád Rivers Valleys, the specific surface area is not.

The correlation analysis between the estimated specific surface area and radon and thoron emanation fractions separately for the three studied areas (*Tab.15.*) did not result in the expected clear linear relationship neither (Chapter 2.3.1.1.). Within Békés County, correlation

coefficients close to 0 (zero) were found (*Tab.15.*). At E-Mecsek Mts. and Sajó and Hernád Rivers Valleys the correlation coefficients of estimated specific surface area with thoron emanation fraction are more positive than that with radon emanation fraction, but not statistically significant relationship is indicated (*Tab.15.*). These observations may indicate the non-homogeneous distributions of parent nuclides within the grains (also see varying correlation coefficients for ^{226}Ra and ^{232}Th activity concentrations in *Tab.13.*, *14.* and consider the role of mineral coatings described by Greeman and Rose 1996). However, note the possibly important role of different type and amount of organic materials added to adobe at different studied areas.

Based on these observations of the study, there is not a general, clear relationship of neither external (^{226}Ra, ^{232}Th and ^{40}K activity concentrations), nor internal (radon and thoron emanation and consequently exhalation) radiation hazard variation of adobe building materials and their textural properties. Other important influencing factors not studied in this work have to be considered. However, generally, it can be stated that high radon and thoron emanation fractions are determined for Hungarian adobe building material samples with medians of 27 and 18 %, respectively (*Tab.9.*, *Fig.18.*). In the studies of Sas et al. (2012) and Sas (2012), the radon emanation fraction of clay samples is decreasing from 18 to close to 0 % with the increase of heat treatment temperature. This observation is explained by the structural changes in pore diameter, pore volume and specific surface area of samples. Since adobe building materials samples of this study have not gone through heat treatment, the comparably elevated emanation fraction values are understandable. Since comparably low ^{226}Ra and ^{232}Th activity concentrations were determined for the same samples it can be stated that these building materials act as important radon and thoron sources for the reason of the elevated emanation fractions.

7.2.3. Observed connections between indoor radon and thoron activity concentrations and weather condition

MW tests satisfy the criteria of significant difference for seasons more frequently than for type and age of geological formations. Therefore, the weather conditions seem to be more relevant radon and thoron activity concentration affecting factors than the local geology. Below, the results (***RnC-S-H*** and ***TnC-S-H***) are evaluated considering the environmental parameters changing through the seasons of the measurement period.

Radon median seasonal pattern (*Tab.20.*, *Fig.28.*) basically follows the typical seasonal temperature changes of the studied area. It is explained by the outdoor/indoor temperature gradient (Schubert and Schulz 2002) and the resulted pressure gradient because radon is always leaving the adobe walls and the soil towards the warmer, i.e. lower pressure side (e.g. observed in a Hungarian cave, results published in **SJ1.**). However, in case of thoron isotope, the median values decrease during the whole measurement period (*Tab.20.*, *Fig.28.*), i.e. they do not increase again by autumn when outdoor temperature drops and indoor heating usually starts. Statistical variabilities (MAD/median) of both radon and thoron levels are much lower in autumn compared to other seasons. These results all indicate the strong influence of another environmental parameter, which has the maximum effect at the end of the measurement period (**SJ6.**).

During the field campaigns, it was experienced that the studied area (Békés County) received an extreme amount of precipitation in 2010 but extremely low amount in 2011 (*Fig.33.*, OMSZ, http://www.met.hu/eghajlat/magyarorszag_eghajlata/). Since the moisture content of building materials influences their radon and thoron emanation and exhalation (e.g. Hassan et al. 2011, Hosoda et al. 2007, Porstendörfer 1994, Strong and Levins 1982, Tanner 1980, Chapter 2.3.1.2.), it can indirectly influence the indoor activity concentration values. Adobe building material, especially, tends to absorb water from the ground and release the moisture during dry spells. Therefore, the strongly decreasing amount of precipitation (*Fig.33.*) and consequently decreasing moisture content of adobe is considered to possibly cause the decreased thoron results in autumn (**SJ6.**). This is possible if the decrease is all happening below the "optimal" value of moisture content in the exhalation process (determined to be 8% in Hosoda et al. 2007, Chapter 2.3.1.2.). Other studies seem to be consistent with our thoron results (Dwivedi et al. 2001, Prasad et al. 2008, Ramola et al. 2005). If we accept the reasoning above, it has to be assumed that indoor radon data in this study are not as strongly affected by the moisture content of the building material because of the much longer half-life of this isotope and its additional source, i.e. the soil below the dwellings.

The statistical distributions of measured radon and thoron activity concentrations also show seasonal variations. In case of radon the results generally show a lognormal distribution but not in the hot summer period. Since it is known (Bossew 2010, Tóth et al. 2006) that deviation from the lognormal distribution is connected to sampling heterogeneity, it is assumed that at least two types of dwellings are formed by summer, i.e. well and poorly

ventilated ones. Consequently, the level of ventilation via opening the windows is considered to have a significantly reducing, but unpredictable effect on the radon activity concentration (**SJ6.**). The low Pearson's linear correlation coefficients for only the summer season (*Tab.21.*) also support this generally accepted process. The effect of ventilation on the thoron activity concentration is more complicated than that on that of radon. An experimental study (Shang et al. 2005) for example pointed out that indoor radon activity concentration is significantly reduced by the increase of airflow, but it does not have a similar effect on thoron.

The effects of two weather conditions were observed in the data (**SJ6.**) and additionally a third one is considered. The seasonal variations of radon and thoron activity concentrations are influenced by the temperature and ventilation weather conditions and might be affected by the amount of precipitation. Radon follows the average temperature changes and affected by the increased ventilation in summer, however thoron seems to be characterized by the amount of precipitation, i.e. the moisture content of adobe building material.

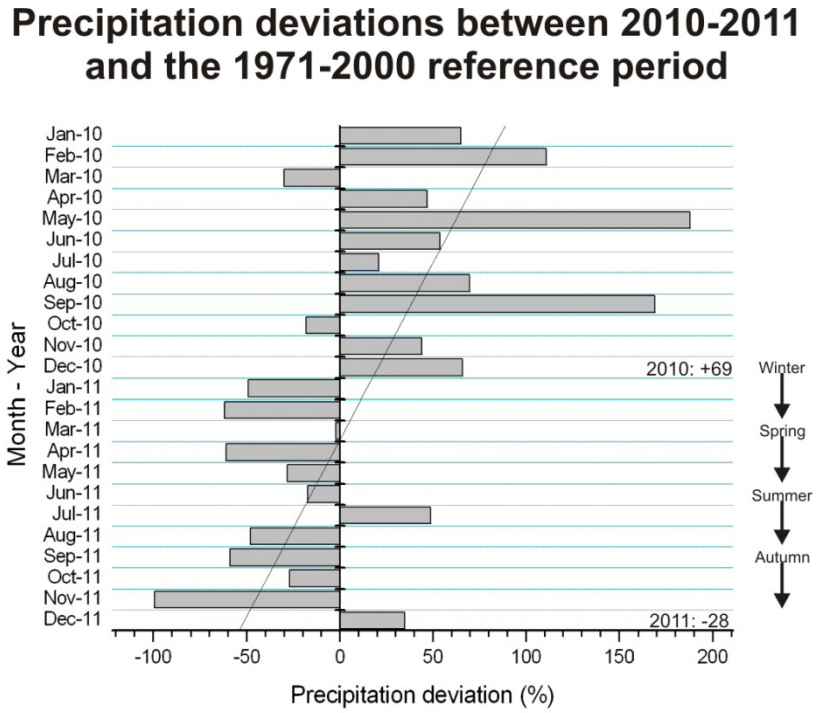

*Fig.33.: Deviation of monthly averages of measured precipitation (%) in 2010 and 2011 from the average of 1971-2000 period, Hungary (OMSZ, http://www.met.hu/eghajlat/magyarorszag_eghajlata/). The radon and thoron activity concentration measurements started in the winter of 2010, earlier months before the start of measurements are able to influence the results (**SJ6.**).*

8. CONCLUSIONS AND RECOMMENDATIONS

As fulfilling specific aims of this study, the results and their evaluation have provided two methodology achievements, one regarding radon, the other thoron emanation determination. Now it is better possible to deal with radon leakage in the experimental setup in a time saving measurement protocol for high number of samples and also with thoron decay in the sample and also RAD7 radon-thoron detector and the resulted attenuation in the sample container, while measuring the thoron activity concentrations.

The assumed elevated terrestrial radiation risk in Hungarian adobe dwellings have been studied by direct indoor (Békés County) and indirect laboratory measurements of adobe building material samples (Békés County, E-Mecsek Mts., Sajó and Hernád Rivers Valleys). The results prove that the external radiation of adobe building material does not carry added radiation risk, however, the elevation of internal (inhalation) radiation exposure due to the exhaled and accumulated radon and thoron is not negligible. It has been shown that more attention should be paid to thoron in these dwellings since its contribution to the total internal exposure is significantly above the available estimated world average values.

The ^{226}Ra and ^{232}Th activity concentrations and radon emanation fraction show significant differences for adobe sample groups originated from the three distinct areas with different geological backgrounds. Among Quaternary sedimentary formations of Békés County, both the highest indoor radon and thoron activity concentrations in adobe dwellings are expected on clay formations. However, here the weather conditions are shown to be even more significant internal exposure variation affecting factors: the average temperature of seasons, the increased ventilation in summer and an indication was found for the amount of precipitation.

Summarizing all results of this study, besides pointing out the need of continuous methodology improvements in environmental radioactivity measurements, it has been cleared that more attention should be paid to the elevated levels of indoor radon and thoron activity concentration in Hungarian adobe dwellings. Their mitigation, in the opinion of the author, should consider the typical spatial and seasonal variations and should be easily acceptable by the residents. The measured levels and experiences on the numerous field campaigns suggest that it could be recommended by regular airing.

Based on the results of this study, eight detailed scientific achievements (thesis) of the author have been raised and summarized in a separate chapter.

9. THESIS

1. I have tested a time saving – for large number of samples – radon emanation measurement method, the so-called equilibrium method regarding its sensitivity to the radon leakage from the experimental setup, which cannot be measured inside the method. I used another radon emanation measurement method, the growth curve (ingrowth) method to compare, which provides a value for the radon leakage rate in addition. The results show that for the appropriate usage of the less time consuming equilibrium method, a proven maximum 0.0025-0.003 h^{-1} radon leakage rate (α, about 30-40 % of the value of radon decay constant) has to be ensured by the design (careful sealing) of the experimental setup (**PV6.**).

2. I have described in an experiment a non-linear RAD7 detector thoron activity concentration response as a function of the thickness of a cylindrical sample. Thus, I have contributed to the final form of a model which is necessary in thoron emanation determination taking into account the sample geometry, the thoron decay in RAD7 detector and the resulted thoron activity concentration attenuation in the sample container. This model matches my experimental results, and provides an estimate for the thoron diffusion coefficient (D) in adobe building material, which is in the range of 1 to 3×10^{-6} m^2 s^{-1} (**SJ4.**). I applied this value in the thoron emanation determination of other samples.

3. I have verified that the external radiation of adobe building material does not carry any radiation risk. The building material radiation hazard indices considered (radium equivalent index, Ra_{eq} and activity concentration index, I) for the 46 adobe samples – from Békés County, E-Mecsek Mts. and Sajó and Hernád Rivers Valleys – are far below their given threshold values (370 Bq kg^{-1} and 1, unit) and also lower than for similar types of building materials reported in other countries. Both estimated annual external effective doses and in-situ measured γ dose rates confirm that the building material excess in adobe dwellings is in all cases below the accepted criterion of 1 mSv y^{-1} (**SJ2.**).

4. I have concluded that the inhaled radon, thoron and their progenies present an important internal radiation risk in adobe dwellings. I have measured annual indoor radon and thoron activity concentrations at 10 cm distance from adobe walls with medians of 188 and 232 Bq m^{-3}, respectively. Accepting lognormal distribution I have demonstrated that 14-17 % of the adobe dwellings at Békés County have radon activity concentration higher than the WHO reference level of 300 Bq m^{-3}. For comparison, accepting normal distribution, 29-32 % of them will have higher thoron activity concentration than the same value. I have estimated

the radon inhalation doses to exceed 10 mSv y^{-1} in 7 % of the 53 studied adobe dwellings and additionally thoron contributes with an elevated estimated average of 30 % in the total inhalation dose (**SJ6.**).

5. I have stated that the adobe building material acts as generally important radon and thoron source for the reason of its high radon and thoron emanation fractions. I have measured high radon and thoron emanation fractions (27 and 18 %, respectively) but comparably low ^{226}Ra and ^{232}Th activity concentrations (28 and 32 Bq kg^{-1}, respectively, **SJ2.**) for the 46 adobe samples from Békés County, E-Mecsek Mts. and Sajó and Hernád Rivers Valleys.

6. I have pointed out that among determined parameters, the ^{226}Ra and ^{232}Th activity concentrations, radon emanation fraction and estimated specific surface area show significant differences for adobe sample groups originated from different distinct areas of Békés County, E-Mecsek Mts. and Sajó and Hernád Rivers Valleys with different geological backgrounds. In this study, the ^{226}Ra and ^{232}Th activity concentrations in adobe building materials are elevated on the loess covered E-Mecsek Mts. with granite bedrock (**SJ2.**). The radon emanation fractions are the highest at Sajó and Hernád Rivers Valleys. However, the specific surface area estimated from grain size distribution is significantly higher at Békés County.

7. I have observed that the in-situ measured radioactivity levels at Békés County, i.e. the annual indoor radon and thoron activity concentrations and the average γ dose rates have characteristic spatial distributions on the type of local Quaternary sedimentary formations. Among clay, loess and turf, the highest values are always observed and hence can be expected on clay formations (**SJ6.**). Comparing the age of the same formations, Pleistocene, Holocene, values slightly higher (<95 % confidence level) are detected on Holocene age formations.

8. I have described and explained different seasonal indoor activity concentration variations for radon than for thoron. Radon median displays a close to typical seasonal variation with high values in winter and autumn, lower values in spring and low values in summer. At the same time thoron median is steadily decreasing during the measurement period from winter to autumn. I have also presented different statistical distribution (lognormal, normal) variations for the two isotopes. Based on these results I have pointed out that the radon data follow the average temperature changes and are affected by the increased ventilation in summer and I observed that seasonal thoron data is moving together with the amount of precipitation (moisture content of adobe building material) through a one year measurement period (**SJ6.**).

9. TÉZISEK

1. Meghatároztam egy – nagy mintaszám esetén – időtakarékos egyensúlyi aktivitás-koncentrációt mérő radonemanáció meghatározási módszer érzékenyégét a mérési elrendezés radon kiszökésének mértékére. Erre a radon feltöltődését mérő, és a radon eresztés mértékéről is információt adó időigényesebb módszerrel történő összehasonlítás nyújtott lehetőséget. Az eredmények alapján 0.0025-0.003 h^{-1} (α), kb. a radon bomlási állandójának 30-40 %-a alatt kell bizonyítottan tartani a radon kiszökést az időtakarékos egyensúlyi aktivitás-koncentrációt mérő módszer megfelelő, pontos eredményt adó használatához (**PV6.**).

2. Egy kísérletben kimértem a minta vastagságától függő RAD7 detektor toronaktivitás-koncentráció választ, amely egy nem-lineáris összefüggést mutat. Ezzel hozzájárultam az ezt leíró modellhez is, amely a minta geometriája mellett azt is figyelme veszi, hogy a toron felhígul a mintatartó kamrában a RAD7 detektorból visszaérkező csökkent toronaktivitás-koncentrációval. A modell jól illeszkedik a kísérleti eredményeimre. Ennek az illesztésnek a segítségével egy $1–3\times10^{-6}$ m^2 s^{-1} értékű toron diffúziós állandót becsültem a vályog építőanyagban, amelyet felhasználtam egy új módszerben a vizsgált minták toronemanáció meghatározására (**SJ4.**).

3. Igazoltam, hogy a magyarországi vályog építőanyag külső dózisterhelés szempontjából nem jelent semmilyen kockázatot. A megfontolásra javasolt építőanyag kockázati indexek (rádium ekvivalens index, Ra_{eq} és aktivitás-koncentráció index, I) mind a 46 – Békés megyéből, a Mórágyi-rög területéről és a Sajó-Hernád völgyéből származó – vályog építőanyag minta esetén jóval a határértékek (370 Bq kg^{-1} és 1, egységnyi) alatt voltak és szintén kisebbek, mint más országok hasonló építőanyagaira meghatározott értékek. Emellett, mind a becsült éves külső effektív dózis és a helyszínen mért beltéri γ-dózisteljesítmény értékek alapján a vályog építőanyagtól származó külső effektív dózisjárulék minden esetben az 1 mSv a^{-1} megkövetelt érték alatt marad (**SJ2.**).

4. Bemutattam, hogy magyarországi vályogépületekben, mind a radontól, mind a torontól és leányelemeiktől származó belső dózisterhelés nem elhanyagolható számú esetben meghaladja a WHO által ajánlott maximális radonaktivitás-koncentrációnak (300 Bq m^{-3}) megfelelő értéket. Az általam mért radon- és toronaktivitás-koncentráció medián értékek rendre 188 és 232 Bq m^{-3} voltak Békés megye területén. Elfogadva az adatok lognormális eloszlását, a vályogházak 14-17 %-ában várható a 300 Bq m^{-3}-es szintnél nagyobb radonaktivitás-koncentráció, amíg normális eloszlást tapasztalva 29-32 %-ukban lesz ugyanennél nagyobb

toronaktivitás-koncentráció 10 cm-re a faltól. A radontól származó becsült éves effektív dózis a vizsgált 53 vályogépület 7 %-ában meghaladta a 10 mSv a^{-1} szintet. Ugyanitt az elérhető legjobb dózisbecslés alapján, a toron még átlagosan 30 % növekményt okozhat (**SJ6.**).

5. Igazoltam, hogy a vályog építőanyag fontos radon- és toronforrás szerepének az oka azok emelkedett radon- és toronemanációs együtthatói. Mind a 46 – Békés megyéből, a Mórágyi-rög területéről és a Sajó-Hernád völgyéből származó – vályog építőanyag mintára általánosságban emelkedett radon- és toronemanációs együtthatókat (rendre 27 és 18 %) határoztam meg, ugyanakkor viszonylag kicsi ^{226}Ra- és ^{232}Th-aktivitás-koncentrációkat (rendre 28 és 32 Bq kg^{-1}, **SJ2.**).

6. Bemutattam, hogy a vályog építőanyag ^{226}Ra- és ^{232}Th-aktivitás-koncentrációja, radonemanációs együtthatója, valamint becsült fajlagos felülete szignifikáns különbségeket mutat a három különböző geológiai hátérrel rendelkező vizsgált területen (Békés megyében, a Mórágyi-rögön és a Sajó-Hernád völgyében). A legnagyobb vályog építőanyagban mérhető ^{226}Ra- és ^{232}Th-aktivitás-koncentrációk a lösszel fedett Mórágyi-rög gránitos alapkőzetéhez köthetők (**SJ2.**). A Sajó-Hernád völgy mintáiban pedig a radonemanációs együttható szignifikánsan nagyobb. Azonban, a szemcseméret eloszlásból becsült fajlagos felület értéke Békés megye mintáiban emelkedett.

7. Kimutattam, hogy a helyszínen mért beltéri radon-, toronaktivitás-koncentrációk és γ-dózisteljesítmény karakterisztikus területi eloszlással rendelkeznek a vizsgált Békés megyei vályogházakban. Ezeket az értékeket a helyi, negyedidőszaki üledékes geológiai képződmények szerint csoportosítva, mindegyik esetén, agyagon detektáltam és így itt várhatók a legnagyobb értékek a löszös és tőzeges területekkel szemben (**SJ6.**). A geológiai képződmények korát – pleisztocén és holocén – összehasonlítva, mérsékelten (<95 % konfidencia szint) nagyobb értékeket mértem a holocén korú formációkon.

8. Különböző szezonális változékonyságot határoztam és magyaráztam meg a helyszínen, vályogházakban mért radon- és toronaktivitás-koncentrációkra és azok statisztikai, vagyis lognormális és normális eloszlásaira. A radon értékek mediánja télen és ősszel nagy, tavasszal közepes, majd nyáron kicsi így egy közel tipikus eloszlást mutatnak. A toron medián ugyanakkor folyamatos csökkenést mutat téltől őszig. A radon változásait az évszakra jellemző átlaghőmérséklethez, valamint a nyári szellőztetés megnövekedett mértékéhez kapcsoltam, amíg a toron, a megfigyelés szerint, a csapadék mennyiségével mozgott együtt az egyéves mérési időszak során (**SJ6.**).

PUBLICATIONS OF THE AUTHOR

Papers in scientific journals

SJ1.: Nagy, H.É., **Szabó, Zs.**, Jordan, G., Szabó, Cs., Horváth, Á. & Kiss, A. (**2012**) Time variations of ^{222}Rn concentration and air exchange rates in a Hungarian cave. *Isotopes in Environmental and Health Studies* 48, 464–472. (2012 **IF**: 0.767)

SJ2.: **Szabó, Zs.**, Völgyesi, P., Nagy, H.É., Szabó, Cs., Kis, Z. & Csorba, O. (**2013**) Radioactivity of natural and artificial building materials – a comparative study. *Journal of Environmental Radioactivity* 118, 64–74. (5-Year **IF**: 1.927)

SJ3.: Nagy, H.É., **Szabó, Zs.**, Scheuer, Gy. & Szabó, Cs. (**2013**) Radioactivity of medicinal springs in Eger (in Hungarian with English abstract). *Hidrológiai Közlöny* 93, 20–26.

SJ4.: Csige, I., **Szabó, Zs.** & Szabó, Cs. (**2013**) Experimental technique to measure thoron generation rate of building material samples using RAD7 detector. *Radiation Measurements* 59, 201–204. (5-Year **IF**: 1.185)

SJ5.: Kis, Z., Völgyesi, P. & **Szabó, Zs.** (**2013**) DÖME – revitalizing a low-background counting chamber and developing a radon-tight sample holder for gamma-ray spectroscopy measurements. *Journal of Radioanalytical and Nuclear Chemistry* 298, 2029–2035. (2012 **IF**: 1.467)

SJ6.: **Szabó, Zs.**, Jordan, G., Szabó, Cs., Horváth, Á., Holm, Ó., Kocsy, G., Csige, I., Szabó, P. & Homoki, Zs. (**in press**) Radon and thoron levels, their spatial and seasonal variations in adobe dwellings – a case-study at the Great Hungarian Plain. *Isotopes in Environmental and Health Studies*, DOI:10.1080/10256016.2014.862533 (2012 **IF**: 0.767)

Papers in proceeding volumes

PV1.: **Szabó, Zs.** & Boros, Á. (**2009**) Applicability of RAD7 radon detector at high thoron activity concentration (in Hungarian). 5th Environmental Scientific Conference of the Carpathian Basin, March 26-29, 2009, Kolozsvár (Cluj-Napoca), Transylvania, 457–462.

PV2.: **Szabó, Zs.**, Boros, Á., Horváth, Á. & Szabó, Cs. (**2009**) Thorium anomaly at Nagy-Kopasz Hill (Buda Mts.): a case study for correction of the RAD7 detector (in Hungarian). 5th Hungarian Radon Forum, May 18, 2009, Veszprém, Hungary, 123–128.

PV3.: Boros, Á, **Szabó, Zs.**, Szabó, K.Zs., Völgyesi, P., Horváth, Á. & Szabó, Cs. (**2010**) Evaluation of radon risk using GIS (Geographic Information System) techniques in the Central Hungarian Region. 3rd European IRPA Congress, June 14-18, 2010, Helsinki, Finland, 609–615, *http://www.irpa2010europe.com/pdfs/proceedings/S03-P03.pdf*

PV4.: Grosch, M., **Szabó, Zs.**, Boros, Á., Müller, M. & Szabó, Cs. (**2011**) Environmental geochemical study of thorium anomaly in the Buda Mts. (in Hungarian). 2nd Terrestrial Radioisotopes in the Environment Conference, May 12, 2010, Veszprém, Hungary, 99–104.

PV5.: **Szabó, Zs.**, Szabó, Cs. & Horváth, Á. (**2011**) Experiences of thoron measurements on Hungarian adobe (in Hungarian). 7th Environmental Scientific Conference of the Carpathian Basin, March 24-27, 2011, Kolozsvár (Cluj-Napoca), Transylvania, 129–133.

PV6.: **Szabó, Zs.**, Szabó, Cs. & Horváth, Á. (**2011**) Comparison of two ^{222}Rn mass exhalation rate measurement methods by study of Hungarian adobe building materials. Nordic Society for Radiation Protection Conference: Current Challenges in Radiation Protection, August 22-25, 2011, Reykjavik, Iceland, *http://www.nsfs.org/NSFS-2011/documents/session-12/S12-O7.pdf*

PV7.: **Szabó, Zs.**, Szabó, Cs. & Horváth, Á. (**2012**) Complex radon and thoron study on Hungarian adobe dwellings. 6th Hungarian Radon Forum, May 16-17, 2011, Veszprém, Hungary, 197–202.

PV8.: Völgyesi, P., **Szabó, Zs.**, Nagy H.É., Somlai, J., & Szabó, Cs. (**2012**) Radiation hazard of different Hungarian building materials. 6th Hungarian Radon Forum, May 16-17, 2011, Veszprém, Hungary, 203–209.

PV9.: Zacháry, D., Nagy H.É., **Szabó, Zs.**, Szabó, K.Zs., Horváth, Á.& Szabó, Cs. (**2012**) Radon emanation fractionation measurements of soils developed on different source rocks from Hungary. 6th Hungarian Radon Forum, May 16-17, 2011, Veszprém, Hungary, 211–218.

Popular science articles

Nagy, H. É., Szabó, K. Zs. & **Szabó, Zs.** (**2009**) Our radioactive roommate (in Hungarian). *Természet Világa* 140/5, 234–235.

Summary of conference presentations (first and/or presenting author)

10 oral presentations

12 poster presentations

Awards:

2009: 1st prize at the National Scientific Conference of Students held at the Western Hungarian University, Szombathely, Hungary

2011: Young Scientist Award of the Nordic Society for Radiation Protection Conference: Current Challenges in Radiation Protection, Reykjavik, Iceland

REFERENCES

Al-Hamarneh, I.F., Awadallah M.I. (2009) Soil radioactivity levels and radiation hazard assessment in the highlands of northern Jordan. Radiation Measurements 44, 102–110.

Al-Sulaiti, H., Alkhomashi, N., Al-Dahan, N., Al-Dosari, M., Bradley, D.A., Bukhari, S., Matthews, M., Regan, P.H., Santawamaitre, T. (2011) Determination of the natural radioactivity in Qatarian building materials using high-resolution gamma-ray spectrometry. Nuclear Instruments and Methods in Physics Research A 652, 915–919.

AMC (Analytical Methods Committee) (2001) What should be done with results below the detection limit? Mentioning the unmentionable. Technical Brief No. 5. Royal Society of Chemistry, London, 2 pages.

Andersen, C.E. (2001) Numerical modeling of radon-222 entry into houses: an outline of techniques and results. The Science of the Total Environment 272, 33–42.

ASI (Austrian Standards Institute) (2009) Radioactivity in construction materials. ENTWURF ÖNORM S 5200:2009, Vienna, 14 pages.

Beretka, J., Mathew, P.J. (1985) Natural radioactivity of Australian building materials, industrial wastes and by-products. Health Physics 48, 87–95.

Bochicchio, F. (2008) The radon issue: Considerations on regulatory approaches and exposure evaluations on the basis of recent epidemiological results. Applied Radiation and Isotopes 66, 1561–1566.

Bossew, P. (2010) Radon: exploring the log-normal mystery. Journal of Environmental Radioactivity 101, 826–834.

Chougaonkar, M.P., Eappen, K.P., Ramachandran, T.V., Shetty, P.G., Mayya, Y.S., Sadasivan, S., Venkat Raj, V. (2004) Profiles of doses to the population living in the high background radiation areas in Kerala, India. Journal of Environmental Radioactivity 71, 275–297.

Cozmuta, I., van der Graaf, E.R. (2001) Methods for measuring diffusion coefficients of radon in building materials. The Science of the Total Environment 272, 323–335.

Csige, I. (personal communication, 2013) Atomki (Institute for Nuclear Research), Hungarian Academy of Sciences, Debrecen, Hungary.

Damla, N., Cevik, U., Kobya, A.I., Celik, A., Yildirim, I. (2011) Assessment of natural radioactivity and mass attenuation coefficients of brick and roofing tile used in Turkey. Radiation Measurements 46, 701–708.

Darby, S., Hill, D., Auvinen, A., Barros-Dios, J.M., Baysson, H., Bochicchio, F., Deo, H., Falk, R., Forastiere, F., Hakama, M., Heid, I., Kreienbrock, L., Kreuzer, M., Lagarde, F., Mäkeläinen, I., Muirhead, C., Oberaigner, W., Pershagen, G., Ruano-Ravina, A., Ruosteenoja, E., Rosario, A.S., Tirmarche, M., Tomásek, L., Whitley, E., Wichmann, H.E., Doll, R. (2005) Radon in homes and risk of lung cancer: collaborative analysis of individual data from 13 European case-control studies. British Medical Journal 330, 223–226.

Deka, P.C., Sarkar, S., Bhattacharjee, B., Goswami, T.D., Sarma, B.K., Ramachandran, T.V. (2003) Measurement of radon and thoron concentration by using LR-115 type-II plastic track detectors in the environ of Brahmaputra Valley, Assam, India. Radiation Measurements 36, 431–434.

Di Stefano, C., Ferro, V., Mirabile S. (2010) Comparison between grain-size analyses using laser diffraction and sedimentation methods. Biosystems Engineering 106, 205–215.

Dowdall, M., Selnaes, Ø.G., Gwynn, J.P., Davids, C. (2004) Simultaneous determination of ^{226}Ra and ^{238}U in soil and environmental materials by gamma-spectrometry in the absence of radium progeny equilibrium. Journal of Radioanalytical and Nuclear Chemistry 261, 513–521.

Durridge Co. (2013) RAD7 Radon Detector User Manual (Revision 7.2.1.). Boston, 77 pages, 49–63.

Dwivedi, K.K., Mishra, R., Tripathy, S.P., Kulshreshtha, A., Sinha, D., Srivastava, A., Deka, P., Bhattacharjee, B., Ramachandran, T.V., Nambi, K.S.V. (2001) Simultaneous determination of radon, thoron and their progeny in dwellings. Radiation Measurements 33, 7–11.

Ebaid, Y.Y., El-Mongy, S.A., Allam, K.A. (2005) ^{235}U–γ emission contribution to the 186 keV energy transition of ^{226}Ra in environmental samples activity calculations. International Congress Series 1276, 409–411.

EC (European Comission) (1999) Radiological protection principles concerning the natural radioactivity of building materials. Radiation Protection Report No. 112, Luxemburg, 16 pages.

Eisenbud, M., Gesell, T. (1997) Environmental radioactivity from natural, industrial, and military sources (4th Edition). Elsevier, ISBN: 978-0-12-235154-9.

Greeman, D.J., Rose, A.W. (1996) Factors controlling the emanation of radon and thoron in soils of the eastern U.S.A. Chemical Geology 129, 1–14.

Gyalog, L. (2005) 1:100 000 Geological map of Hungary (digital version). Former MÁFI (Geological Institute of Hungary), Budapest.

Hamilton, E.I. (1971) The relative radioactivity of building materials. American Industrial Hygiene Association Journal 32, 398–403.

Hámori, K. (2006) Nukleáris méréstechnika radioaktív gázok vizsgálatára (Nuclear measurement techniques for analysis of radioactive gases). Ph.D. thesis, University of Debrecen, Hungary.

Hámori, K., Tóth, E. (2004) A lakótéri radon Magyarországon (The indoor radon in Hungary). RAD Labor, Budapest, 14 pages.

Hámori, K., Váradi, M,. Csikai, J. (2006) Space charge effect on the electrostatic collection of thoron decay products. Applied Radiation and Isotopes 64, 854–857.

Harley, N., Chittaporn, P., Medora, R., Merrill, R. (2010) Measurement of the indoor and outdoor ^{220}Rn (thoron) equilibrium factor: application to lung dose. Radiation Protection Dosimetry 141, 357–362.

Hassan, N.M., Ishikawa, T., Hosoda, M., Iwaoka, K., Sorimachi, A., Sahoo, S.K., Janik, M., Kranrod, C., Yonehara, H., Fukushi, M., Tokonami, S. (2011) The effect of water content on the radon emanation coefficient for some building materials used in Japan. Radiation Measurements 46, 232–237.

Hellevang, H. (personal communication, 2013) Department of Geosciences, University of Oslo, Oslo, Norway.

Hewamanna, R., Sumithrarachchi, C.S., Mahawatte, P., Nanayakkara, H.L.C., Ratnayake, H.C. (2001) Natural radioactivity and gamma dose from Sri Lankan clay bricks used in building construction. Applied Radiation and Isotopes 54, 365–369.

Hopke, P.K., Jensen, B., Li C.S., Montassier, N., Wasiolek, P., Cavallo, A.J., Gatsby, K., Socolow, R.H., James A.C. (1995) Assessment of the exposure to and dose from radon decay products in normally occupied homes. Environmental Science and Technology 29, 1359–1364.

Hosoda, M., Shimo, M., Sugino, M., Furukawa, M., Fukushi, M. (2007) Effect of soil moisture content on radon and thoron exhalation. Journal of Nuclear Science and Technology 44, 664–672.

HZM (Helmholtz Zentrum München, German Research Center for Environmental Health, Institute of Radiation Protection), *http://www.helmholtz-muenchen.de*, Indoor thoron and radon. Significance of thoron in radiation protection.

IAEA (International Atomic Energy Agency) (1986) Environmental migration of radium and other contaminants present in liquid and solid wastes from the mining and milling of uranium. IAEA-TECDOC-370, Vienna, 23 pages (without Appendixes).

IAEA (International Atomic Energy Agency) (2003) Radiation protection against radon in workplaces other than mines. Safety Report Series No. 33. Vienna, 74 pages.

ICRP (International Commission on Radiological Protection) (1990) Recommendations of the ICRP. ICRP Publication 60. Ann. ICRP 21(1-3).

ICRP (International Commission on Radiological Protection) (2005) Low-dose extrapolation of radiation-related cancer risk. ICRP Publication 99. Ann. ICRP 35(4).

ICRP (International Commission on Radiological Protection) (2007) The 2007 recommendations of the ICRP. ICRP Publication 103. Ann. ICRP 37(2-4).

ICRP (International Commission on Radiological Protection) (2008) Review, New ICRP recommendations. Journal of Radiological Protection 28, 161–168.

ICRP (International Commission on Radiological Protection) (2009) Statement on radon. ICRP Ref 00/902/09, 2 pages.

ICRU (International Commission on Radiation Units and Measurements) (1985) Determination of dose equivalents resulting from external radiation sources. ICRU Report 39. Bethesda.

Ingersoll, J.G. (1983) A survey of radionuclide contents and radon emanation rates in building materials used in the U.S. Health Physics 45, 363–368.

Jonassen, N. (1983) The determination of radon exhalation rates. Health Physics 45, 369–376.

Kaste, J.M., Bostick, B.C., Heimsath, A.M., (2006) Determining ^{234}Th and ^{238}U in rocks, soils, and sediments via the doublet gamma at 92.5 keV. Analyst 131, 757–763.

Kávási, N., Németh, Cs., Kovács, T., Tokonami, S., Jobbágy, V., Várhegyi, A., Gorjánácz, Z., Vígh, T., Somlai, J. (2007) Radon and thoron parallel measurements in Hungary. Radiation Protection Dosimetry 123, 250–253.

Kemski, J., Siehl, A., Stegemann, R., Valdivia-Manchego, M. (2001) Mapping the geogenic radon potential in Germany, Science of the Total Environment 272, 217–230.

Khokhar, M.S.K., Kher, R.S., Rathore, V.B., Pandey, S., Ramachandran, T.V. (2008) Comparison of indoor radon and thoron concentrations in the urban and rural dwellings of Chhattisgarh state of India. Radiation Measurements 43, 405–409.

Kocsy, G. (2012) Lower limit of detection with RADUET detectors. Radosys Ltd., Budapest, 4 pages.

Kohli, S., Sahlén, K., Löfman, O., Sivertun, Å, Foldevi, M., Trell, E., Wigertz, O. (1997) Individuals living in areas with high background radon: a GIS method to identify populations at risk. Computer Methods and Programs in Biomedicine 53, 105–112.

Kovács, T. (2010) Thoron measurements in Hungary. Radiation Protection Dosimetry 141, 328–334.

Krieger, R., (1981) Radioactivity of construction materials. Betonwerk Fertigteil Techn 47, 468–473.

Krishnaswami, S., Cochran, J.K. (2008) Appendix B: Systematics of Radioactive Decay, Volume 13: U-Th Series Nuclides in Aquatic Systems in: Baxter, M.S. Radioactivity in the environment, A companion series to the Journal of Environmental Radioactivity. Elsevier, ISBN: 9780080450124.

Luo, Y., Zhuo, W., Wei, M., Tokonami, S., Wang, W., Yamada, Y., Chen, J., Chen, M. (2005) Natural radiation levels in Fuan city in Fujian Province of China. International Congress Series 1276, 311–312.

Madas, B.G., Balásházy, I. (2011) Mutation induction by inhaled radon progeny modeled at the tissue level. Radiation and Environmental Biophysics 50, 553–570.

Mann, H.B., Whitney, D.R. (1947) On a test of whether one of two random variables is stochastically larger than the uther. Annals of Mathematical Statistics 18, 50–60.

Megumi, K., Mamuro, T. (1974) Emanation and exhalation of radon and thoron gases from soil particles. Journal of Geophysical Research 79, 3357–3360.

MFGI (Geological and Geophysical Institute of Hungary), *http://loczy.mfgi.hu/fdt100/*, 1:100 000 Geological map of Hungary (online version).

Milić, G., Jakupi, B., Tokonami, S., Trajković, R., Ishikawa, T., Čeliković, I., Ujić, P., Čuknić, O., Yarmoshenko, I., Kosanović, K., Adrović, F., Sahoo, S.K., Veselinović, N., Žunić, Z.S. (2010) The concentrations and exposure doses of radon and thoron in residences of the rural areas of Kosovo and Metohija. Radiation Measurements 45, 118–121.

Minda, M., Tóth, G., Horváth, I., Barnet, I., Hámori, K., Tóth, E. (2009) Indoor radon mapping and its relation to geology in Hungary. Environmental Geology 57, 601–609.

Moura, C.L., Artur, A.C., Bonotto, D.M., Guedes, S., Martinelli, C.D. (2011) Natural radioactivity and radon exhalation rate in Brazilian igneous rocks. Applied Radiation and Isotopes 69, 1094–1099.

Nazaroff, W.W., Moed, B.A., Sextro, R.G. (1988) Soil as source of indoor radon: generation, migration and entry. 57–112. in: Nazaroff, W.W., Nero, A.V. Radon and its decay products in indoor air. Wiley, ISBN: 978-0-471-62810-1.

Németh, C., Tokonami, S., Ishikawa, T., Takahashi, H., Zhuo, W., Shimo, M. (2005) Measurements of radon, thoron and their progeny in a dwelling in Gifu prefecture, Japan. International Congress Series 1276, 283–284.

NuDat 2.6, *http://www.nndc.bnl.gov/nudat2/*, online database of the National Nuclear Data Center, Brookhaven National Laboratory.

OECD (Organization for Economic Cooperation and Development) (1979) Exposure to radiation from the natural radioactivity in building materials. Report by an NEA (Nuclear Energy Agency) Group of Experts, Paris, 34 pages.

Omori, Y., Prasad, G., Sagar, V., Sahoo, S.K., Sorimachi A., Janik, M., Ishikawa, T., Tokonami, S., Ramola R.C. (2013) Thoron Equilibrium Factors Based on Long-term Measurements of Thoron and Its Progeny Concentration around a High Background Radiation Area in Orissa, India. Oral presentation at the 7th Hungarian Radon Forum and Radon in environment Satellite workshop, May 16-17, Veszprém, Hungary *http://rri.vein.hu/conferences/radon/2013/presentations/session3/3_omori.pdf*

OMSZ (Hungarian Meteorological Service), *www.met.hu/eghajlat/magyarorszag_eghajlata*, Climate of Hungary (online database),

Papachristodoulou, C.A., Assimakopoulos, P.A., Patronis, N.E., Ionnadis, K.G. (2003) Use of HPGe γ-ray spectrometry to assess the isotopic composition of uranium in soils. Journal of Environmental Radioactivity 64, 195–203.

Petropoulos, N.P., Anagnostakis, M.J., Simopoulos, S.E. (2001) Building materials radon exhalation rate: ERRICCA intercomparison exercise results, Science of the Total Environment 272, 109–118.

Porstendörfer, J. (1994) Properties and behaviour of radon and thoron and their decay products in the air. Journal of Aerosol Science 25, 219–263.

Prasad, G., Prasad, Y., Gusain, G.S., Ramola, R.C. (2008) Measurement of radon and thoron levels in soil, water and indoor atmosphere of Budhakedar in Garhwal Himalaya, India. Radiation Measurements 43, 375–379.

Ramachandran, T.V., Subba Ramu, M.C. (1994) Variation of equilibrium factor F between radon and its short-lived decay products in an indoor atmosphere. International journal of radiation applications and instrumentation, Part E, Nuclear geophysics 8, 499–503.

Ramola, R.C., Negi, M.S., Choubey, V.M. (2005) Radon and thoron monitoring in the environment of Kumaun Himalayas: survey and outcomes. Journal of Environmental Radioactivity 79, 85–92.

Reimann, R.C., Filzmoser, P., Garrett, R.G., Dutter, R. (2008) Statistical data analysis explained: Applied environmental statistics. Wiley, ISBN: 978-0-470-98581-6.

Rogers, V.C., Nielson, K.K. (1991) Correlations for predicting air permeabilities and ^{222}Rn diffusion coefficients of soils. Health Physics 61, 225–230.

Saidou, Bochud, F., Laedermann, J.P., Kwato Njock, M.G., Froidevaux, P. (2008) A comparison of alpha and gamma spectrometry for environmental natural radioactivity surveys. Applied Radiation and Isotopes 66, 215–222.

Sakoda, A., Hanamoto, K., Ishimori, Y., Nagamatsu, T., Yamaoka, K. (2008) Radioactivity and radon emanation fraction of the granites sampled at Misasa and Badgastein. Applied Radiation and Isotopes 66, 648–652.

Sas, Z. (2012) Építőanyagok radonemanációját és exhalációját befolyásoló paraméterek meghatározása (Parameters influencing the radon emanation and exhalation of building materials). Ph.D. thesis, University of Pannonia, Veszprém, Hungary.

Sas, Z., Somlai, J., Szeiler, G., Kovács, T. (2012) Radon emanation and exhalation characteristic of heat-treated clay samples. Radiation Protection Dosimetry 152, 51–54.

Schubert, M., Schulz, H. (2002) Diurnal radon variations in the upper soil layers and at the soil-air interface related to meteorological parameters. Health Physics 83, 91–96.

Sciocchetti, G., Bovi, M., Cotellessa, G., Baldassini, P.G., Battella, C., Porcu, I. (1992) Indoor radon and thoron surveys in high radioactivity areas of Italy. Radiation Protection Dosimetry 45, 509–514.

Shang, B., Chen, B., Gao, Y., Wang, Y.W., Cui, H.X., Li, Z. (2005) Thoron levels in traditional Chinese residential dwellings. Radiation and Environmental Biophysics 44, 193–199.

Shapiro, S.S., Wilk, M.B. (1965) An analysis of variance test for normality (complete samples). Biometrika 52, 591–611.

Sreenath Reddy, M., Yadagiri Reddy, P., Rama Reddy, K., Eappen, K.P., Ramachandran, T.V., Mayya, Y.S. (2004) Thoron levels in the dwellings of Hyderabad city, Andhra Pradesh, India. Journal of Environmental Radioactivity 73, 21–28.

Steinhäusler, F. (1996). Environmental ^{220}Rn: A review. Environment International 22, 1111–1123.

Stojanovska, Z., Bossew, P., Tokonami, S., Žunić, Z.S., Bochicchio, F., Boev, B., Ristova, M., Januseski, J. (2013) National survey of indoor thoron concentration in FYR of Macedonia (continental Europe – Balkan region). Radiation Measurements 49, 57–66.

Stojanovska, Z., Januseski, J., Bossew, P., Žunić, Z.S., Tollefsen, T., Ristova, M. (2011) Seasonal indoor radon concentration in FYR of Macedonia. Radiation Measurements 46, 602–610.

Stranden, E. (1988) Building materials as a source of indoor radon. 113–130. in: Nazaroff, W.W., Nero, A.V. Radon and its decay products in indoor air. Wiley, ISBN: 978-0-471-62810-1.

Stranden, E., Kolstad, A.K., Lind, B. (1984) The influence of moisture and temperature on radon exhalation. Radiation Protection Dosimetry 7, 55–58.

Strong, K.P., Levins, D.M. (1982) Effect of moisture content on radon emanation from uranium ore and railings. Health Physics 42, 27–32.

Szabó K.Zs., Jordan G., Horváth, Á., Szabó, Cs. (2013) Dynamics of soil gas radon concentration in a highly permeable soil based on a long-term high temporal resolution observation series. Journal of Environmental Radioactivity 124, 74–83.

Takeno, N., (2005) Atlas of Eh-pH Diagrams. Intercomparison of thermodynamic databases. Open File Report No. 419. Geological Survey of Japan, 285 pages.

Tan, Y., Xiao, D. (2013) The method for recalibration of thoron concentration reading of RAD7 and obtaining the thoron exhalation rate from soil surface. Nuclear Technology and Radiation Protection 28, 92–96.

Tanner, A.B. (1964) Radon migration in the ground: a review. 161–190. in: Adams, J.A.S., Lowder, W.M. The natural radiation environment. University of Chicago Press, Chicago.

Tanner, A.B. (1980) Radon migration in the ground: supplementary review. 5–56. in: Gesell, T.F., Lowder, W.M. Proceedings natural radiation environment III, National Technical Information Service, Washington.

Thermo Scientific (2007) The modular system for radioactivity measurements, FH 40 G/GL Digital Survey Meter and FHT 6020 Display Unit. Thermo Scientific, 16 pages (*http://www.thermo.com/eThermo/CMA/PDFs/Product/productPDF_2635.pdf*).

Tokonami, S. (2010) Why is ^{220}Rn (thoron) measurement important? Radiation Protection Dosimetry 141, 335–339.

Tóth, E. (1999) Radon a magyar falvakban (Radon in Hungarian villages). Fizika Szemle 2, (*http://epa.oszk.hu/00300/00342/00110/radon.html*)

Tóth, E., Hámori, K., Minda, M. (2006) Indoor radon in Hungary (lognormal mysticism). (*http://www.geology.cz/extranet/vav/geochemie-zp/radon/sympozia/2006*, Last Accessed 30.11.2009). in: Barnet, I., Neznal, M., Pacherová, P. Radon Investigations in the Czech Republic XI and the 8th International Workshop on the Geological Aspects of Radon Risk Mapping. Proceedings. Czech Geological Survey, Prague.

Trevisi, R., Risica, S., D'Alessandro, M., Paradiso, D., Nuccetelli, C. (2012) Natural radioactivity in building materials in the European Union: a database and an estimate of radiological significance. Journal of Environmental Radioactivity 105, 11–20.

Tuccimei, P., Moronic, M., Norcia, D. (2006) Simultaneous determination of ^{222}Rn and ^{220}Rn exhalation rates from building materials used in Central Italy with accumulation chambers and a continuous solid state alpha detector: Influence of particle size, humidity and precursors concentration. Applied Radiation and Isotopes 64, 254–263.

Tukey, J.W. (1977) Exploratory Data Analysis, Behavioral Science. Addison-Wesley, Boston, ISBN-10: 0201076160, ISBN-13: 978-0201076165.

Ujić, P., Čeliković, I., Kandić, A., Žunić, Z.S. (2008) Standardization and difficulties of the thoron exhalation rate measurements using an accumulation chamber. Radiation Measurements 43, 1396–1401.

UNSCEAR (United Nations Scientific Committee on the Effects of Atomic Radiation) (2000) Annex B, Exposures from natural radiation sources. 83–156. in: UNSCEAR. Sources and effects of ionizing radiation, Report to the General Assembly with Scientific Annexes. New York.

UNSCEAR (United Nations Scientific Committee on the Effects of Atomic Radiation) (2006) Annex E, Sources-to-effects assessment for radon in homes and workplaces. 197–334. in: UNSCEAR. Effects of ionizing radiation, Report to the General Assembly with Scientific Annexes. New York

Urosevic, V., Nikezic, D., Vulovic, S. (2008) A theoretical approach to indoor radon and thoron distribution. Journal of Environmental Radioactivity 99, 1829–1833.

van der Graaf, E.R., Schaap, L.E., Bosmans, G. (2001) Radiation performance index for Dutch dwellings: consequences for some typical situations. Science of the Total Environment 272, 151–158.

Vaupotic, J., Kávási, N. (2010) Preliminary study of thoron and radon levels in various indoor environments in Slovenia. Radiation Protection Dosimetry 141, 383–385.

Völgyesi, P., Nagy, H.É., Szabó, Cs. (2011) Radiometric and environmental geochemical study of building materials from certain settlements within the central region of Hungary. 119–123. in: Mócsy, I., Urák, I., Farkas, G., Nagy, K., Szacsvai, K., Tóth, A., Zsigmond, A. VII. Environmental Scientific Conference of the Carpathian Basin. Proceedings. Kolozsvár (Cluj-Napoca). ISSN: 1842-9815.

Wattananikorn, K., Emharuthai, S., Wanaphongse, P. (2008) A feasibility study of geogenic indoor radon mapping from airborne radiometric survey in northern Thailand, Radiation Measurements 43, 85–90.

Weiszburg, T., Tóth E. (2011) I. Környezetünk szilárd anyagai és szerepük a környezeti folyamatokban. 8–58. in: Weiszburg, T. Környezeti ásványtan, Környezettudományi alapok tankönyvsorozat. Typotex. ISBN 978-963-279-541-6.

WHO (World Health Organization) (2009) WHO handbook on indoor radon: a public health perspective. WHO Press. 110 pages. ISBN: 978 92 4 154767 3.

Wunsch, A. (2009) Soil Texture Utility 2.0., USDA soil texture triangle, *inside.mines.edu/~awunsch/pubs/Soil%20Texture%20Utility%202.0.xls*, Colorado School of Mines.

Yamada, Y., Tokonami, S., Zhuo, W., Yonehara, H., Ishikawa, T., Furukawa, M., Fukutsu, K., Sun, Q., Hou, C., Zhang, S., Akiba, S. (2005) Rn-Tn discriminative measurements and their dose estimates in Chinese loess plateau. International Congress Series 1276, 76–80.

Yonehara, H., Tokonami, S., Zhuo, W., Ishikawa, T., Fukutsu, K., Yamada, Y. (2005) Thoron in the living environments of Japan. International Congress Series 1276, 58–61.

Yücel, H., Çetiner, M.A., Demirel, H. (1998) Use of the 1001 keV peak of ^{234m}Pa daughter of ^{238}U in measurement of uranium concentration by HPGe gamma-ray spectrometry. Nuclear Instruments and Methods in Physics Research A 413, 74–82.

Yücel, H., Solmaz, A.N., Köse, E., Bor, D. (2009) Spectral interference corrections for the measurement of ^{238}U in materials rich in thorium by a high resolution γ-ray spectrometry. Applied Radiation and Isotopes 67, 2049–2056.

Zagyvai, P. (personal communication, 2013) Centre for Energy Research, Hungarian Academy of Sciences, Budapest, Hungary.

Žunić, Z.S., Celiković, I., Tokonami, S., Ishikawa, T., Ujić, P., Onischenko, A., Zhukovsky, M., Milić, G., Jakupi, B., Cuknić, O., Veselinović, N., Fujimoto, K., Sahoo, S.K., Yarmoshenko, I. (2010) Collaborative investigations on thoron and radon in some rural communities of Balkans. Radiation Protection Dosimetry 141, 346–350.

LIST OF TABLES

LIST OF FIGURES

The views and opinions of the author expressed herein do not necessarily state or reflect those of any department and institute connected to this work.

SUMMARY

TERRESTRIAL RADIOACTIVITY IN HUNGARIAN ADOBE BUILDING MATERIAL AND DWELLINGS WITH A FOCUS ON THORON (^{220}RN)

Radon (^{222}Rn) and thoron (^{220}Rn) isotopes are responsible for approximately the half of the annual effective dose to an average human from natural sources. Thoron can significantly contribute to the internal radiation dose in some special environments, like adobe dwellings. The main objective of this study was to evaluate the assumed elevated terrestrial radiation risk in Hungarian adobe dwellings. The spatial distribution and seasonal variation of the measured levels are also considered. This work also provides solutions to some problems occurred in the radon and thoron emanation determination methods of building material samples.

Altogether 46 adobe samples were collected from three distinct areas of Hungary. These are Békés County, E-Mecsek Mts. and Sajó and Hernád Rivers Valleys. At Békés County in-situ measurements were also carried out in 53 adobe dwellings. The adobe samples were studied in laboratory and their radon and thoron emanations, emanation fractions, ^{226}Ra, ^{232}Th and ^{40}K activity concentrations, different building material hazard indices, excess to the external dose received outdoors and grain size distributions were determined. In the selected adobe dwellings indoor radon and thoron activity concentrations in four seasons and γ dose rates were measured. Based on the results the inhalation does is estimated. The obtained data were evaluated by statistical methods: basic statistic, Mann-Whitney (Wilcoxon) and Shapiro-Wilk hypothesis tests and correlation analysis.

Regarding radon and thoron emanation methodology achievements, now it is better possible to deal with radon leakage from generally the experimental setup in a time saving measurement protocol and also with thoron decay in the RAD7 radon-thoron detector and attenuation in the sample container while measuring the thoron activity concentrations. The evaluation of the measured levels shows that the external radiation of adobe building material does not carry any radiation risk, however, the elevation of internal (inhalation) radiation exposure due to the exhaled and accumulated radon and thoron is not negligible. The most significant affecting factors are shown to be the weather conditions. These are considered to result different indoor radon and thoron activity concentration seasonal variations in this study. It has been cleared that among Quaternary sedimentary formations of Békés County, the highest values have to be expected on clay formations. For the adobe building materials of the three distinct areas, the highest ^{226}Ra and ^{232}Th activity concentrations (which are the sources of radon and thoron) were shown to belong to the E-Mecsek Mts.

ÖSSZEFOGLALÁS

TERRESZTRIÁLIS RADIOAKTIVITÁS MAGYARORSZÁGI VÁLYOGBAN ÉS VÁLYOGHÁZAKBAN KÜLÖNÖS TEKINTETTEL A TORONRA (^{220}RN)

A radon (^{222}Rn) és toron (^{220}Rn) izotópok egy átlagos ember természetes forrásból származó éves effektív dózisterhelésének kb. feléért felelősek. Ehhez a toron csupán néhány speciális környezetben járulhat hozzá jelentősen, például bizonyítottan vályogházakhoz hasonló épületekben. Ezen kutatás fő célja az volt, hogy értékelje a feltételezetten emelkedett terresztriális radioaktivitás szerepét magyarországi vályogházakban az eredmények eloszlásával és évszakos változásaival együtt. A vályogminták vizsgálata ugyanakkor hozzájárult az alkalmazott radon- és toronemanáció meghatározás módszereit érintő problémák megoldásához is.

A kutatás során 46 vályogminta került begyűjtésre Békés megye, a Mórágyi-rög és a Sajó-Hernád völgy területein. Ezen minták laboratóriumi vizsgálata mellett Békés megyében helyszíni mérések is történetek 53 vályogházban. A laboratóriumi vizsgálatok során a vályogminták radon- és toronemanációja, emanációs együtthatója, ^{226}Ra-, ^{232}Th- és ^{40}K-aktivitás-koncentrációja, különböző építőanyag kockázati indexei, becsült külső dózisjáruléka és szemcseméret eloszlása került meghatározásra. A kiválasztott vályogházakban helyszíni mérések történtek, ezek radon- és toronaktivitás-koncentráció négy évszakban, valamint γ-dózisteljesítmény adatokat szolgáltattak. Az eredmények alapján megbecsülhető a belső dózisterhelés. Az adatokat statisztikai módszerek, alapstatisztikai elemzés, Mann-Whitney (Wilcoxon) és Shapiro-Wilk hipotézis tesztek és korreláció analízis segítségével értékeltem.

Az eredmények hozzájárultak ahhoz, hogy egy időtakarékos radonemanáció mérési módszerben megfelelően lehessen értékelni a radon kiszökés jelenségét, valamint, hogy a RAD7 radon-toron detektorban történő toron elbomlás majd az ezt követő mintatartó kamrában történő felhígulás is kezelhető legyen a toronemanáció meghatározás során. Továbbá kijelenthető, hogy a magyarországi vályog építőanyag külső dózisterhelés szempontjából nem jelent semmilyen kockázatot. Ugyanezekben az épületekben viszont mind a radontól, mind a torontól származó belső dózisterhelés nem elhanyagolható. Az értékeket az időjárási körülmények befolyásolják legjelentősebben, amelyek lehetséges eredménye a detektált radon és toron évszakos változásainak különbözősége. A Békés megyében található negyedidőszaki üledékes geológiai képződmények közül agyagon várhatók a legnagyobb beltéri értékek. A három vizsgált terület közül a Mórágyi-rög vályog építőanyagához köthető a legnagyobb ^{226}Ra- és ^{232}Th-aktivitás-koncentráció (amelyek a radon és toron forrásai).